UNIVERSITY OF NAPLES FEDERICO II

Faculty of Engineering

PH.D. PROGRAMME in MATERIALS and STRUCTURES
COORDINATOR PROF. DOMENICO ACIERNO
XXII CYCLE

LUDOVICA ELEFANTE

PH.D. THESIS

Dealing with Uncertainties in the Assessment of Existing RC Buildings

TUTOR PROF. GAETANO MANFREDI
CO-TUTOR ING. IUNIO IERVOLINO, ING. FATEMEH JALAYER

Index

VI

Introduction

From a literature review it has been possible to point out, starting from Greek and Latin literature references, the development of at least 160 catastrophic seismic events in the Mediterranean area in the last two century. Studies and researches have shown that about 60% of such events have been recorded in Italy as well as more than 50% of the recorded damages. This data can be ascribed to the high intensity of the recorded earthquakes in Italy, but also to both the high density of population and the presence of many structures under-designed or designed following old codes and construction practice: for this reasons the seismic risk in Italy is very high.

In fact, the seismic risk is defined by the convolution of three terms: hazard vulnerability and exposure. The hazard is linked to the probability that, in the analyzed area, a seismic event occurs in a given period of time. The vulnerability, also known as fragility, is related to the propensity of people and goods to be injured or damaged during a seismic event. The exposure is rather closely related to the aftermath analysis of a seismic event and in particular to location, consistency, quality and value of goods and activities on the territory that may be affected directly or indirectly from the event of earthquake.

Moreover by analysing the data provided by the 14th census of population and buildings (2001) in Italy, it is possible to have a clear idea regarding the period of construction of the existing reinforced concrete buildings (see Figure I.1); such data show that about one million of building units (35%) have been

built before the first code with seismic provisions, Legge 2/2/74 n.64 [1], was issued.
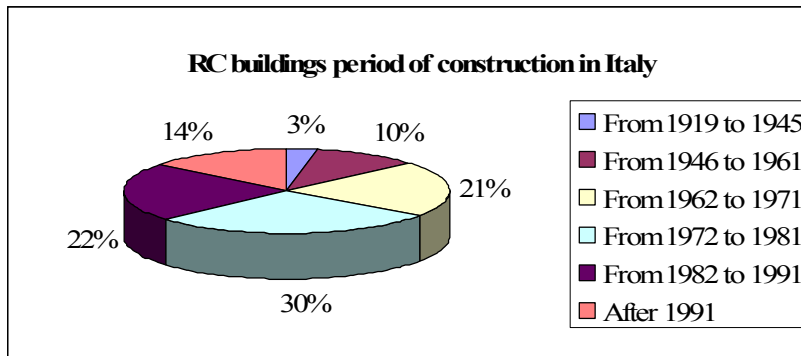
Figure I.1. RC buildings period of construction in Italy – census 2001

As a result a significant portion of the total seismic risk in Italy, evaluated in economic terms, comes from the various type of damages endured by the existing buildings. This is the case for several other European countries in which the average service life for buildings is larger than that of countries like the United States. Therefore, management of existing building stock is a major concern in such regions.

This is the reason why, more recent European seismic guidelines (e.g., EC8 [2], OPCM [3], NTC [4]) pay particular attention to seismic assessment of existing structures, which is distinguished from that of the new construction by lack of information about both the original features and the current state of building in consideration. The assessment of existing structures is subjected to numerous sources of uncertainty.

I.1   Objectives

One of the most challenging aspects of the seismic assessment of existing buildings is the characterization of structural modeling uncertainties.

Many European countries are subjected to a considerable seismic hazard. Quite a few of these countries enjoy a rich patrimony of existing buildings,

which for the most part were built before the specific seismic design provisions made their way into the constructions codes. Therefore, the existing buildings can potentially pose serious fatality and economic risks in the event of a strong earthquake. One very recent and very unfortunate case is the L'Aquila Earthquake of 6 April 2009 in central Italy. One main feature distinguishing the assessment of existing buildings from that of the new construction is the large amount of uncertainty present in determining the structural modeling parameters. Recent codes such as Eurocode 8 [2] seem to synthesize the effect of structural modeling uncertainties in the so-called confidence factors (CFs) that are applied to mean material property values. The confidence factors are classified and tabulated as a function of discrete knowledge levels acquired based on the results of specific in-situ tests and inspections.

With the emerging of probability-based concepts such as life-cycle cost analysis and performance-based design, the question arises as to what the CF would signify and would guarantee in terms of the structural seismic reliability [5,6]. This would not be possible without a thorough characterization of the uncertainties in the structural modeling parameters [5,7].

A fully probabilistic method coupled with non-linear dynamic analysis would be the best method in order to incorporate all relevant sources of uncertainties; however pragmatism oblige the adoption of a simplified format, calibrated on the fully probabilistic method, able to put the engineer in the condition to approach the problem by incorporating the uncertainties of different nature in the assessment procedure.

The objective of this thesis work is to investigate how dealing with the different sources of uncertainty that affect the assessment of existing RC buildings.

Methods alternative to the code based confidence factors are proposed and adopted for the case study structure.

These methods employ a Bayesian framework in order to update the global structural performance-based reliability in relation of different knowledge levels obtained for the analyzed structure.

I.2   Problems of Existing RC Buildings

The problem of structural safety for existing buildings must be addressed by identifying the technical and social reasons that make a large number of buildings potentially at risk. The quality of constructions in Italy, especially in the last fifty years, is poor with respect to the constructions of the same period in other European country [8]. This situation is probably due to the "construction-boom" which gave rise, in the last fifty years, to a considerable urbanization phenomenon; this buildings, often unlawful, are characterized by insufficient design standards, lack of attention in structural details and use of poor quality materials. Most of reinforced concrete (RC) existing structures have been designed mainly for gravity loads and the seismic provisions considered in the design process are very poor or non-existent. In addition, this buildings, which are often subjected to load conditions not foreseen during the design process and used for purposes other than those they were designed for, may experience significant degradation.

The assessment of existing structures is distinguished from that of the new construction by lack of information about both the original features and the current state of building in consideration. In fact, design documentation for this buildings tends to be poor and original design calculations and working drawings usually are unavailable.

Even in cases in which the original documentation is available, it may be that, during the construction process (which is rarely subjected to quality control) something has been changed from the original documents due to lack of attention, unavailability of materials or speculative reasons. Furthermore design codes, materials and construction practices are changed, and material specifications may be difficult to obtain. Moreover not all members may be accessible for inspection and previous maintenance operation, even if conducted, may have caused undesirable strength and stiffness variations. In any case; full documentation relative to the maintenance operations performed in the past are often unavailable.

In short determining the structural modelling parameters such as, materials properties and structural detailing parameters in existing RC structures is not an easy task and is subjected to a significant level of uncertainty.

I.3   Evolution of the Legislation and Practice Project

While new buildings are designed based on Performance-Based design principles, the existing buildings are designed based on an engineering conception founded on deterministic models of actions and resistances. Thus the structure would be verified only in relation to the maximum resistance of its composing structural elements.

Moreover, as stated previously, most of existing RC structures have been designed mainly for gravity loads and the seismic provisions considered in the design process are very poor or non-existent.

In fact the first identification of seismic zones in Italy, took place in early 900 through the instrument of the Regi Decreti, issued following the destructive earthquake of Messina and Reggio Calabria 28/12/1908. A list of the cities which were hit by the earthquake was compiled. The hit towns were divided into two categories, in relation to their degree of seismicity and their geological formation. After occurrence of each strong earthquake, the so-called list was updated by simply adding new towns affected by seismic event.

The first code in which was established a framework for classifying national seismic hazard with special requirements for seismic zones, as well as drafting of technical regulations, is the Legge 2/2/1974, n. 64 [1], *"Provvedimenti per le costruzioni con particolari prescrizioni per le zone sismiche"*.

It should be noted that the distinctive character of this law was the opportunity to update the rules whenever it was warranted by evolving knowledge of seismic phenomena; instead for the seismic classification was made, as in the past, simply by appending to the list the new towns affected by the new earthquakes.

Seismological characterizations conducted in the aftermath of the earthquakes of Friuli Venezia Giulia, 1976, and of Irpinia, 1980, have led to a significant increase in knowledge on the seismicity of the national territory and

have led to a proposal for seismic classification of the national territory. This has been translated into a series of decrees approved between 1980 and 1984, which defined the Italian seismic classification, until the OPCM [3].

As much as it concerns the technical standards, the first seismic provisions were already enacted with the DM 3/3/1975 [9], subsequently supplemented by a series of successive decrees, with some relevant technical information contained in the accompanying ministerial circulars.

Immediately after the earthquake of 31 October 2002, which hit the territories on the border between the Molise and Puglia, the Department of Civil Protection (DPC) has adopted the OPCM [3], in order to provide an immediate response to the need for updating the seismic zonation and seismic provisions.

Among the major innovations of this new legislation, one can name the extension of the seismic zonation throughout the country, the replacement of the allowable stress method in favor of the limit state method of verification, and attention to proper structural modeling analysis.

Unlike the earlier seismic provisions, in the OPCM [3], and subsequent modifications, the entire national territory has been classified as seismic and is divided into 4 zones, characterized by decreasing seismic hazard; these areas have been identified by 4 classes of peak ground acceleration with a probability of exceedance of 10% in 50 years. In this new classification the three zones of high, medium and low seismicity, were provided the standards of seismic design with different levels of severity, while for zone 4, a new feature was introduced, which gave the regions the option to to require the standards for seismic design.

It should be stressed, moreover, the close link between the rules contained in the OPCM [3] and the system of laws already established in Europe, Eurocode 8 [2].

The main difference between the new generation codes, such as EC8 [2] and OPCM [3], and the traditional ones, is the substitution of conventional design and purely prescriptive approach with a performance-based approach in which the objectives of design are declared, and the set of rules and methods used for

this purpose (the procedures for structural analysis and sizing of elements) are individually justified. Another innovative aspect of the OPCM [3] is that for the first time the problem of evaluation of existing structures was explicitly addressed and an entire chapter was dedicated to it.

Together with the DM 14/09/2005 [10] the "Technical standards for construction" have been approved, which represent a first attempt towards unification of a highly fragmented and inhomogeneous framework. In fact, the design and assessment criteria for various building types are all outlined in one text. This includes both the mechanical material properties and the definition of loading. In this uniform code, the set of external actions are fixed base on the level of safety to be achieved and the minimum performance expectations for structures.

Regarding the characterization of seismic actions the general approach introduced by OPCM [3] is maintained; however the operative design procedures described in detail in the OPCM [3] must be taken only as illustrative suggestions and are not obligatory.

Together with the DM 14/01/2008, the new "Technical standards for construction" (NTC) [4] is published that is the result of the revision of standards approved in 2005.

These new rules, which generally confirm the basic approach in the 2005 rules, introduce some changes and provide a series of clarifications on specific aspects, some of which were taken from OPCM [3] and its subsequent modifications. Among the most important change include;

- the definition of seismic intensity parameters as a function of the coordinates of the location and class of use of the building;
- slight variations in load factors and their combination;
- redefinition of the parameters relating to verification of the load-bearing capacity of foundations;
- redefinition of the shear capacity assessment for RC elements;
- definition of design rules for performance-based design and the parameters that govern the achievement of the high and low ductility classification;

- changes in expressions of the structural factor (q);
- recommendation of the use of static pushover analysis as complementary or alternative method with respect to linear analysis methods for checking the safety of buildings subject to earthquake.

This research work has been developed during the last steps of the described code evolution, therefore we will refer to both the OPCM [3] and the NTC [4].

As stated previously, more recent European seismic guidelines pay particular attention to seismic assessment of existing structures. In particular, existing buildings are distinguished from those of the new design since the project reflects the state of knowledge at the time of construction and may contain conceptual flaws of various kinds including those related to the construction process. Moreover, these buildings may have been subjected to past earthquakes or other accidental actions whose effects are not evident. Consequently the assessment of existing structures appears highly sensitive to uncertainties that maybe comparable to those related to the representation of seismic ground motion.

European and Italian seismic guidelines synthesize the effect of structural modeling uncertainties in the so-called *confidence factors* (CF) which have to be applied to mean material properties, assumed a priori or obtained by performing in-situ tests on the structure. The primary scope for introduction of these confidence factors is to allow for a certain level of conservatism, through the use of material strength values smaller than that of the corresponding mean values determined based on available knowledge, in the seismic assessment of existing structures.

Evaluation of these confidence factors is based on three increasing levels of knowledge about the structure, each of which are required for specific sets of tests (destructive and non-destructive) and inspections. The quantity and quality of data collected determines the method of analysis and values of the confidence factor applicable to the properties of materials to use later on in the safety checks.

In particular there are three levels of knowledge:

- KL1 - *Limited*;
- KL2 - *Extended*;
- KL3 - *Comprehensive*.

The aspects that define the levels of knowledge are:

- *geometry*, i.e., the geometric characteristics of structural elements;
- *structural details*, namely, the quantity and the arrangement of steel reinforcement, including the stirrup spacing and closure;
- *materials*, i.e., the mechanical properties of materials.

In general, as shown in the tables below (Table I.1 and Table I.2) taken from EC8 [2], which can also be found in the OPCM [3] and in the Circolare 2/2/2009, n.617 [11] "Instructions for the application of new technical standards for construction", larger amount of information corresponds to a lower value of the confidence factor, in order to stimulate an increase in the number of tests and inspections.

Table I.1. Recommended minimum requirements for different levels of inspection and testing

KL	Inspections of reinforcement details (% structural elements)	Testing of Materials (sample/floor)
Limited	20	1
Extended	50	2
Comprehensive	80	3

Table I.2. Knowledge levels and corresponding methods of analysis (LF: Lateral Force procedure, MRS: Modal Response Spectrum analysis) and confidence factors (CF)

Knowledge Level	Geometry	Details	Materials	Analysis	CF
KL1	From original outline construction drawings with sample visual survey *or* from full survey	Simulated design in accordance with relevant practice and from limited *in-situ* inspection	Default values in accordance with standards of the time of construction *and* from limited *in-situ* testing	LF-MRS	CF_{KL1}
KL2		From incomplete original detailed construction drawings with limited *in-situ* inspection *or* from extended *in-situ* inspection	From original design specifications with limited *in-situ* testing *or* from extended *in-situ* testing	All	CF_{KL2}
KL3		From original detailed construction drawings with limited *in-situ* inspection *or* from comprehensive *in-situ* inspection	From original test reports with limited in-situ testing or from comprehensive in-situ testing	All	CF_{KL3}

Although the confidence factors are applied to the properties of materials, the uncertainties in structural modeling are not limited to them and include also other structural detailing parameters (e.g., reinforcement detailing, cover thickness, etc.) entering into the seismic assessment problem. The variations in structural detailing parameters can prove quite significant to the extent that they may change the structural collapse mechanism.

It seems that this structural details are taken into account only in an implicit way and the extent to which they could affect the seismic assessment of existing structures seems not yet to be studied in depth.

I.4   Evolution of Structural Materials

The importance of materials properties is evident in the approach prescribed for the assessment of existing buildings in the recent European and Italian seismic codes.

The mechanical properties of structural materials are important for sizing the elements in relation to the design action as well as for evaluating the structural capacity.

The material properties in an existing RC building can be determined from the following sources of information:

- common value used by the practice at the time of the construction;
- original specifications of the original project or test certificates;
- in-situ tests.

The extent of in-situ tests depends on the chosen level of knowledge and on other information available.

Particularly important is the estimation of the concrete compressive strength not only for the role it has on the load-bearing capacity and durability of the structure, but also because other properties of concrete such as the elastic modulus and tensile strength can be obtained directly or indirectly from it. In order to evaluate this quantity in existing RC structures, various methods of investigation both of destructive (i.e., involving localized removal of material as the carrot test) and non-destructive (e.g., rebound hammer test, ultrasonic test and the Sonreb combined method) nature can be used.

Moreover, chemical tests may be useful in order, for example, to detect the presence and the degree of carbonization, which can led to the corrosion of steel reinforcement.

It should be noted that these methods have undergone a substantial evolution in recent years but are efficient and reliable only when used properly. Nevertheless, a crucial role in the inspection process is still assumed by a visual direct examination [12].

The knowledge of historical data, namely the properties required by technical regulations in force at the construction time and / or quality of

materials usually adopted in different periods of time and different regions, such as the specifications derived from the manuals (e.g., [13,14]), are very important for the estimation of material properties, especially reinforcing steel.

In fact the mechanical properties of steel are difficult to assess with non-destructive in-situ tests. Therefore their evaluations generally requires the removal of reinforcement to be tested later in the laboratory. These pieces have to be taken under particular conditions and from locations that would not compromise the integrity of the structural element and would minimize the resulting damage.

However both concrete and reinforcement steel mechanical properties have had a substantial improvement in quality and in performance, thanks to new technology for their production and also to the development of more severe acceptance criteria as a result of updating of constructions codes.

I.5   Open Issues in the Current Code-Based Approach

At a first glance, the application of the confidence factor seems to be a deterministic method for addressing an inherently probabilistic problem.

In the code approach, the effect of the application of the confidence factors on structural reliability is not explicitly stated. Instead, with the emerging of probability-based concepts such as life-cycle cost analysis and performance-based design, the question arises as to what the CF would signify and would guarantee in terms of the structural seismic reliability [5,6]. This would not be possible without a thorough characterization of the uncertainties in the structural modeling parameters [5,7].

Another issue regards the definition of the level of knowledge (KL). The current code definition in Table I.2 leaves a lot of room for interpretation. For example, it does not explicitly specify the spatial configuration and the outcome of the test results. Moreover, the logical connection between the numerical values for the CFs and the onset of the KLs is not clear.

These problems underline the necessity of developing simple and approachable methods, based on structural reliability concepts, in order to

assess the structural performance of existing RC structures in the presence of modeling uncertainties.

I.6   Variability of the Assessment Results

As it is well addressed in the work of Franchin at al. 2008 [6], the current approach of the code related to the assessment of existing RC buildings leaves the engineer with a series of subjective choices that, together with different sources of uncertainty that characterize the problem, contribute to a relatively large dispersion in estimating the state of the structure.
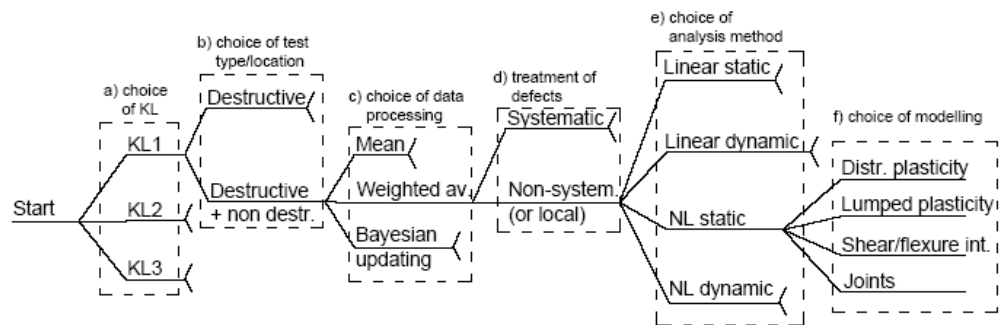
Figure I.2. Degrees of freedom left to the analyst [6].

Starting from the information initially available about the existing RC building and following the code assessment procedure, the engineers are faced with a number of options that can lead to different outcomes.

In fact in relation to the knowledge level that the engineer wants to reach, he has to choose the amount and type of additional information to be collected to complement the initial set. The planning of tests and inspections, in relation to the identified homogeneous zones, is left to the engineer; in particular, each engineer can choice the type of tests (destructive or non-destructive) and their spatial location. It is evident that different engineers can make different choices.

Also the elaboration of the test results requires some choices in relation to the parameters adopted in the data processing. Furthermore, once the results

have been collected, these have to be integrated with the initial data set. It could happen that the results contradict the initial data set: one engineer might accept the discrepancy, within certain limits, while another may choose to rely entirely on in-situ information adopting a comprehensive survey on the structure.

Therefore, for the same existing building, different engineers can obtain different structural models; moreover they could choose different analysis methods.

If the chosen analysis method is the dynamic one, another relevant source of uncertainty could affect the assessment results, that is the uncertainty in the representation of the ground motion. This source of uncertainty is strictly related to the selection of the ground motion records to be used in the structural assessment employing time-history analysis procedures. In fact, the seismic input selection represents one of the main issues in assessing the seismic response of a structure through numerical dynamic analysis; this choice may be affected by the interface variable used to measure the intensity of ground motion and may cause bias in assessment results.

Therefore, at the end of the assessment process, for the same existing RC structure we can have a large variability of results.

I.7   The Organization of the Thesis

In this thesis the problem of the seismic assessment of existing RC buildings is addressed, with particular attention to the various sources of uncertainty associated with it.

In chapter I, different approaches to the structural safety problem are briefly presented and discussed. Particular attention is given to how dealing with uncertainties in engineering safety problems and decision making under uncertainty. The probability-based performance assessment framework is described in details.

In chapter II a review of some interesting research works concerning the problem of the seismic assessment of existing RC buildings, with particular attention to the confidence factors defined in the code, is presented. The relation between confidence factor and structural reliability for the case study

structure is investigated accounting for both material properties uncertainty and structural detailing uncertainty. A proposal for a probability-based definition of confidence factor in relation to the global structural performance is presented.

In chapter III, the representation of ground motion in the seismic assessment and the uncertainties associated with it is discussed. A graphical and statistical tool is implemented in order to evaluate the fulfillment of the condition of sufficiency for different intensity measures adopted to represent the ground motion in the assessment; a simplified method using the statistical tool of the weighted regression is presented and adopted when this condition is not verified in order to modify the assessment of the structural performance in relation to the observed dependencies. The weights are assigned in relation to the results of the seismic hazard disaggregation for the site of interest.

In chapter IV an efficient simulation method that allows the robust estimation of the structural fragility with a small number of analysis is presented and implemented for the case study structure, accounting for the uncertainty in the materials properties and the construction detail parameters. The efficient simulation method is implemented using both static and dynamic non-linear analysis; in the case of dynamic analysis, also the uncertainty in the ground motion representation is taken into account.

In chapter V, in the framework of demand and capacity factor design, an alternative probabilistic-based formulation of the confidence factors for the estimation of structural safety of existing buildings is presented for both static and dynamic non-linear analysis procedures, in relation to different knowledge levels. The proposed approach, similar to that adopted by the SAC-FEMA guidelines [15], takes into account the uncertainty about the structural modeling parameters (materials and details), and those related to the ground motion representation. This alternative formulation is applied to the case study structure for different hypotheses related to the outcome of tests and inspections. A code-based implementation of the proposed alternative performance-based safety-checking format is presented.

Finally, in chapter VI a survey for professional engineers is presented in order to obtain a database based on expert opinion for characterizing prior

probability distributions for structural details. Preliminary testing results obtained by interviewing a small group of professionals are presented.

I.8   References

[1]   Legge 2 febbraio 1974 n. 64, "*Provvedimenti per le costruzioni con particolari prescrizioni per le zone sismiche*" (*in Italian*).

[2]   CEN, European Committee for Standardisation TC250/SC8/ [2003] "*Eurocode 8: Design Provisions for Earthquake Resistance of Structures, Part 1.1: General rules, seismic actions and rules for buildings*," PrEN1998-1.

[3]   Ordinanza del Presidente del Consiglio dei Ministri (OPCM) n. 3431, "Ulteriori modifiche ed integrazioni all'ordinanza del Presidente del Consiglio dei Ministri n. 3274 del 20 marzo 2003". Gazzetta Ufficiale della Repubblica Italiana n. 107 del 10-5-2005 (Suppl. Ordinario n.85), 2005 (*in Italian*).

[4]   CS..LL.PP, DM 14 gennaio, *Norme Techniche per le Costruzioni* (NTC). Gazzetta Ufficiale della Repubblica Italiana, **29**, 2008 (*in Italian*).

[5]   Jalayer F., Iervolino I., Manfredi G., "Structural modeling uncertainties and their influence on seismic assessment of existing RC structures", submitted to *Structural Safety*, 2008.

[6]   Franchin P., Pinto P. E., Pathmanathan R., Assessing the adequacy of a single confidence factor in accounting for epistemic uncertainty, Convegno RELUIS "*Valutazione e riduzione della vulnerabilità sismica di edifici esistenti in cemento armato*", Roma 29-30 maggio 2008.

[7]   Monti G., Alessandri S., Confidence factors for concrete and steel strength, Convegno RELUIS "*Valutazione e riduzione della vulnerabilità sismica di edifici esistenti in cemento armato*", Roma 29-30 maggio 2008.

[8]   "*Valutazione riduzione della vulnerabilità sismica di edifici esistenti in cemento armato*", Cosenza E., Manfredi G., Monti G. editors, Polimetrica publisher, 2008.

[9]   Decreto Ministero per i lavori pubblici, 3 marzo 1975, "*Disposizioni concernenti l'applicazione delle norme tecniche per le costruzioni in zone sismiche*", (*in Italian*)..

[10] Decreto del Ministero delle infrastrutture e dei trasporti, 14 settembre 2005, "*Norme Tecniche per le costruzion*i", (*in Italian*)..

[11] Circolare del Ministero delle infrastrutture e dei trasporti n.617, 2 febbraio 2009, "*Istruzioni per l'applicazione delle Nuove norme tecniche delle costruzioni di cui al DM 14 gennaio 2008*", (*in Italian*)..

[12] "*Valutazione degli edifici esistenti in cemento armato*", G. Manfredi, A. Masi, R. Pinho, G. M. Verderame, M. Vona, Manuale IUSS Press, 2007.

[13] Santarella L. "*Il cemento armato – Le applicazioni alle costruzioni civili ed industriali*", Edizione Hoepli 1968.

[14] Pagano M. "*Teoria degli edifici - Edifici in cemento armato*", Napoli, Edizione Liguori 1968.

[15] Federal Emergency Management Agency (FEMA), 2000. *Pre-Standard and Commentary for the Seismic Rehabilitation of Buildings*. FEMA 356, Washington, D.C.

Chapter I

Approaches to Structural Safety Problems

1.   Introduction

Recent significant advances in the engineering design and the revolution in information technology and computing have made possible to predict the behavior and performance of complex engineered system with an increasing level of accuracy.

However numerous sources of uncertainties arise in the analysis and assessment process, causing a significant impact on technical, economic and social decisions. Some of these uncertainties stem from randomness inherent in nature, others arise from a lack of knowledge and ignorance. Both sources of uncertainty are equally important and must be considered in engineering safety problems [1].

The inevitable consequence of these uncertainties is that the engineering system may fail to perform as intended by the owner, occupant or user, or society as a whole.

It is not feasible to eliminate risk entirely; rather, the risk must be managed in the public interest by engineers, code bodies and political system.

Engineers traditionally have dealt with risk and uncertainty by making conservative assumptions in analysis and design, postulating worst-case scenarios, and applying factors of safety. Such approaches provide an unknown

margin of safety against the failure state, however it is defined. Often, the decision is so conservative as to be wasteful of resources; occasionally, it errs in the non-conservative direction.

In recent years, there has been a growth in the use of reliability and risk analysis, founded in the mathematics of probabilistic and statistics, to support decision making in the presence of uncertainty.

2.   Engineering Safety Problems

In this section a brief review of different approaches that can be used in order to solve engineering safety problems are presented.

2.1.   Deterministic Approach

The first non-empirical approach to engineering safety problems is for sure the "allowable stress" method introduced at the beginning of 1900 and widely used till last few years. This approach consists in verifying that the maximum calculated tension in the most stressed section, in relation to the most unfavourable load condition, should be smaller than a certain allowable stress level. This allowable stress value is evaluated in relation to the material fracture stress, scaled by a safety factor that accounts for the uncertainties related to load and stress conditions.

2.2.   Semi-Probabilistic Approach

Recent codes and provisions have introduced the evaluation of structural safety through a semi-probabilistic approach based on the definition of the limit states; this approach is closer to the probabilistic one, that will be discussed later, but is based on the introduction of partial safety coefficients to the characteristic values of the load and resistance. This approach is also known as the first level method.

Within this method the engineer has only to ensure that:

$$\gamma_S S_k \leq \frac{R_k}{\gamma_R}$$ Eq.1.1

where R_k and S_k are defined as a lower and an upper percentile p, respectively.

$$P[R < R_k] = p \qquad\qquad P[S > S_k] = p$$ Eq.1.2

where p is a little number (usually 0.05).

The coefficients γ_S and γ_R in equation 1.1 are the partial safety coefficients, both greater than 1.

This approach is named semi-probabilistic because the evaluation of input data and coefficients comes from probabilistic and statistical considerations; however, from an engineering point of view, the partial safety coefficients approach is still similar to the allowable stresses with a modified comparsion between load and resistance.

2.3.   Probabilistic Approach

Due to the discrepancy between the safety problem analyzed with the admissible stresses method, that is a fully elastic method, and the real behavior of structures that are characterized by non-linear behavior, and the uncertainties related to the allowable stresses method, engineers have tried to approach the safety problem from a different point of view by defining structural safety through probabilistic methods.

From a probabilistic point of view the load and resistance of the structural elements are modelled through aleatory variables, that are able to describe the intrinsic uncertainty of this parameters caused by a very large number of phenomena that can not be modelled in a deterministic framework [2]. This probabilistic approach is founded on the definition of the limit states. In this case the safety problem can be expressed by this equation:

$$S \le R$$ Eq.1.3

where S is the demand expressed in performance terms and R is the available capacity; the equality in the previous equation corresponds to the threshold of the limit state.

In general for each limit state it is possible to define a function and identify a domain of significant variables; for example an R-S space for the equation 1.3, a "safe domain" Σ where inequality is verified and a "failure domain" Ω in which it is not.

We can then determine the probability of failure and reliability of the system, respectively, as the probability that the limit state function is less than zero or not:

$$P_{failure} = P[S > R]$$
$$P_{success} = 1 - P_{failure} = P[S \le R]$$ Eq.1.4

2.3.1. Exact Probabilistic Approach

Introducing the joint probability density function (JPDF) $f(X)$ of the vector X representative of the random variables characterizing the problem under consideration, we can define the probability of collapse (failure) as:

$$P_{failure} = \int_{\Omega} f_X(\mathbf{X}) dx$$ Eq.1.5

Moreover, one can define a limit state function $G=G(X)$ as:

$$\{G(\boldsymbol{X}) > 0\} \rightarrow \{success\}$$
$$\{G(\boldsymbol{X}) < 0\} \rightarrow \{failure\}$$

Eq.1.6

If for example we refer to two random variables *S* and *R* (load and resistance) the most basic limit state is $G(R,S) = R\text{-}S$. With the introduction of *G*, we can write:

$$P_{failure} = \int_{G(\mathbf{X}) \leq 0} f_X(\mathbf{X}) dx$$

Eq.1.7

The structural reliability problem is reduced (apparently) to the solution of this multidimensional integral; in reality the solution in closed form of the integral is possible only in very rare cases and under very restrictive circumstances.

To solve the structural reliability problem with an entirely probabilistic approach, the JPDF for *X* must be determinate; then we the functional form of the limit state function needs to be defined; finally the multiple integral in equation 1.7 needs to be solved.

Determining the JPDF for X will be substantially based on the hypothesis of statistical independence between the variables. Determining the limit state function is a specific problem of reliability theory: in many cases we know the analytical form of the limit state function *G*, but in other cases this function must be estimated from the data and is known only in numerical form. In these cases, we must use special approaches (such as surface response) to determine the shape of *G*. Integration of equation 1.7 is a purely computation problem with multidimensional integration domains defined in implicit form (generally inequalities within a *n*-dimensional area).

In general, however, that integral can be solved only numerically through simulation methods which are typically very computationally expensive.

However in the case of the two-dimensional problem of independent load and resistance variables and linear limit state function, it is possible to find a closed form solution of the integral.

For example in the case of the formulation of structural reliability problem based on the limit state function defined as $G(R,S) = R\text{-}S$, where R and S are independent variables for which the functions of marginal probability density PDFs (Probability Density Functions), $f_R(r)$ and $f_S(s)$, are known, equation 1.7 can be written in this form:

$$P_{failure} = P_f = \iint\limits_{[R-S<0]} f_{R,S}(r,s)drds \qquad \text{Eq.1.8}$$

Since the independence of the variables we can write:

$$f_{R,S}(r,s) = f_R(r)f_S(s) \qquad \text{Eq.1.9}$$

and by substitution in equation 1.8:

$$P_f = \iint\limits_{[R-S<0]} f_{R,S}(r,s)drds = \int_0^\infty f_S(s)\left[\int_0^s f_R(r)dr\right]ds = \int_0^\infty f_S(s)F_R(s)ds \qquad \text{Eq.1.10}$$

and then the probability of failure is given by the convolution integral of two functions of *s*, where $f_S(s)$ is the PDF of *S* and $F_R(s)=P[R<S]$ is the CDF (Cumulative Distribution Function) of *R*.

In general, cases where the integral is solved analytically coming to the exact solution are extremely rare. However, there are numerical methods for solving the problem of calculating the probability of failure. These simulation methods sample the variables in the safety-checking problem from their JPDF.

For each realization of these variables, the limit state function is checked to see whether the sample lies in the failure space or not. These procedures, more or less refined, are all characterized by an accuracy inversely proportional to the number of simulations.

The easier simulation method, but also the best known, is the so-called Monte Carlo method. It calculates the integral defining an auxiliary function *I*, called indicator function, which takes the value zero for values of the vector **X** for which the limit state function *G* is positive (safe space) and unit value for values of the vector **X** for which the limit state function takes negative values (failure space).

$$I(\mathbf{X}) = \begin{cases} 0 & if & G(\mathbf{X}) > 0 \\ 1 & if & G(\mathbf{X}) \leq 0 \end{cases} \qquad \text{Eq.1.11}$$

The indicator function is used to calculate the probability of collapse by extending the integral to the whole space of definition of **X**, thus overcoming the problem of having to determine the failure domain Ω. It can be shown that, in this way, the integral in equation 1.7 is approximated by the ratio between the number of repetitions of the experiment that have given a negative result (N_f) and the total number of tests performed.

$$P_f = \int_{\Omega} f_X(\mathbf{X})dX = \int_{R^n} I(\mathbf{X})f_X(\mathbf{X})dX \cong \frac{N_f}{N_{TOT}} \qquad \text{Eq.1.12}$$

It can be shown that the coefficient of variation of probability of collapse is equal to the following expression:

$$C.O.V.(P_f) = \sqrt{\frac{1 - Pf}{N \cdot Pf}} \qquad \text{Eq.1.13}$$

Therefore, for example in order to estimate a probability of collapse equal to 10^{-3} with a coefficient of variation around 30%, one needs to perform at least 10^4 simulations .

Since the probability of collapse in structures is generally very small and each simulation requires a complete structural analysis, the computational effort can be prohibitive even for computers. Therefore alternative simulation methods, called *smart simulation methods*, have been developed. Generally speaking, these methods represent modifications of the Monte Carlo method in order to try to reduce the number of simulations needed to calculate the reliability with a given accuracy.

2.3.2. Simplified Probabilistic Approach

The integral in equation 1.5 in most cases can only be solved numerically. As described in the previous section, numerous numerical simulations will result very costly in terms of time and computing power.

As stated before, the main problems related to the calculation of the integral can be summarized as follows [3]:
1) the domain of integration is known only in implicit form;
2) the domain of integration is generally "far" from the mean of the vector **X**;
3) the integrand may have a steep slope in the domain of integration.
The first point makes it difficult to find the limits (bounds) for the domain of integration. The second point makes it difficult to efficiently generate the random numbers, while the third point requires an accurate choice of the integration pattern in order to avoid losing some peak value of the integrand. For these reasons, several authors have proposed the idea of assess the reliability with an index β, called *reliability index* [4]. This index measures, in units of standard deviation, the distance between the average value of the vector *X* and the boundary of the domain of failure, or the distance between this average value and the point of the limit state function ($G(X)=0$) which is closest

to the average value (*design point*). The evaluation of the index β is therefore a constrained minimization problem.

Once this index has been calculated, it is possible to calculate the probability of collapse and compare it with the reference values to assess the degree of reliability of the structure, obviously the greater the value of β, the lower the probability of collapse.

In the case of the load-resistance model, assuming that the vector of random variables R and S is normally distributed, the function $G = R-S$ is still normally distributed. Assuming that R and S are also uncorrelated, the mean and standard deviation of G are given by:

$$\mu_G = \mu_R - \mu_S$$
$$\sigma_G = \sqrt{\sigma_R^2 + \sigma_S^2}$$

Eq.1.14

In this particular case the probability of collapse can be calculated simply by recalling the Gauss integral:

$$P_f = \frac{1}{\sqrt{2\pi}\sigma_G} \int_{-\infty}^{0} e^{-\frac{1}{2}\left(\frac{g-\mu_G}{\sigma_G}\right)^2} dg = \Phi\left(-\frac{\mu_R - \mu_S}{\sqrt{\sigma_R^2 + \sigma_S^2}}\right) = \Phi(-\beta) = 1 - \Phi(\beta) \qquad \text{Eq.1.15}$$

where β is the value at which the Gaussian function is calculated in order to obtain the probability of collapse. This result is susceptible to a geometric interpretation: indeed posing $y_2 = (r-\mu_R)/\sigma_R$ and $y_1 = (s-\mu_S)/\sigma_S$, the limit state function can be expressed as follows:

$$G(R,S) = y_2\sigma_R - y_1\sigma_S + \mu_R - \mu_S$$

Eq.1.16

In the space of standardized variables, it can be easily shown that the distance between the boundary surface (linear) and the origin is equal to β; thus the probability of collapse is related to the distance between the limit state surface and origin. In relation to Figure 1.1, the point P takes the name of a *design point* while β is the reliability index.
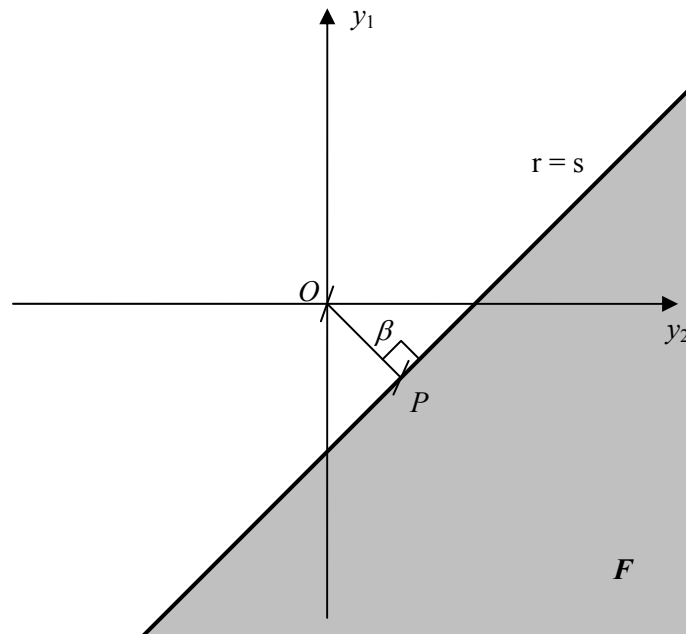
Figure 1.1. Trace of the linear limit state surface in the space of standardized variables.

Generalizing, it can be argued that in all cases in which the limit state function G is a linear combination of the random variables that influence the structural behaviour, characterized by a jointly Gaussian distribution, the calculation of the probability of collapse through the reliability index is exact. This method can even be adopted if the described conditions are not fully satisfied. In these cases an approximation of the probability of collapse is obtained that depends on the shape of the limit state function, the nature of the random variables involved and the possible correlation between the variables (i.e., FORM and SORM methods [5]).

3. Aleatory and Epistemic Uncertainties

It is common in risk analysis and engineering safety problems to distinguish between uncertainty that reflects the variability of the outcome of a repeatable experiment (*aleatory* uncertainty) and uncertainty due to limited or imperfect knowledge (*epistemic* uncertainty). The times and magnitudes of future earthquakes in a region, record-to-record variability in acceleration time-history amplitudes and phases are examples of the former type, while uncertainty on the age of the universe, the geologic profile of a site, or the earthquake capability of a fault are examples of the latter [1].

It may thus appear that the labeling of any given uncertainty as aleatory or epistemic is self-evident, but in fact the aleatory/epistemic quality is not an absolute attribute of uncertainty. Rather, it depends on the deterministic or stochastic representation that we make of a phenomenon [6].

However, the importance of distinguishing between aleatory and epistemic uncertainty it is not relevant for decision making, but serves the useful practical purpose of forcing the analyst to consider all sources of uncertainty.

4. Statistical and Non-Statistical Information

In essence, uncertainty about the applicable model (and its parameters) is epistemic, whereas uncertainty given the model (and its parameters) is aleatory.

Classical and Bayesian statistics handle epistemic uncertainty in different ways. In Bayesian statistics one first identifies the set of plausible models and then assigns to each model a probability of being correct based on all available information. In principle, the initial selection of models can be arbitrarily broad, since the implausible models can subsequently be assigned zero probability, without affecting the final result.

By contrast, classical statistics does not assign probabilities to models and deals exclusively with statistical data (with information in the form of outcomes of statistical experiments). Any non-statistical information (for example theoretical arguments, physical constraints, expert opinion) constrains

the set of plausible models, but is not subsequently used to quantify uncertainty within the chosen set of models.

Therefore, the selection of plausible models is usually a more sensitive operation in classical statistics than in Bayesian statistics.

5.   Decision Making Under Uncertainty

There are two main approaches to decision making under uncertainty, namely classical decision theory and Bayesian decision theory. Bayesian decision theory is conceptually simpler because it treats aleatory and epistemic uncertainty in the same way. It is also the more broadly applicable one, because as previously noted it can handle also non-statistical information.

5.1.   Bayesian Decision Theory

In this framework a utility function can be defined to express the relative desirability of alternative actions (e.g. seismic design decisions) taken when confronting with possible future events (future earthquakes and their consequences). An action is then considered optimal if it maximizes the expected utility relative to all uncertain quantities.

Bayesian decision theory involves three basic steps:

1. *Identify all uncertain quantities that affect the utility U(A) for each action A.*
   We denote by X the vector of such uncertain quantities.
2. *Quantify uncertainty on (X|D).* This is done by separately considering statistical and non-statistical information. Non-statistical information is used to produce a prior distribution of X ("the prior"). Statistical data are subsequently accounted for by calculating the likelihood of (X|D). The posterior distribution of (X|D) is given by the normalized product of the prior and the likelihood function:

$$P(X \mid D) = \frac{P(D \mid X)}{P(D)} P(X)$$

Eq.1.17

3. *Specify a utility function U(A,X) to measure the relative desirability of alternative (A,X) combinations.* Decisions are ranked according to the utility U(A), given by:

$$U(A) = \int_{allX} U(x, A) dF_{X|D}(x)$$

Eq.1.18

where $F_{X|D}$ is the posterior distribution of $(X|D)$. Hence, a decision A^* is considered optimal if it maximizes $U(A)$ in equation 1.18 [1].

It should be noted that the posterior distribution accounts for all available information on $(X|D)$, whether statistical or not, and all uncertainty, whether aleatory or epistemic. Hence neither of these distinctions is influential on the decision and all that ultimately matters is the total uncertainty.

5.2.   Classical Decision Theory

Classical decision analysis differs from Bayesian decision analysis in that it does not represent quantities with epistemic uncertainty as random variables. While this leads to certain complications and limitations, decisions involving epistemic uncertainty can still be made.

Contrary to the Bayesian case, non-statistical information cannot be incorporated in the decision-making problem.

However, for complex decision problems, the classical procedure becomes inadequate, first of all because in cases that involve many random variables and uncertain parameters (for example in earthquake loss estimation problems, which combine earthquake recurrence, attenuation, system response and damage models) it may be difficult to define functions with distributions that do not depend on the unknown parameters. In these cases a practical way to make decisions is to set the unknown parameters to conservative values such as upper or lower confidence limits. This "confidence approach" is frequently used in practice, but is not satisfactory since there is no objective way to choose the acceptable level of confidence.

6.   The Total Probability Theorem

The total probability theorem is one of the most useful theorems of the probability theory. Given a set of mutually exclusive and collectively exhaustive *events*, *B₁*, *B₂*, *…*, *Bn*, the probability *P[A]* of another event *A* can always be expanded in terms of the following joint probabilities:

$$P[A] = \sum_{i=1}^{n} P[A \mid B_i] \cdot P[B_i]$$

Eq.1.19

7.   Probabilistic performance-based assessment

This section focuses on the general performance assessment methodology developed by Pacific Earthquake Engineering Research (PEER) Center for buildings in the framework of Performance-Based Earthquake Engineering (PBEE). The approach is aimed at improving decision making related to seismic risk associated with direct losses, downtime and life safety [7].

7.1.   Decision Variables

By definition PBEE is based on achieving desired performance objectives that are of concern to society as a whole or to specific groups or individual owners, such as life safety, dollar losses and downtime (or loss of function). It is postulated that the performance objective can be expressed in terms of a quantifiable entity and, for instance, its annual probability of exceedance. For instance the mean annual frequency[1] (MAF) of collapse, or of the loss exceeding a certain quantity *y* of dollars, can be used as performance objectives. The quantifiable entities, on which the performance assessment is based, are referred to as decision variables (*DV*s). In the assessment methodology the key issue is to identify and quantify decision variables of

---

[1] The MAF is approximately equal to the annual probability for the small probability values of interest here.

primary interest for the decision makers, with due consideration given to all important uncertainties.

In order to compute DVs and their uncertainties, other variables that define the seismic hazard, the demands imposed on the building systems by the hazard and the state of damage have to be defined and evaluated.

7.2. Intensity Measures

The seismic hazard is quantified in terms of a vector of intensity measures (IMs), which should comprehensively define the seismic input to the structure.

The vector can have a single component (scalar IM), such as spectral acceleration at the first mode period of the structure, $S_a(T_1)$, or can have several components [8], as it will be discussed in chapter III. If a scalar IM is adopted, such as $S_a(T_1)$, the hazard is usually defined in terms of a hazard curve.

The outcome of hazard analysis, which forms the input to demand evaluation, is usually expressed in terms of the MAF of exceeding the IM vector and denoted by $\lambda(IM)$.

7.3. Engineering Demand Parameters

Given ground motion hazard, a vector of engineering demand parameters (EDPs) needs to be computed, which define the response of the building in terms of parameters that can be related to DVs. Relationships between EDPs and IMs are typically obtained through non-linear time-history analyses of the structure subject to a set of ground motion records. The outcome of this process, which may be referred to as probabilistic seismic demand analysis, can be expressed as $G(EDP|IM)$ or more specifically as $G[EDP \geq y \mid IM = x]$, which is the probability that the EDP exceeds a specified value y, given (conditional) that the IM is equal to a particular value x.

7.4.   Damage Measures

In order to close the loop, *EDP*s have to be related to the *DV*s of interest. In most cases an intermediate variable, called damage measure (*DM*), has to be inserted between the *EDP* and the *DV* simply to facilitate the computation of *DV*s from *EDP*s. A *DM* describes the damage and the consequences of damage to a structure. The term *G*(*DM*|*EDP*) represents the fragility function for a specific damage (failure) state or, in other words, the probability of being in or exceeding a specific damage state, given a value of *EDP*. If the fragility functions for all relevant damage states are known, the *DV*s of interest can be evaluated either directly or by the means of cost function that relate the damage states to repair and replacement costs. The results of this last operation is *G*(*DV*|*DM*), the conditional probability that *DV* exceeds a specified value, given a particular value of *DM*.

7.5.   PBEE Probability Framework Equation

These steps, which form the basis of performance assessment can be expressed in the following equation for a desired realization of the *DV*, such as the MAF of exceeding *DV*, dented by $\lambda(DV)$, based on the total probability theorem:

$$\lambda(DV) = \iiint G(DV \mid DM)\,dG(DM \mid EDP)\,dG(EDP \mid IM)\,d\lambda(IM) \qquad \text{Eq.1.20}$$

This equation, which is often referred to as the framework equation for performance assessment, suggests a generic structure for coordinating, combining and assessing the many considerations implicit in performance-based seismic assessment.

Through this equation, it is possible to "de-construct" the assessment problem into the four basic elements of hazard analysis, demand prediction, modelling of damage states and loss estimation, by introducing the three intermediate variables, *IM*, *EDP* and *DM*. These elements are then re-coupled

by integration over all levels of the selected intermediate variables [7]. This integration required that the conditional probabilities $G(EDP|IM)$, $G(DM|EDP)$ and $G(DV|DM)$ must be characterized over a suitable range of *DM*, *EDP* and *IM* levels.

The form of equation 1.20 implies that the intermediate variables (*DM*s and *EDP*s) are chosen such that the conditional probabilities are independent of one another and conditioning information need to be carried forward. This implies, for example, that given the structural response described by *EDP,* the damage measures (*DMs*) are conditionally independent of the ground motion intensity (*IM*), i.e., there are no significant effects of ground motion that influence damage and are not reflected in the calculated *EDPs*. The same can be said about the conditional independence of the decision variables (*DV*) from ground motion *IM* or structural *EDP*, given $G(DV|DM)$. Likewise, the intensity measure (*IM*) should be chosen such that the structural response (*EDP*) is not also further influenced by, say, magnitude or distance, which have already been integrated into the determination of $d\lambda(IM)$. Apart from facilitating the probability calculation, this independence of parameters serves to compartmentalize discipline-specific knowledge necessary to evaluate relationships between the key variables.

8.   References

[1]   Y. K. Wen, B. R. Ellingwood, D. Veneziano, and J. Bracci "Uncertainty Modeling in Earthquake Engineering", MAE Center Project FD-2 Report February 12, 2003.

[2]   O. Ditlevsen, H.O. Madsen, "Structural Reliability Methods", John Wiley & Sons Ltd, Chichester, 1996

[3]   F. Casciati, J. Roberts, "Models for structural reliability analysis", CRC Press, 1996.

[4]   C.A. Cornell, "Bounds on the reliability of structural systems", *Journal ofstructural division*, ASCE, Vo. 93, No. ST1, February 1967.

[5]   C.A. Cornell, "A probability based structural code", *J. Am. Concr. Inst.*, 66, pp.974-985, 1969.

[6]   W. M. Bulleit, "Uncertainty in Structural Engineering", Practice Periodical on Structural Design and Construction, Vol. 13, No. 1, February 1, 2008. ©ASCE.

[7]   G.G. Deierlein, H. Krawinkler, and C.A. Cornell, "A framework for performance-based earthquake engineering", Pacific Conference on Earthquake Engineering (2003).

[8]   J. W. Baker, C. A. Cornell, "Uncertainty propagation in probabilistic seismic loss estimation", Structural Safety 30 (2008) 236–252.

Chapter II

Confidence Factor: the State of Research

1.   Some Interesting Works

As it has been stressed in the introduction of this thesis, the problem of the assessment of existing RC buildings is of primary concern, not only for the engineers, but also for the political and research world. In fact the Italian Civil Protection has financed through RELUIS (Rete Laboratori Universitari di Ingegneria Sismica) different scientific tasks concerning the evaluation and reduction of seismic vulnerability of existing reinforced concrete buildings. In particular, a special task has been dedicated to the confidence factors.

In this context, some interesting works have addressed the open issues in the current code-based approach, obviously analyzing the problems from different points of view.

In particular, in the work of G. Monti and S. Alessandri (2008) [1], the authors chose to distinguish information about the strength of materials, that is affected by both inherent and epistemic uncertainties, from the information relative to construction details, affected only by epistemic uncertainties. For this reason a different approach has been proposed, in which confidence factors are evaluated separately for each material type. In particular, a method is proposed for the calibration of CF's for the resistance of materials based on a Bayesian framework. This method allows to use the results obtained from

destructive and non-destructive tests to update the a priori probability distribution, taking into account the accuracy of individual tests. Thus a benchmark for the strength of materials is obtained in relation to a lower level percentile of the updated probability distribution for material properties.

The work by G. Monti and S. Alessandri focus on materials and evaluate the CF's for different material properties. This CF's are calibrated based on the material's resistance and not on the global response of the structure.

In the work developed by P. Franchin et al.(2009) [2] a single value of the CF was adopted, taking into account all types of uncertainty. A reference structure was created in order to represent the complete state of knowledge and several realization of structural models were generated in which, for each knowledge level, the structure was known partially. The paper discusses the fact that, for each given level of knowledge, every analyst can develop a different (incomplete) picture of the structure. This way, probability distributions for the global response of the structure can be constructed , representing the variability of the choices each analyst can make (adhering to code specifications). The confidence factor was calibrated by setting a chosen lower percentile of the response value (say 10%) equal to one (the onset of collapse limit state).

The following describes, a fully probabilistic method for the assessment of the structural response developed by Jalayer et al. ([3,4]). This method calibrates the CF based on the probability distribution for the variable that describes the global performance of the structure, accounting for the uncertainties involved in the analysis of an existing structure. The uncertainties related to seismic motion were not taken into account in this work in order to use the typical analysis tools for the professional engineers: the static *push-over* and the *capacity spectrum method* [5] (Appendix C).

2.   Confidence Factor and Structural Reliability

As mentioned in the precedent section, in a previous work by Jalayer et al., 2008 [4], here briefly presented and discussed, the authors have strived to quantify and to update both the modeling uncertainties and the structural

reliability for a case-study existing RC building, given the state of knowledge about the existing structure and given a specific level of seismic intensity, inside a Bayesian probabilistic framework. The focus of the study is on the uncertain parameters that are specific to an existing building as opposed to a building of new construction; thus, the uncertainties in the seismic action and the modeling uncertainties in the component capacities (e.g., the modeling uncertainty in determining the ultimate rotation in a section) were not taken into account.

The characterization of uncertainties in this framework is preformed in two levels. In the first level, prior probability distributions for the uncertain modeling parameters are constructed based on information available from original design documents and professional judgment. In the second level, the results of in-situ tests and inspections are implemented in the Bayesian framework in order to both update the prior distributions for the modeling parameters and also to update the distribution for structural reliability using simulation-based reliability methods. The Bayesian updating procedure employed allows for updating the probability distributions for both structural modeling parameters and the structural global response within the simulation routine. Moreover, it is general enough to allow for both consideration of various types of inspections ranging from carrot tests, pacometric tests to pseudo-dynamic health-monitoring tests and also consideration of the corresponding measurement errors.

The updating of structural reliability across increasing amount of test results makes the authors able to, (i) introduce a performance-based probabilistic definition of the confidence factor as the value that, once applied to the mean material properties, leads to a value for structural performance measure with a specified probability of being exceeded (e.g., 5%), (ii) evaluate the code-based recommendations regarding confidence factors and the corresponding knowledge levels. The methodology presented allows for characterizing structural modeling uncertainties specific to existing buildings using a rigorous probabilistic framework. The relevant information has been implemented in

this framework in order to update both the modeling uncertainties and the probabilistic performance assessments.

2.1.   The Case-Study Structure

As the case-study, an existing school building in the city of Avellino, Italy, is considered herein. Avellino is a city located in the Irpinia region, which is an historical and geographical region of central-southern of Italy. This region is notorious for the Irpinia Earthquake, that occurred on 23th of November 1980 and struck the central Campania and Basilicata. Characterized by a magnitude 6.9 on the Richter scale, with its epicenter in the town of Conza (AV), caused about 280,000 displaced persons, 8848 injured and 2914 deaths.

The Irpinia region was classified in the Italian seismic guidelines OPCM [6, 7] as seismic zone II. According to this classification, for this seismic zone a value of 0.25g is indicated for the maximum horizontal acceleration on the soil category A, with a probability of exceedance equal to 10% in 50 years.

The structure consists of three stories and a semi-embedded story and its foundation lies on soil type B. For the structure in question, the original design notes and graphics have been gathered.

The building is constructed in the 1960's and it is designed for gravity loads only, as it is frequently encountered in the post second world war construction.

In Figure 2.1a, the tri-dimensional view of the structure is illustrated; it can be observed that the building is highly irregular both in plane and elevation. The main central frame in the structure is extracted and used as the structural model (Figure 2.1b).
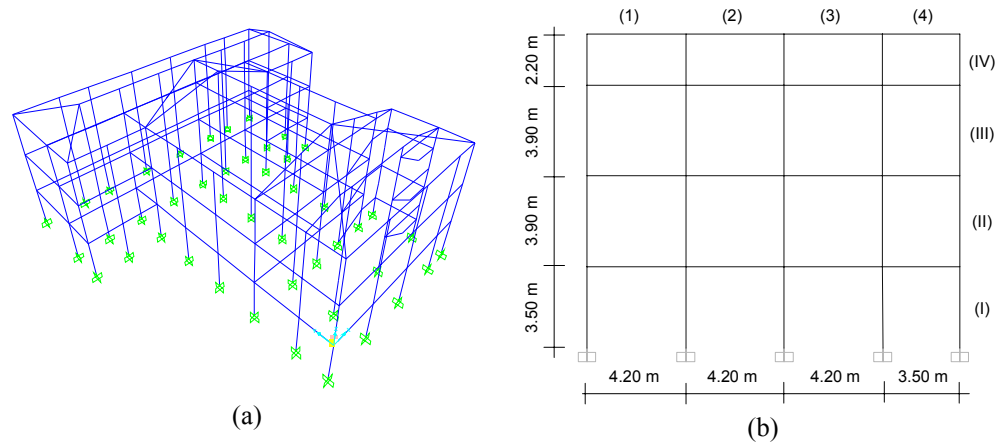
Figure 2.1: (a) The tri-dimensional view of the scholastic building (b) The central frame of the case-study building

The columns have rectangular sections with the following dimensions: first storey: 40x55 cm^2, second storey: 40x45 cm^2, third storey: 40x40 cm^2, and forth storey: 30x40 cm^2. The beams, also with rectangular section, have the following dimensions: 40x70 cm^2 at first and second floors, and 30x50 cm^2 for the ultimate two floors.

It can be inferred from the original design notes that the steel rebar is of the type Aq42 (nominal minimum yield resistance f_y = 2700 kg/cm^2) and the concrete has a minimum resistance equal to 180 kg/cm^2 (R.D.L. 2229, 1939 [8]).

The finite element model of the frame is constructed assuming that the non-linear behavior in the structure is concentrated in plastic hinges located at the element ends (Appendix A). Each beam or column element is modeled by coupling in series of an elastic element and two rigid-plastic elements (hinges). The stiffness of the rigid-plastic element is defined by its moment-rotation relation which is derived by analyzing the reinforced concrete section at the hinge location. In this study, the section analysis is based on the Mander-Priestly [9] constitutive relation for reinforced concrete, assuming that the

concrete is not confined[2], and the reinforcing steel behavior is elastic-perfectly-plastic.

The behavior of the plastic hinge is characterized by four phases, namely: rigid, cracked, post-yielding, and post-peak. In addition to flexural deformation, the yielding rotation takes into account also the shear deformation and the deformation related to bar-slip based on the code recommendations (OPCM [7]) (Appendix B). Moreover, the shear span used in the calculation of the plastic rotation is based on the code formulas. As it regards the post-peak behavior, it is assumed that the section resistance drops to zero, resulting in a tri-linear curve which is sketched in Figure 2.2.
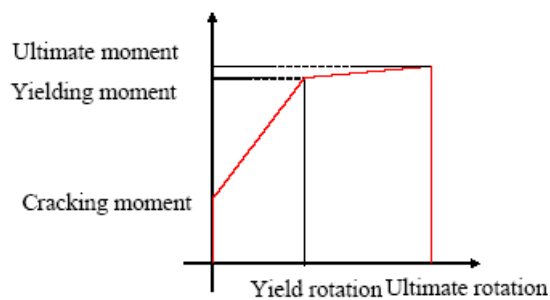
Figure 2.2. Schematic diagram of the typical tri-linear behavior characterizing the rigid-plastic hinge.

Moreover Table 2.1 demonstrates the actual test results available for the case study structure which consist of (non-destructive) ultrasonic results (6 data per floor), (destructive) carrot tests (2 data per floor) for determining the concrete resistance and the tension test for reinforcing steel (1 data).

---

[2] For a building that is not designed according to seismic provisions, it is unlikely the number of stirrups inside and outside the section are sufficient to assure that the concrete is confined everywhere inside the stirrups.

Table 2.1.Test results available for the structure

Test	# data	Type	Standard Error
Carrot test Basement	2	destructive	0.150
Carrot test Ground floor	2	destructive	0.150
Carrot test Fisrt floor	2	destructive	0.150
Ultrasonic test Basement	6	non-destructive	0.335
Ultrasonic test Ground floor	6	non-destructive	0.335
Ultrasonic test First floor	6	non-destructive	0.335
Tension test Reinforcing steel	1	destructive	0.080

It should be noted that the standard error assigned to the ultrasonic tests is larger than that assigned to the carrot tests to take into account the fact that the ultrasonic results are calibrated (using regression analysis) with respect to the carrot tests.

2.2.   Evaluation of Robust Reliability

In the presence of structural modeling uncertainty, instead of a unique structural model, a set of plausible structural models can be identified. A robust assessment of structural reliability takes into account a whole set of possible structural models that are weighted by their corresponding plausibility. A Bayesian updating framework can be implemented in order to update both the structural modeling properties and the reliability based on test results [10]. Nevertheless, model updating is not an end by itself, and it is normally desirable to also improve the predictions of structural reliability.

Let the vector $\underline{\theta}$ denote the set of uncertain model parameters. Let D denote some test data and consider that the set of possible structural models can be defined by M to specify (both the structural and the probabilistic) modeling assumptions used in the analysis. The Bayesian framework used provides a rigorous method for updating the plausibility of each of the models in representing the structure. The plausibility of a model is quantified by a

probability distribution over the vector of model parameters $\underline{\theta}=[\theta_1,...,\theta_n]$ that define a model within the set of possible models. The updated probability distribution can be defined using the Bayes Theorem [11]:

$$p_D(\underline{\theta}) = p(\underline{\theta}|D,M) = \frac{p(D|\underline{\theta},M)}{p(D|M)} p(\underline{\theta}|M)$$ Eq.2.1

where $p(\underline{\theta}|M)$ is the prior probability distribution for $\underline{\theta}$ specified by M, $p(D|M)$ is the probability distribution for data D specified by M, and $p(D|\underline{\theta},M)$ is the (updated) probability distribution for observed data D given the vector of parameters $\underline{\theta}$ specified by M.

Updated response predictions can be made implementing data D through $p_D(\underline{\theta})$ given by equation 2.1. For example, if the probability of a failure event F based on modeling parameters $\underline{\theta}$ is denoted by $P(F|D,M)$, the robust failure probability can be calculated from the following integral defined over the whole domain of $\underline{\theta}$:

$$P(F|D,M) = \int P(F|\underline{\theta},M) p(\underline{\theta}|D,M) d\underline{\theta}$$ Eq.2.2

where $P(F|\underline{\theta},M)$ is the failure probability for the structural model defined by $\underline{\theta}$. In particular, given a specific representation of ground motion, $P(F|\underline{\theta},M)$ reduces to a deterministic index function $I_F(\underline{\theta},M)$. This index function is equal to one in the event of failure and equal to zero otherwise:

$$P(F|D,M) = \int I_F(\underline{\theta},M) \frac{p(D|\underline{\theta},M)}{p(D|M)} p(\underline{\theta}|M) d\underline{\theta}$$ Eq.2.3

2.3.   The Algorithm for Calculating the Structural Reliability

The cited paper utilizes a Markov Chain Monte Carlo (MCMC) simulation method to evaluate the robust reliability in equation 2.3 [11]. The MCMC method employs the Metropolis-Hastings (MH) algorithm [12] in order to generate samples as a Markov chain sequence which are used later to estimate the robust reliability by statistical averaging. The Metropolis-Hastings algorithm is normally used to generate samples according to an arbitrary PDF when the target PDF is known only up to a scaling constant.

2.4.   Calculating the Failure Probability using Subset Simulation

In order to calculate the small failure probabilities encountered in the seismic reliability problem, the failure probability can be calculated using a simulation method known as Subset Simulation [13], in which the failure region is modeled as the last element in a sequence of embedded failure regions $F = F_m \subset F_{m-1} \subset ... \subset F_1$. Therefore, the failure probability can be derived as the following:

$$P(F) = P(F_1) \prod_{i=1}^{m-1} P\left(F_{i+1} \middle| F_i\right)$$

Eq.2.4

where, F_1 is the first element in the failure sequence (i.e., largest failure region) and $F = F_m$ is the target failure region and the last element in the failure sequence. The first term in the second member of equation 2.4 $P(F_1)$ can be calculated using standard Monte Carlo simulation, generating samples from the original PDF for the modeling parameters:

$$P(F_1) = \int I_{F_1}(\underline{\theta}) p(\underline{\theta}) d\underline{\theta}$$

Eq.2.5

And the intermediate failure probabilities $P(F_{i+1}|F_i)$ is equal to:

$$P\left(F_{i+1}|F_i\right) = \int I_{F_{i+1}|F_i}\left(\underline{\theta}\right)p\left(\underline{\theta}|F_i\right)d\underline{\theta} \qquad\qquad \text{Eq.2.6}$$

Again the MH algorithm can be used to generate samples as the states of a Markov chain with target distribution equal to the conditional PDF $p(\underline{\theta}|F_i)$ for each intermediate failure region (see [14] for details on how to choose the candidate PDF). The subset simulation is shown to be especially efficient for modeling rare failure events.

2.5.   Structural Performance and Conventional Collapse

The failure event F can be defined as when structural demand, denoted as $D(\underline{\theta})$, exceeds structural capacity $C(\underline{\theta})$: $F=\{\underline{\theta}: D(\underline{\theta}) > C(\underline{\theta})\}$.

Assuming scalar demand and capacity, the (scalar) demand to capacity ratio can be defined as $Y(\underline{\theta})=D(\underline{\theta})/C(\underline{\theta})$ [15]. Therefore, the failure region F can be defined as $F=\{\underline{\theta}: Y(\underline{\theta})=1\}$ and the sequence of embedded intermediate failure regions can be generated as $F=\{\underline{\theta}: Y(\underline{\theta})>.y_i\}$ where $0<y_1<\dots<y_m=1$.

In the study, the structural capacity is obtained using the pushover analysis as the global displacement at which the first element is loses its load bearing capacity (i.e., 3/4th of the of ultimate chord rotation in the member).

The structural demand is defined as the global displacement corresponding to the intersection of the capacity curve for the equivalent SDOF system and the corresponding code-based seismic response spectra for the seismicity and the soil characteristics at the site of the project.

It should be mentioned that the code-based seismic response spectra can be applied to represent the seismic action for both the existing structures and the new construction; therefore, the uncertainties in representation of the seismic action are not taken into account herein.

2.6. Characterization of Uncertainties

As it is mentioned in the previous section, in a general case the vector of parameters $\underline{\theta}$ includes all the uncertain parameters in the problem such as the uncertainty in the seismic action, the uncertainty in the property of the materials and the uncertainty involved in the structural detailing.

The work discussed here focuses on the uncertainty in structural modeling parameters for resisting elements, since it is characterized differently in existing structures and new construction. Hence, the seismic assessment is performed conditioned on a given ground motion intensity level.

The structural modeling uncertainty is directly related to the quantity (and the quality) of information that is available on the structure.

In the work of Jalayer et all. 2008 [4], two different sources of uncertainty are considered: (1) uncertainty in the mechanical properties of materials used in construction (2) the reinforcement details that affect the component capacity in terms of moment-rotation relation.

2.6.1. Materials

Uncertainties related to the properties of materials, particularly the value of the yield stress of steel and that of compressive strength of concrete were considered in relation to each floor of the analyzed structure. The probability distributions were then constructed, before in-situ testing. In order to characterize the prior probability distributions, the results of statistical studies conducted on the variability of mechanical properties in the existing buildings in 1960's ([16,17]) were used.

In the following table the characteristic statistical parameters related to the prior distributions of material properties are illustrated.

Table 2.2. Probabilistic characterization of the mechanical property of RC.

Variable	Distribution	Mean [kg/cm^2]	COV
f_y	LogNormal	165	0.15
f_c	LogNormal	3200	0.08

2.6.2. Structural Details

The uncertainty in structural details can be both due to limited information about the design of a specific structure and/or local construction practice and also due to low quality control in construction (also known in the engineering jargon as *structural defects,* not uncommon in structures built after the second world war in Italy). As uncertainties in structural detailing, those related to the percentage of rebar present in the element, rebar diameter (e.g., different from that specified in the original design notes), the anchorage quality and the cover thickness are considered.

Table 2.3. Probabilistic characterization of the structural detailing parameters.

Defects	Possibilities	Probabilities	Type
Insufficient anchorage (Beams)	sufficient (100% effective)	0.900	Systematic over floor
	absent (50% effective)	0.100	
Error in diameter (Columns)	$\phi 16$	0.950	Systematic over floor and section type
	$\phi 14$	0.050	
Superposition (Columns)	100% of the area effective	0.950	Systematic over floor
	75% of the area effective	0.050	
Errors in configuration (columns)	More plausible configuration	0.950	Systematic over floor and section type
	Less plausible configuration	0.050	
Absence of a bar (beams)	Absence of a bar	0.100	Systematic over floor and section type
	Presence of a bar	0.900	
Conceret cover	2 cm	0.125	Systematic over floor
	3 cm	0.750	
	4 cm	0.125	

The uncertainties in structural detailing are modeled as discrete uncertain variables that can assume a range of possible values with corresponding

plausibilities/weights. In the absence of test results and in situ inspections, the a priori plausibility of each possible value is assigned qualitatively based on engineering consensus, judgment and experience.

It should be mentioned that once the test results are available on the quantity in question, they can be used applying the Bayesian methodology described in the previous sections to update the plausibility of each possible value for the corresponding discrete uncertain variable.

As it regards the correlation between different uncertain parameters, a simplified model of correlation is constructed by classifying different sets of correlated uncertain parameters within groups that are not cross-correlated [14].

2.7.   A Proposal for a Probabilistic Definition of Confidence Factor

Using the results of this work the authors have proposed a probability-based definition of the confidence factor.

In Figure 2.3 the histograms and the lognormal curves fitted for the demand to capacity ratio for three increasing levels of data considered in the work are shown. The first level corresponds to the prior lognormal probability distribution for the demand to capacity ratio before taking into consideration the test results. The second level corresponds to the updated distribution after considering the carrot test results for concrete and the tension test result for reinforcing steel. The last level illustrates the updated distribution for structural performance variable after considering also the ultrasonic test results for concrete.

For all three values of confidence level suggested by the code (i.e., CF=1,1.2,1.35) the corresponding demand to capacity ratios for the structure is calculated. The resulting three values for demand to capacity ratio are marked on the curves illustrated in Figure 2.3. Note that the failure threshold is also marked at the value of $\ln Y = \ln 1.0 = 0.0$.
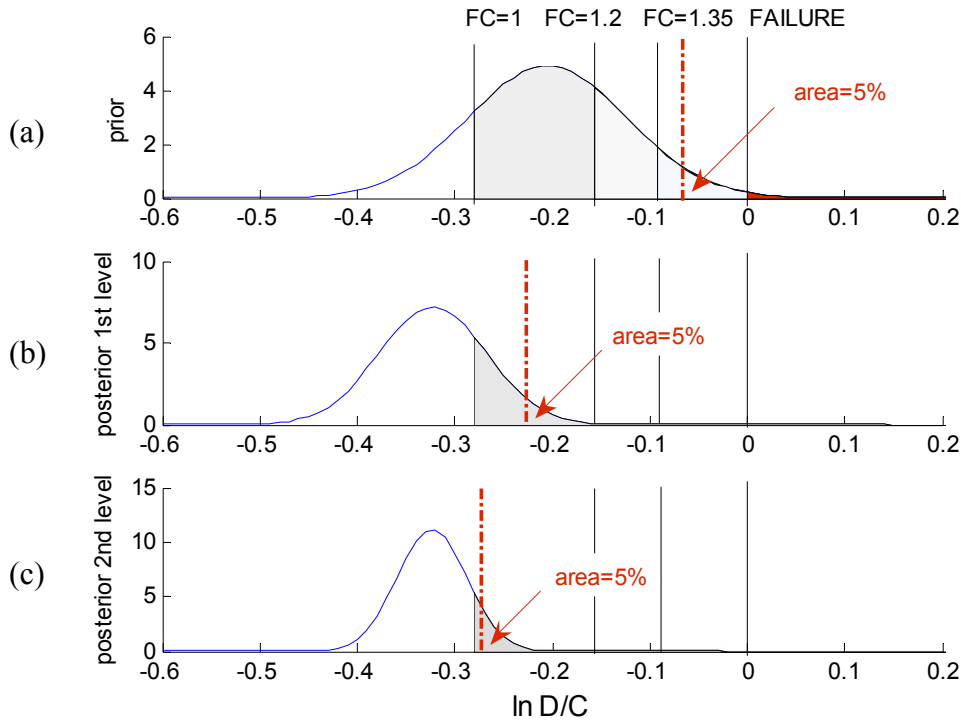
Figure 2.3: Distribution of the demand to capacity ratio when both the uncertainty in the material property and in the structural defects are taken into account: (a) The prior lognormal PDF fit to the demand to capacity ratio before test results are being considered, (b) The updated lognormal PDF fit to the demand to capacity ratio after implementing the destructive test results, (c) The updated lognormal PDF fit to the data after the non-destructive test results are also implemented. The probability of failure is indicated by the area under the curve for demand to capacity ratios great than unity (0 on the logarithmic scale). The demand to capacity ratios corresponding to the code-specified values for the confidence factor are also marked on the figure.

The authors propose the estimation of the confidence factors as the value of CF that leads to a demand to capacity ratio with, for example, say 5% probability of exceedance. It can be observed that, in the prior stage (Figure 2.3a), the confidence factor corresponding to a value of demand to capacity ration with 5% probability of exceedance is larger than (but close to) CF=1.35. In Figure 2.3b, after the distribution for demand to capacity ratio is updated

after the destructive test results are considered, the demand to capacity ratio with 5% probability of exceedance corresponds to a confidence factor between CF=1.0 and CF=1.20. In Figure 2.3c, after the non-destructive test results are also considered, the demand to capacity ratio with 5% probability of exceedance corresponds to a confidence factor slightly greater than 1.0 which corresponds to the code-recommended value for the most complete level of knowledge.

3.   Conclusions

In this chapter some interesting works which have addressed the open issues in the current code-based approach, obviously from different points of view, have been briefly discussed.

The present thesis work deals with the uncertainty in the assessment of existing RC buildings, analyzing the problem from the same point of view highlighted in the recent work of Jalayer et all, 2008 [4]. As in this chapter briefly presented and discussed, in this work the authors demonstrated that uncertainties in structural detailing can affect the structural reliability significantly. It was shown that considering the uncertainty in structural detailing parameters increases both the mean and standard deviation of the demand to capacity ratio for the structure. This finding, in the context of the code-based approach in which the confidence factors are applied to the mean material strength values only, emphasizes on the importance of calibrating them with respect to the global structural performance.

In order to characterize the uncertainties in the structural detailing parameters, prior probability mass functions are constructed based on all the information available excluding the test results. It was shown how a qualitative database of possible detailing parameters can be created by identifying the set of possibilities for each parameter and the corresponding plausibilities. This type of database, in lieu of test results and complete information about the structure, can be constructed based on both the qualitative judgment of the profession and also based on the construction practice at the time when the structure in question has been built.

The Bayesian updating algorithm implemented is general with respect to the type of in-situ test (e.g., also pseudo-dynamic test results can be implemented) performed and the standard error associated with it. Moreover, it allows for implementing the test data gradually and across increasing levels of knowledge with the goal of studying the changes in the updated representation of the structural performance. It was also demonstrated that the quality and quantity of the acquired test data significantly affects the updated (robust) reliability of the structure. It can observed that even a very small number of tests (e.g., only one in the case of steel resistance) can affect the distribution of demand to capacity ratio.

Moreover, defining the confidence factor as the value which leads to a demand to capacity ratio with a specified probability of being exceeded (e.g., 5%) in contrast to the code-specified values that are applied to mean values for material strength, has the advantage of measuring these factors in terms of the eventual structural performance instead of a modeling parameter. Nevertheless, for the case-study structure, the confidence factors, associated to each increasing level of knowledge, calculated based on the updated distribution of structural performance variable were consistent with the code-specified values.

4. References

[1] Monti G., Alessandri S., "Confidence factors for concrete and steel strength", *Convegno RELUIS "Valutazione e riduzione della vulnerabilità sismica di edifici esistenti in cemento armato"*, Roma 29-30 maggio 2008.

[2] Franchin P., Pinto P. E., Pathmanathan R., "Confidence in confidence factor", *Convegno Finale RELUIS – REte Laboratori Universitari Ingegneria Sismica, Napoli, Italia, 1-3aprile 2009.*

[3] Jalayer F., Iervolino I., Manfredi G., "Influenza dei parametri di modellazione e dell'incertezza associata nella valutazione sismica di edifici esistenti in cemento armato", *Proceedings XII Convegno ANIDIS*, Giugno 2007.

[4] Jalayer F., Iervolino I., Manfredi G., "Structural modeling uncertainties and their influence on seismic assessment of existing RC structures", *submitted to Structural Safety*, 2008.

[5] Fajfar, P. "Capacity spectrum method based on inelastic demand spectra", *Earthquake Engineering and Structural Dynamics*; 28:979–93, 1999.

[6] Ordinanza del Presidente del Consiglio dei Ministri (OPCM) n. 3431, Ulteriori modifiche ed integrazioni all'ordinanza del Presidente del Consiglio dei Ministri n. 3274 del 20 marzo 2003. *Gazzetta Ufficiale della Repubblica Italiana* n. 107 del 10-5-2005 (Suppl. Ordinario n.85), 2005.

[7] Ordinanza del Presidente del Consiglio dei Ministri (OPCM) n. 3519. Criteri per l'individuazione delle zone sismiche e la formazione e l'aggiornamento degli elenchi delle medesime zone. *Gazzetta Ufficiale della Repubblica Italiana* n. 108, 2006.

[8] Regio Decreto Legge (R.D.L.) 2229. *Norme per l'esecuzione delle opere in conglomerato cementizio semplice o armato*, 1939.

[9] Mander J.B., Priestley M.J.N., Park R., Theoretical stress-strain model for confined concrete, *Journal of Structural Engineering*, vol.114, n.8, August 1988, pp.1804-1826.

[10] Beck, J.L., Katafigiotis, L.S. "Updating models and their uncertainties. I: Bayesian statistical framework", *Journal of Engineering Mechanics*, Vol. 124, no. 4, April 1998.

[11] Beck J.L., Au S.K., "Bayesian updating of structural models and reliability using Markov chain Monte Carlo simulation", *Journal of Engineering Mechanics*, Vol.128, no. 4, April 2002.

[12] Hastings, W.K. Monte-Carlo sampling methods using Markov Chains and their applications. *Biometrika*; 57(1), 97-109, 1970.

[13] Au S.K., Beck J.L. First excursion probabilities for linear systems by very efficient importance sampling. *Probabilistic Engineering Mechanics*; Vol. 16:193-207, 2001.

[14] Au, S.K., Beck, J.L. "Subset simulation and its application to probabilistic seismic performance assessment", *Journal of Engineering Mechanics*, Vol. 16, no. 4, 2003.

[15] Jalayer, F., Franchin, P. and Pinto, P.E. "A Scalar Decision Variable for Seismic Reliability Analysis of RC Frames", *Earthquake Engineering and Structural Dynamics Special Issue on Structural Reliability*, Vol. 36 (13): 2050-2079, 2007a.

[16] Verderame, G.M., Manfredi, G., Frunzio G., "Le proprietà meccaniche dei calcestruzzi impiegati nelle strutture in cemento armato realizzate negli anni '60", *X Congresso Nazionale "L'ingegneria Sismica in Italia"*, Potenza-Matera 9-13 settembre 2001a.

[17] Verderame, G.M., Stella, A., Cosenza, E., "Le proprietà meccaniche degli acciai impiegati nelle strutture in cemento armato realizzate negli anni '60", *X Convegno Nazionale "L'Ingegneria Sismica in Italia"*, Potenza e Matera 9-13 Settembre 2001b.

Chapter III

Uncertainty in the
Representation of Ground Motion

1.   Introduction

The uncertainty in the representation of ground motion is strictly related to the selection of the ground motion records to be used in the structural assessment employing dynamic analysis.

The seismic input selection represents one of the main issues in assessing the seismic response of a structure through numerical dynamic analysis. In some cases the records are selected to have response spectra that approximate the uniform hazard spectrum or other "design" response spectrum (e.g., [1, 2]). In general, it is reasonable to choose ground motion records whose magnitude, distance, site conditions and mechanisms of fault are representative for the seismic hazard at the site of the structure under consideration. This choice may be guided by the disaggregation of the seismic hazard [3] for the site of interest. However, once the set of records is chosen, there are several techniques to evaluate the structural seismic response [4].

In the framework of PBEE (chapter II), the choice of the ground motions may be affected by the interface variable used to measure the intensity of ground motion, known as the intensity measure *IM*.

According to criteria proposed by Luco and Cornell [5] a preferred *IM* is both "sufficient" with respect to the ground motion characteristics and also "efficient". A sufficient *IM* renders the structural response conditionally statistically independent of other ground motion characteristics such as event magnitude, while an efficient *IM* predicts the structural response with (relatively) small record-to-record variability.

Theoretically, careful record selection is not essential if the *IM* is demonstrated to be sufficient with respect to ground motion characteristics [6]. It has to be recalled that sufficiency of a specific *IM* depends on the structure, the structural response parameters and the ground motion characteristics. Ground motion parameters such as site amplification and/or directivity may prove particularly troublesome because they may imply strong sensitivity of spectral shape to certain ground motion parameters [7].

A useful strategy, in cases where the adopted scalar intensity measure IM_1 does not prove to be sufficient, is to introduce an additional intensity measure, IM_2. That is, one can adopt a vector-valued intensity measure $\mathbf{IM}=[IM_1,IM_2]$, consisting of two scalar *IM*'s, in order to render a more complete description of the ground motion characteristics [8].

2.   Ground Motion Record Selection

In this chapter, an approximate method based on linear regression is used in order to establish possible correlation between the structural response conditional on the primary intensity measure IM_1 and the secondary intensity measure IM_2. Moreover, a weighting scheme based on seismic hazard disaggregation is used, in the framework of the scalar intensity measure IM_1, in order to adjust the structural response for possible correlations with a candidate secondary intensity measure. This weighting scheme can be implemented in non-linear dynamic analysis procedure both for a wide range of ground motion intensities and also for a limited range of ground motion intensities.

The efficiency of the weighting scheme is evaluated in terms of seismic risk which is represented herein by the mean annual frequency (MAF) of exceeding the critical component demand to capacity ratio. The seismic risk curves are

obtained related to the adoption of both scalar and vector-valued intensity measures.

The chapter begins by an overview of the procedure for probabilistic performance assessment of buildings based on both scalar and vector ground motion intensity measures. Then the structural model chosen as the case-study and the ground motion record selections used for non-linear dynamic analysis are presented. In subsequent sections the *IM*'s studied in this work for predicting structural response and the structural engineering parameter used to measure the global performance of the structure are introduced. It is demonstrated how site-specific seismic hazard disaggregation can be used in order to obtain the conditional probability distribution for the secondary *IM* given the primary *IM*. Moreover, the application of the so-called residual-residual plots in establishing sufficiency of the adopted *IM* is discussed.

Distinguished by the amount of structural analysis required, two alternative non-linear dynamic analysis procedures, namely the cloud and the stripe method are introduced. The weighted cloud and the weighted stripes methods are then introduced as analysis procedures which manipulate the structural response to the selected ground motion records by employing the information provided from the seismic hazard analysis. Finally, the mean annual frequency of exceeding a global structural performance variable is used in order to benchmark the candidate intensity measures for the case-study structure.

3.   Probabilistic Assessment based on Non-Linear Dynamic Analysis

As discussed in chapter II, a probabilistic performance-based criterion for seismic assessment of existing structures can be written as:

$$\lambda_{DM} \leq P_0 \qquad\qquad\qquad\qquad \text{Eq.3.1}$$

where λ_{DM} refers to the MAF of exceeding a specified damage level[3] and P_0 is the allowable probability threshold for the assessment[4].

In order to calculate λ_{DM} using non-linear time-history analyses, it is common to use an intermediate parameter known as the *IM* in order to relate the characteristics ground motion record to the structural performance. The annual rate of exceeding a specified limit state can be expanded, using the principles of probability theory, with respect to the adopted (scalar) *IM* in the following:

$$\lambda_{DM}(y) = \int P_{DM|IM}(DM > y|x)|d\lambda_{IM}(x)| \qquad \text{Eq.3.2}$$

The first term in the integrand $P_{DM|IM}(DM > y|x)$ is the conditional probability of exceeding the damage threshold *y* for a given value of the *IM=x*. This term is also known as the structural *fragility*. The second term in the integrand is the absolute value of the derivative of the annual rate of exceeding *IM=x*; this second term is known as the *hazard* for the adopted *IM*. Ideally, the hazard function for the adopted *IM* is obtained from the results of site-specific probabilistic seismic hazard analysis (PSHA, see [9]).

The non-linear dynamic analysis procedures based on a limited suite of ground motion records can be used to estimate the fragility term in the integrand in equation 3.2. Depending on the amount of structural analysis and also on the range of limit states for which the performance assessment is done, two alternative non-linear dynamic analysis procedures are considered in this work, the *cloud method* and the *stripes method* [10, 4, 11].

---

[3] It is desirable to express the performance objectives in terms of life-cycle cost [9]. However, the focus of this work is on ground motion record selection for the purpose of estimating non-linear structural response. Therefore, the performance objective is hereby stated in terms of a structural damage index instead of economic indices.

[4] Note that in equation 3.1 it has been assumed that the numerical value for rate of exceedance is close to that of the probability of exceedance; this is true for small values of the exceedance probability representing very rare events.

The cloud method employs the linear least squares scheme to the specified *DM* based on non-linear structural response (*cloud response*) for a suite of ground motion records (un-scaled) in order to estimate the conditional mean and standard deviation of *DM* given *IM*. A linear relationship (determined using regression) between the logarithms of the two variables provides a reasonable estimate of the mean value of the logarithm of *DM*. Moreover, by assuming that the errors of the least square estimate are independent and identically distributed (i.i.d.), and assuming a Gaussian distribution for the logarithm of *DM* given *IM)*, the $P_{DM|IM}(DM > y|x)$ can be estimated using the Complementary Cumulative Distribution Function (CCDF):

$$P_{DM|IM}(DM > y|x) = G_{DM|IM}(y|x) = 1 - \Phi\left(\frac{\ln y - \eta(\ln y|x)}{\sigma(\ln y|x)}\right) \qquad \text{Eq.3.3}$$

where $\eta(\ln y|x)$ and $\sigma(\ln y|x)$ are the conditional mean and standard deviation of the logarithm of *DM* given a specific *IM* level respectively.

Alternatively, the stripes method provides the non-linear structural response parameters for the suite of records that are scaled to successively increasing *IM* levels: this is referred to as the *stripe response*. Subsequently, the statistical properties of the stripe responses for various *IM* levels, calculated based on the response to the suite of records, can be employed to obtain the probability of exceeding a specified damage level.

In the case where a vector-valued **IM**=[*IM$_1$,IM$_2$*] consisting of two scalar *IM*'s is adopted, the fragility term in equation 3.2 for the annual rate of exceeding *DM=y* can be expanded with respect to *IM$_2$* and re-arranged as following:

$$\lambda_{DM}(y) = \iint P_{DM|IM_2,IM_1}(DM > y|x,z)f_{IM_2|IM_1}(z|x)\left|d\lambda_{IM_1}(x)\right| \qquad \text{Eq.3.4}$$

The first term in the integrand is the conditional probability of exceeding $DM=y$ given IM_1 and IM_2 and the second term is the conditional probability density function (PDF) for $IM_2=z$ given $IM_1=x$. Similar to the case regarding scalar *IM*, both cloud method and stripes method can be employed in order to perform probabilistic seismic risk assessments. In the context of cloud method, the two-variable linear least squares scheme can be used to estimate the statistical parameters for the damage measure conditional on both IM_1 and IM_2. Also in this case, by assuming that the errors of the multiple linear least square estimate are independent and identically distributed (i.i.d.), and assuming a Gaussian distribution for the logarithm of *DM* given IM_1 and IM_2, the $P_{DM|IM_1,IM_2}(DM>y|x,z)$ can be estimated using the Complementary Cumulative Distribution Function (CCDF):

$$P_{DM|IM_1,IM_2}(DM>y|x,z) =$$
$$= G_{DM|IM_1,IM_2}(y|x,z) = 1 - \Phi\left(\frac{\ln y - \eta(\ln y|x,z)}{\sigma(\ln y|x,z)}\right) \qquad \text{Eq.3.5}$$

where $\eta(\ln\ y|x,z)$ and $\sigma(\ln\ y|x,z)$ are the conditional mean and standard deviation of the logarithm of *DM* given $IM_1=x$ and $IM_2=z$. Alternatively, using the stripes methods, the simple linear least squares can be applied to the stripe response at various IM_1 level with IM_2 as the independent variable.

3.1.   The Intensity Measures for Predicting Structural Response

The *IM*s can be considered either as a scalar or a vector of parameters that are proxies for the ground motion potential with respect to structural response. In this chapter, both scalar and vector *IM*'s are studied.

As scalar *IM*'s, the peak ground acceleration (PGA) and the spectral acceleration at the first mode denoted as $S_a(T_1)$ are considered. As vector *IM*'s, the pairs consisting of PGA and magnitude M, $S_a(T_1)$ and the deviation from the ground motion prediction model, ε, are considered. Furthermore, the pair

consisting of $S_a(T_1)$ and the spectral acceleration at a period $T_2 \neq T_1$, $(S_a(T_2))$ is considered. In particular, as will be explained later, T_2 is the second period whose spectral acceleration is most efficient in predicting structural response.

PGA has been widely used as the ground motion *IM* in the past. Recently, $S_a(T_1)$ is considered and verified to be a more suitable choice of an *IM*, as it reflects the elastic response of a single degree of freedom (SDOF) system with a period equal to the first-mode period of the structure and hazard curves are also available for this *IM*. However, it is unable to reflect the effect of higher frequencies (higher modes in a structure with several degrees of freedom) or lower frequencies (severe non-linear behavior in the structural elements) or the near-source effects (a single low frequency pulse dominating the ground motion record).

Ideally, one should use a vector consisting of $S_a(T_1)$ and an *IM* related to the spectral shape, for example the ratio $R(T) = S_a(T)/ S_a(T_1)$ [12], where T is the second period whose spectral value is considered as important to the structural response. It has been also demonstrated that *epsilon* may act as a proxy for the spectral shape [8].

3.2.   The Structural Engineering Parameters

The structural engineering parameter used in this work, to measure the global performance of the structure subjected to seismic excitation, is the *critical demand to capacity ratio*.

It is desirable to express the performance objective in terms of a (scalar) system damage measure which reflects how far away the structure is from the threshold of the limit state [13], namely:

$$\lambda_{LS} = \lambda_{DV>1} \leq P_0 \qquad \text{Eq.3.6}$$

The decision variable can be defined as the ratio of system demand D to system capacity C_{LS}, (e.g., ratio of θ_{max} to θ_{CLS}) or it can be defined as a functional of component demand and capacities, which is equal to one at the

onset of failure. This latter formulation is the one adopted in this work. In this work the scalar system decision variable, denoted by Y, is defined as the demand to capacity ratio of the critical component, i.e., that component that brings the system closest to failure:

$$Y = \max_{l=1}^{N_{mech}} \min_{j=1}^{N_l} \frac{D_{jl}}{C_{jl}}$$

Eq.3.7

where N_{mech} is the number of considered potential failure mechanisms and N_l is the number of components taking part in the lth mechanism. This corresponds to the system reliability concept of *cut-set* [14], defined as any set of components whose joint failure, $Y_l = \min_{j=1}^{l} D_{jl}/C_{jl}$, implies the failure of the system, $Y = \max_{l=1}^{N_{mech}} Y_l$.

4.   The Case-Study Structure

The case study structure analyzed is the same considered in the previous chapter that is an existing RC school building in the city of Avellino.

In order to employ non-linear dynamic analysis both for a limited and a wide range of value of the *IM*, the finite element model of the central frame of the structure is constructed using the Open System for Earthquake Engineering Simulation (OpenSees) software. In particular the force-based *beam with hinges* model [15] has been employed assuming that the non-linear behavior in the structure is concentrated in plastic hinges located at the element ends (Appendix A). This type of element consists of three parts. Two hinges at the ends characterized as rigid plastic elements, and a linear-elastic region in the middle. The stiffness of the rigid-plastic element is defined by its moment-rotation relation which is derived by analyzing the reinforced concrete section at the hinge location. In this study, the section analysis is based on the Mander-Priestly [16] constitutive relation for reinforced concrete assuming that the concrete is not confined and the reinforcing steel behavior is elastic-plastic.

As mentioned in the previous chapter the behavior of the plastic hinge is characterized by four phases, namely: rigid phase, cracked phase, post-yielding phase and post-peak phase. In addition to flexural deformation, the yielding rotation takes into account also the shear deformation and the deformation related to bar slip based on the code recommendations [17] (Appendix B). Moreover, the shear span used in the calculation of the plastic rotation is based on the code formulas. As it regards the post-peak behavior, it is assumed that the section resistance drops to zero, resulting in a tri-linear curve.

The length of the two hinges at the ends is approximated by the semi-empirical formulas provided for the plastic hinge length in the Italian code [17] which take into account both the effect of shear and bar slip in the (post peak) ultimate phase of the section behavior. The plastic hinges take into account the superposition of both flexural and axial action. The axial action models, in parallel, the reinforcing steel as elastic-perfectly plastic and concrete as elastic-no tension. In order to model the flexural action in the hinges, the moment-curvature curves calculated for the plastic hinges described above are utilized. The structural damping is modeled based on the Rayleigh model and is assumed to be equal to 5% for the first two modes. The small amplitude period for the first two vibration modes are equal to 0.73 and 0.26 seconds respectively.

5. The Suites of Ground Motion Records and their Properties

Two different suites, respectively of 21 (*Sel_A*) and 20 (*Sel_B*) ground motion records, have been selected for this study. They are all main-shock recordings recorded on stiff soil (400 m/s < V_{s30} < 700 m/s) which is consistent with the soil-type for the site. The first suite of records has been chosen in order to cover a wide range of moment magnitude values; for the second suite of records the same goal has been pursued in terms of the deviation from the ground motion prediction model *epsilon*.

Epsilon is defined as the number of standard deviations by which an observed logarithmic spectral acceleration differs from the mean logarithmic spectral acceleration of a ground-motion prediction (attenuation) equation. The

equation corresponding to this definition is:

$$\varepsilon = \frac{\ln S_a(T) - \hat{\mu}_{\ln S_a(T)}}{\hat{\sigma}_{\ln S_a(T)}}$$ Eq.3.8

where $\ln S_a(T)$ is the natural logarithm of the spectral acceleration value of the record at a specified period T, and $\hat{\mu}_{\ln S_a(T)}$ and $\hat{\sigma}_{\ln S_a(T)}$ are the estimate mean and standard deviation as predicted by an attenuation equation. The definition of ε is valid for any ground motion prediction model, but the model of Sabetta and Pugliese [18] is the only one used in calculations here. It should be noted that epsilon is defined with respect to the unscaled record and will not change in value when the record is scaled.

4.1.   Record Selection A (Sel_A)

The first suite is based on Mediterranean events taken from European Strong-Motion Database or ESD[5] (17 recordings) and Pacific Earthquake Engineering Research Next Generation Attenuation of Ground Motions or PEER NGA[6] Database (4 recordings). The earthquake events have moment magnitude (M_w) between 5.3 and 7.2, and closest distances ranging between 7km and 30km. Table 3.1 illustrates the ground motion recordings, their M_w, the fault mechanism (FM), the velocity of propagations of the shear waves (Vs_{30}, symbol "?" indicates that the value is not available), epicentral distance (ED), fault distance (FD), peak ground acceleration (PGA), spectral acceleration at the first mode ($S_a(T_1)$) and ε values for each record.

---

[5] http://www.isesd.cv.ic.ac.uk/ESD/Database/Database.htm

[6] http://peer.berkeley.edu/nga/flatfile.html

Table 3.1. Selection A of ground motion records.

Record	M_w	FM	Vs_{30} [m/s]	ED [km]	FD [km]	PGA [g]	$S_a(T_1)$ [g]	ε
Basso Tirreno	6.0	oblique	?	18	16	0.15	0.17	-0.121
Valnerina	5.8	normal	?	23	21	0.04	0.03	-0.529
Campano Lucano	6.9	normal	529	16	13	0.16	0.31	-0.519
Preveza	5.4	thrust	?	28	7	0.14	0.10	-0.244
Umbria	5.6	normal	546	19	19	0.21	0.02	0.230
Lazio Abruzzo	5.9	normal	?	36	28	0.07	0.05	-0.219
Etolia	5.3	thrust	405	20	12	0.04	0.01	-0.518
Montenegro	5.4	thrust	399	18	?	0.07	0.09	-0.227
Kyllini	5.9	strike slip	490	14	11	0.15	0.15	-0.231
Duzce 1	7.2	oblique	662	26	13	0.13	0.18	-0.722
Umbria Marche	5.7	normal	400	32	28	0.04	0.05	-0.334
Potenza	5.8	strike slip	494	28	29	0.10	0.08	-0.003
Ano Liosia	6.0	normal	411	20	9	0.16	0.06	-0.308
Adana	6.3	strike slip	?	39	30	0.03	0.05	-0.749
South Iceland	6.5	strike slip	?	15	10	0.21	0.13	-0.344
Tithorea	5.9	normal	665	25	?	0.03	0.02	-0.639
Patras	5.6	strike slip	665	30	?	0.05	0.02	-0.184
Friuli Italy-01	6.5	reverse	425	20	21	0.35	0.35	0.168
Friuli, Italy-02	5.9	reverse	412	18	18	0.21	0.08	0.110
Fruili, Italy-03	5.5	reverse	412	20	21	0.11	0.21	0.034
Irpinia, Italy-01	6.9	normal	600	15	18	0.13	0.30	-0.466
(average)	6.0		501	23	18	0.12	0.12	-0.277

4.2.   Record Selection B (Sel_B)

The second suite is based on Mediterranean events all taken from the ESD. The earthquake events have moment magnitude between 5.9 and 7.2, and closest distances ranging between 0km and 71km. Table 3.2 illustrates the ground motion recordings. It has to be noted that epsilon values of record selection B are all included in a range of values between -1.1 and 0.07.

Table 3.2. Selection B of ground motion records.

Record	M_w	FM	Vs_{30} [m/s]	ED [km]	FD [km]	PGA [g]	$S_a(T_1)$ [g]	ε
Friuli	6.5	thrust	?	42	34	0.06	0.22	-0.015
Friuli	6.5	thrust	?	87	71	0.05	0.11	0.003
Campano Lucano	6.9	normal	472	48	33	0.11	0.25	-0.204
Campano Lucano	6.9	normal	529	16	13	0.16	0.31	-0.493
Kalamata	5.9	normal	486	10	0	0.22	0.48	-0.231
Kalamata	5.9	normal	399	11	0	0.24	0.48	-0.233
Umbria Marche	6.0	normal	546	11	1	0.52	0.56	-0.216
Umbria Marche	6.0	normal	450	38	27	0.09	0.17	0.062
South Iceland	6.5	strike slip	?	7	6	0.63	0.54	-0.288
Duzce 1	7.2	oblique	662	26	13	0.13	0.18	-0.893
Friuli	6.5	thrust	?	42	34	0.09	0.25	0.031
Friuli	6.5	thrust	?	87	71	0.07	0.12	-0.002
Camp. Lucano	6.9	normal	472	48	33	0.14	0.26	-0.187
Camp.Lucano	6.9	normal	529	16	13	0.18	0.31	-0.484
Kalamata	5.9	normal	486	10	0	0.30	0.63	-0.120
Kalamata	5.9	normal	399	11	0	0.27	0.51	-0.208
Umbria Marche	6.0	normal	546	11	1	0.46	0.64	-0.156
Umbria Marche	6.0	normal	450	38	27	0.10	0.18	0.065
South Iceland	6.5	strike slip	?	7	6	0.51	0.74	-0.154
Duzce 1	7.2	oblique	662	26	13	0.16	0.14	-1.004
(average)	6.4		506	30	20	0.22	0.35	-0.236

The acceleration spectra for the original (un-scaled) records for *Sel_A* and *Sel_B* are plotted in Figure 3.1a and 3.1b, together with the EC8 spectrum for the site of interest [19].

(a)

(b)
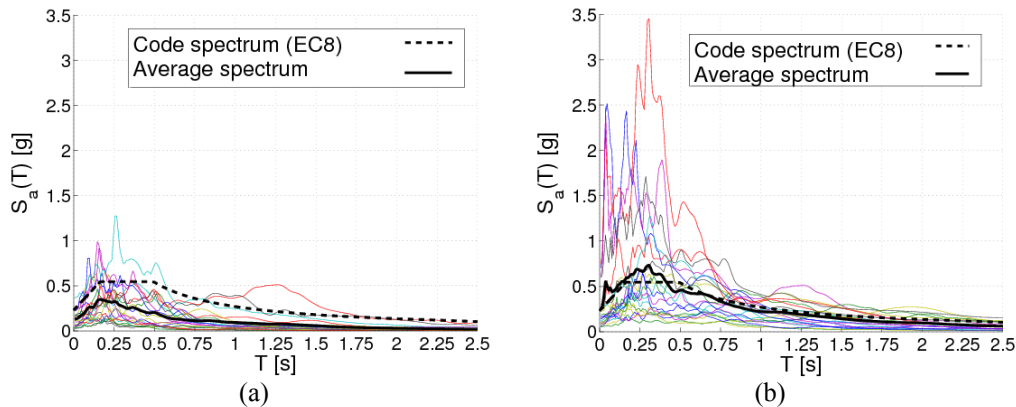
Figure 3.1. (a) Acceleration Spectra *Sel_A*. (b) Acceleration Spectra *Sel_B*.

6.   The Disaggregation of Seismic Hazard

In order to adopt a vector-valued **IM** for representing the ground motion intensity in the seismic assessment outlines in equation 3.4, it is necessary to obtain the conditional probability distribution for the second *IM* given the occurrence of the original *IM*.

This section employs a site-specific seismic hazard analysis performed based on the Italian seismic zonation (ZS9, aerial seismic zones, [20], Figure 3.2) inside a Bayesian framework for inference in order to obtain the conditional probability distribution for magnitude *m*, distance *r* and the deviation from the attenuation law ε given the original *IM* adopted.

As mentioned earlier the ground motion prediction relation adopted in this work is the Sabetta and Pugliese relation [18].

It should be noted that the website of INGV (Istituto Nazionale di Geofisica e Vulcanologia, Progetto DPC-INGV-S1, http://esse1.mi.ingv.it) provides the results of site-specific seismic hazard analysis based on the Italian seismic zonation, but only in terms of PGA. The results of the disaggregation in magnitude (and distance) are also available, but in terms of exceedance probability of the design value of PGA (for a given return period) rather than occurrence probability of a specific PGA value.
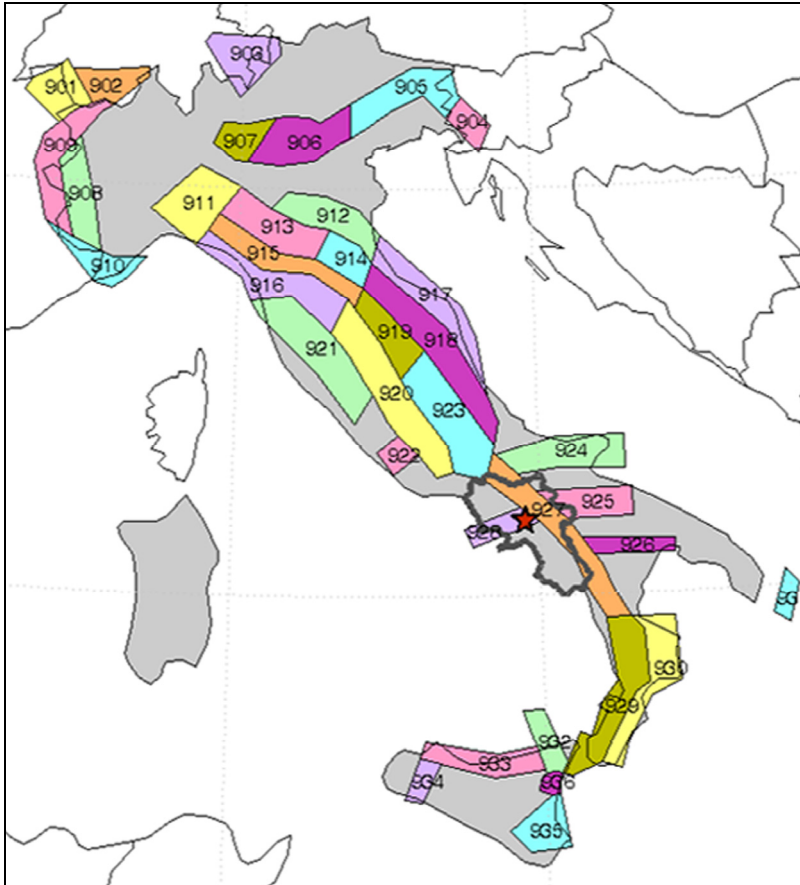
Figure 3.2. Seismogenic zonation ZS9; the different zones are identified by number; the
Campania region is highlighted by a gray polyline and the site of interest is indicated by a red
pentagram.

The seismic hazard can be disaggregated with respect, for example, to
magnitude using the Bayes theorem:

$$f(m|IM) = \frac{f(IM,m)}{\sum f(IM|m)f(m)} \qquad\qquad \text{Eq.3.9}$$

Supposing that the site of interest is surrounded by aerial seismic zones, and using the total probability theorem, the term $f(IM,m)$ can be further expanded with respect to the seismo-genetic areas surrounding the site and the distance r of the points within each area to the site of interest:

$$f(m|IM) = \frac{\sum_i \sum_R \sum_\varepsilon \alpha_i I(IM|m,r,\varepsilon) f(m) f(r) f(\varepsilon)}{p(IM)}$$ Eq.3.10

where α_i is the relative seismicity of seismic area A_i with respect to other seismic zones considered ($\alpha_i = \lambda_i / \Sigma\lambda$, where λ_i is the seismicity of zone i). The term $I(IM \mid m, r, \varepsilon)$ is an indicator function reflecting the fact that given the epsilon, distance and magnitude, the *IM* value is going to be known deterministically from the ground motion prediction relationship. That is $I(IM \mid m, r, \varepsilon)$ can assume only two values, namely, zero and unity. It should be noted that, given that an earthquake takes place in seismic zone A_i, it is assumed that it is equally likely to have its epicenter located anywhere inside the area. Therefore, the probability $f(r)$ of having an earthquake with its epicenter inside the areal increment dA, whose center is individuated by the distance r, can be calculated as dA/A where A is the total area of the seismic zone.

The probability density function (PDF) for the magnitude can be calculated from the Gutenberg-Richter truncated distribution:

$$f(m) = \frac{\beta \cdot e^{-\beta \cdot m}}{e^{-\beta \cdot m_l} - e^{-\beta \cdot m_u}}$$ Eq.3.11

where β is the Richter *b*-value times $\ln(10)$ and m_l and m_u are a lower and an upper bound magnitude, respectively.

Table 3.3 illustrates the seismicity λ, the Richter *b*-value and a lower and upper magnitude bound (m_l and m_u, respectively) for those ZS9 seismic zones surrounding the Campania region.

Table 3.3. Parameters of those ZS9 seismic zones surrounding the Campania region.

Zone	λ	b-value	m_l	m_u
920	0.0600	1.9600	4.7600	6.1400
922	0.3700	2.0000	4.7600	5.4500
923	0.1400	1.0500	4.7600	7.0600
924	0.1300	1.0400	4.7600	6.8300
925	0.1700	0.6700	4.7600	6.8300
926	0.1000	1.2800	4.7600	6.1400
927	0.4300	0.7400	4.7600	7.0600
928	0.2100	1.0400	4.7600	5.9100
929	0.1700	0.8200	4.7600	7.2900
930	0.1700	0.9800	4.7600	6.6000

It should be noted that the term $p(IM)$, in the denominator in equation 3.10 acts as a scaling constant on the nominator. Therefore, it can be calculated by calculating the denominator for an interval covering all possible m values and summing them up. This is because the resulting probability distribution needs to sum to one for all possible m values.

In order to disaggregate the seismic hazard with respect to the epsilon of the ground motion prediction relationship, the same as above, the Bayes theorem and the total probability theorem can be used in order to calculate:

$$f(\varepsilon|IM) = \frac{\sum_i \sum_M \sum_R \alpha_i I(IM|m,r,\varepsilon) f(m) f(r) f(\varepsilon)}{p(IM)} \qquad \text{Eq.3.12}$$

In a similar manner, as described above, the constant term $p(IM)$ in the denominator can be calculating by summing up the nominator in equation 3.12 for all possible values of epsilon. It should be noted that the expansion of the nominator in equation 3.12 is done assuming that the probability distribution for epsilon is independent of other ground motion parameters. It is also assumed that the relative seismicity of each seismic zone is independent of

other parameters. Moreover, it is assumed that the probability distribution for magnitude is the same for all the points within a given seismic area.

The conditional probability distributions of magnitude given peak ground acceleration and of epsilon of the prediction law given the spectral acceleration at first mode, have been obtained through the disaggregation of the seismic hazard for the site of the case study structure using the Bayesian framework here described.
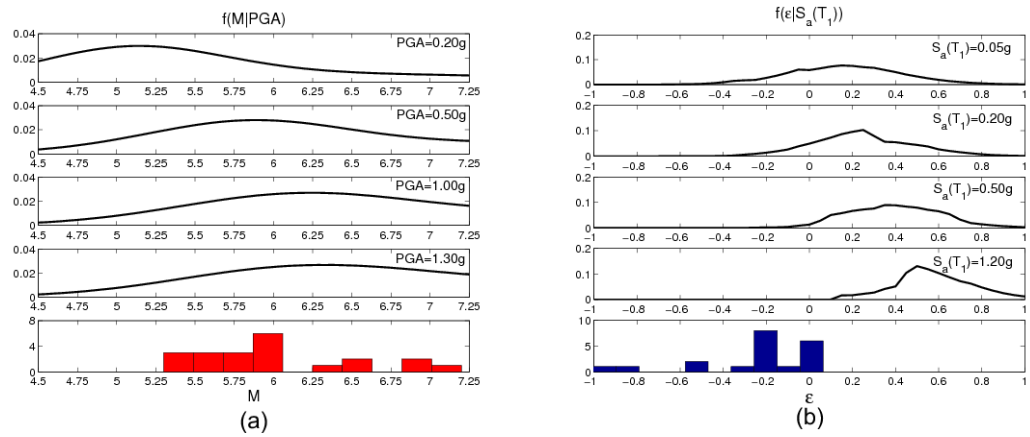
Figure 3.3. (a) Conditional probability distribution of M given some values of PGA and histogram of M values for *Sel_A*. (b) Conditional probability distribution of ε given some values of $S_a(T_1)$ and histogram of ε values for *Sel_B*.

The distributions $f(m|PGA)$ obtained for increasing levels of PGA are illustrated in Figure 3.3a; moreover, the histogram of the values of magnitude of the record selection A is also shown in the bottom of the figure. In the same manner, the distributions $f(\varepsilon|S_a(T_1))$ obtained for increasing levels of $S_a(T_1)$ are illustrated in Figure 3.3b; the histogram of the values of epsilon of the record selection B is also plotted in the bottom of the figure.

7.   Residual – Residual Plot

Linear regression is a useful statistical tool for investigating efficiency and sufficiency criteria for a candidate *IM* (see [21, 22]). The damage measure, Y,

can be predicated as a function of the candidate *IM*, e.g., PGA or $S_a(T_1)$, by performing linear regression (usually in the logarithmic scale). The efficiency of the candidate *IM* can be measured by the variability in the residuals of the regression analysis. In order to establish sufficiency, the effectiveness of ground motion characteristic variables as additional regression variables (i.e., in addition to IM_1) can be investigated. In other words, ground motion characteristic variables cause very little improvement in the regression prediction as regression variables in addition to a "sufficient" *IM*. This improvement may be judged by the reduction in the dispersion of the regression residuals and/or the statistical significance of the regression coefficients corresponding to the ground motion characteristic variables.

In this study, a simplified statistical approach based on regression is implemented for measuring the effectiveness of ground motion characteristics as additional regression variables. This method uses a graphical statistical tool known as the residual-residual plot. The main advantage of the residual-residual plots is that they offer visual means for judging the improvement caused by an additional regression variable.

Residual-residual plots are used in the applied statistics in order to investigate whether adding a second variable to the regression improves the predictions compared to predictions based on the regression on the first variable only. These plots are constructed by: a) performing regression of the dependent variable (e.g., the damage measure, Y) versus the (first) independent variable IM_1 (e.g., PGA or $S_a(T_1)$) b) performing regression of the second independent variable IM_2 (e.g., one of the ground motion characteristics) on also the first variable IM_1 c) plotting the residuals of the two regressions mentioned above against each other.

Roughly speaking, the two regressions on the first variable "eliminate" possible dependence of both the dependent variable (Y) and the second independent variable (one of the ground motion characteristics) on the first independent variable (PGA or $S_a(T_1)$). This facilitates investigating the potential dependence of the dependent variable on the second variable, by observing a (statistically) significant trend, in the residual-residual plot,

between the two sets of residuals explained above. In order to simplify future references to these residuals, the residuals of the regression of the dependent variable on the first variable are also called the "response residuals", and the residual of the regression of the second variable on the first variable are also called the "second-variable residuals". The possible trend between the two sets of residuals may be observed by performing linear regression of "response residuals" on "second variable residuals". The significance of the trend measured by both the variability in the residuals of such regression and/or testing the following hypothesis: *"The slope of the regression line is zero"* (i.e., test of hypothesis). The significance of the slope is usually measured by a quantity known as the *p-value*, assuming that the slope of the regression line is a random variable described by *Student's T-distribution* (see [23]). The hypothesis is rejected (i.e., the slope is non-zero) if the *p-value* is smaller than a certain (small) value, e.g., 0.01. If a two-variable regression of the response on both the first and the second independent variable is performed, it can be shown that the regression coefficient for the second variable is going to be the same as the slope of the (simple) regression of the "response residuals" on "second-variable residuals". Moreover, the results of the hypothesis test are going to be identical.

As it is mentioned above, one way to measure the significance of an additional regression variable is by measuring the amount of reduction it causes in the variability of data around the regression prediction. The variability of data around the regression line can be estimated by the (square) root of the mean of squares (RMS) of regression residuals, which is also referred to as the "sigma" of the regression. It should be noted that the "sigma" of the residual-residual regression is the same as that of the two-variable regression of response (dependent variable) on the two independent variables, i.e., the two approaches are equivalent. The smaller is the ratio of the sigma of the residual-residual regression (explained above) to the sigma of the regression of dependent variable on the first variable (or "original" regression for brevity), the more significant is the role of the second regression variable. In simple terms, an effective second regression variable is going to "explain" part of the

variability in the data that is not captured by the first regression variable. In the context of sufficiency, this means that if the sigma of the residual-residual regression is (significantly) smaller than the sigma of the original regression, this will also confirm (in addition to the test of hypothesis) that the *IM* is not sufficient with respect to the ground motion characteristic in question. It also indicates that the two regression variables together can provide a more "efficient" prediction of response, recalling that the efficiency criterion is based on the variability of response for a given value of the *IM*.

However, it should be noted that in this (simplified) approach the sufficiency of *IM* is questioned for one ground motion characteristic at the time. This would ignore possible interactions between the ground motion characteristics themselves. A more thorough approach consists of performing a multi-variable regression of the damage measure (the dependent variable) on IM_1 and all of the ground motion characteristics in question, and test the (joint) hypothesis of whether all the regression coefficients corresponding to the ground motion characteristics are simultaneously zero. Nevertheless, it is believed that the residual-residual plot approach is still effective in un-covering potential dependencies of response on ground motion characteristics.

8.   The Cloud Method

As described above, in order to estimate the statistical properties of the *cloud response*, the linear least squares scheme is applied on non-linear structural response for a suite of ground motion records (un-scaled) in order to estimate the conditional mean and standard deviation of *DM* given *IM*. This is equivalent to fitting a power-law curve of the form, $a \cdot IM^b$, to the cloud response. The conditional mean of *DM* given *IM* can be estimated with one of the two expression, equivalently:

$$\hat{\eta}_{DM|IM}(y|x) = a \cdot IM^b \Leftrightarrow \ln(\hat{\eta}_{DM|IM}(y|x)) = \ln(a) + b \cdot \ln(IM) \qquad \text{Eq.3.13}$$

where ln(*a*) and *b* are linear regression coefficients. The standard deviation of regression, measuring the second moment of data points around the predicted curve, can be used to estimate the conditional standard deviation of *DM* given *IM*.

$$\hat{\sigma}_{DM|IM} = \sqrt{\frac{\sum (\ln(y_i) - \ln(a \cdot x_i^b))^2}{n-2}}$$ Eq.3.14

where y_i and x_i are the damage measure and the corresponding *IM* for record number *i* within the cloud response set and *n* is the number of records.

It should be noted that the standard deviation of the regression is assumed to be constant with respect to *IM* over the range of *IM*'s in the cloud. This assumption may be un-conservative, in fact for example, for the spectral acceleration it has been proved in [24] that the standard deviation tends to increase for the larger values of spectral acceleration. This stresses the importance of performing linear regression locally, i.e., in a region of *IM* values of interest.

However, if the adopted *IM* is sufficient in relation to other ground motion characteristics, the cloud method is efficient and easy to apply.

In cases where the adopted *IM* is not sufficient, a vector-valued ***IM***=[*IM₁*,*IM₂*] consisting of two scalar *IM*'s could be adopted; the two-variable linear least squares scheme can be used to estimate the statistical parameters for the damage measure conditional on both IM_1 and IM_2.

8.1. The Weighted Cloud Method

If the "primary" adopted *IM* is not sufficient with respect to the ground motion characteristics, instead of adopting a vector-valued *IM*, using a weighted regression scheme [25] (Appendix D) may help in reducing the dependence of the residuals (of the "original" regression on *IM*) on ground motion characteristics. Shome [21] implemented the weighted regression

scheme in order to take into account the effect of the shape factor in predicting the response of special moment resisting frames.

It should be recalled that regression analysis works by minimizing the sum of the squared errors (residuals) between the observed critical demand to capacity ratio and the predicted critical demand to capacity ratio. The weighted regression scheme weights each error term (residual) proportional to its corresponding variance (Appendix D).

It can be argued that the variance of each error term and hence the corresponding weight is positively related to the following ratio:

$$w_i \propto \frac{f_{IM_2|IM_1}(z_i|x)_{disaggregation}}{f_{IM_2|IM_1}(z_i|x)_{data}} \qquad \text{Eq.3.15}$$

where $f_{IM_2|IM_1}(z|x)$ is the fraction of the ground motions with IM_2 equal to z for a given IM_1 equal to x. In this work, it is assumed that it is equally likely to observe IM_2 given IM_1 for each record in the set; therefore, $f_{IM_2|IM_1}(z_i|x)_{data}$ is going to be equal to $1/N_T$, where N_T is the total number of records. $f_{IM_2|IM_1}(z_i|x)_{disaggregation}$ is the fraction of records with IM_2 equal to z_i for a given IM_1 equal to x, estimated from the disaggregation of hazard.

Using the weights calculated as described above, the weighting scheme is implemented later in this work in order to adjust for the magnitude-dependence of the residuals of the "original" regression of lnY on PGA, and to adjust for dependence of the residuals of the original regression of lnY on $S_a(T_1)$, first with regard to the ground motion ε, and then with regard to spectral acceleration at a period $T_2 \neq T_1$, denoted as $S_a(T_2)$.

9.   The Multiple – Stripe Analysis

In the framework of the multiple-stripe methods, the suite of ground motion records are scaled to successively increasing values of the primary *IM*

parameter. The set of corresponding structural damage measures calculated for each primary *IM* value can be referred to as the *stripe response* for the *IM* level. The statistical properties of the stripe responses for various *IM* levels, can be evaluated based on the response to the suite of records, in order to estimate the fragility using equation 3.3.

In cases where the adopted *IM* is not sufficient, a vector-valued ***IM***=[IM_1,IM_2] consisting of two scalar *IM*'s could be adopted. In this case the linear regression analysis can be employed in order to investigate the dependence of the stripe response for each IM_1 level on the secondary IM_2 parameter. In contrast to the cloud method, the constant coefficients *a* and *b* and the standard deviation of the regression residuals, estimated from the observed prediction errors, are re-estimated at every IM_1 stripe and depend on the IM_1 value at each stripe.

9.1.   The Weighted Multiple-Stripe Analysis

Also in the framework of the multiple-stripe analysis, if the "primary" adopted *IM* is not sufficient with respect to the ground motion characteristics, instead of adopting a vector-valued ***IM***, a procedure similar to the one used in the weighted cloud method can be employed, in order to account for additional information available on the correlation between the adopted primary *IM* and a candidate secondary *IM* (e.g, the information extracted from seismic disaggregation). In fact, for a given suite of ground motion records, one could re-weight the stripe response in relation to the conditional probability distribution *f(IM_2|IM_1)* at each IM_1 level. This approximate method, which has been proposed by Shome and Cornell [21] and Jalayer [24], incorporates the available information about a secondary *IM* given that the IM_1 is known, in the framework of seismic assessments based on the scalar intensity measure IM_1.

The first and second central moment (i.e., expected value and variance) of the stripe response for each *IM* level can be calculated as described in the following. It can be recalled first that the sample average and the sample variance of the relevant damage measure Y can be calculated as:

$$\bar{Y} = E[Y] = \frac{1}{N_T} \sum_{i}^{N_T} Y_i \qquad \text{Eq.3.16}$$

$$s_Y^2 = E[Y^2] - (\bar{Y})^2 \qquad \text{Eq.3.17}$$

where $E[\cdot]$ denotes the expected value (mean) estimated by the sample average. The above equations can also be applied to the natural logarithm of the relevant damage measure for a given *IM* level, x:

$$\ln \hat{\eta}_{Y|IM}(x) \cong E[\ln Y | IM] = \frac{1}{N_T} \sum_{i}^{N_T} Y_i \qquad \text{Eq.3.18}$$

$$\beta_Y^2 = \hat{\sigma}_{\ln Y}^2 = E[\ln Y^2 | \text{IM}] - (E[\ln Y | \text{IM}])^2 \qquad \text{Eq.3.19}$$

where the (log of) median has been approximated by the sample average of the logarithm of the response. Nevertheless, for a lognormal variable, the mean of the logarithm is exactly equal to the logarithm of the median.

   Expanding the estimated median and the standard deviation (of the logarithm) with respect to IM_2, the mean of the logarithm of the stripe response can also be calculated as:

$$\ln \hat{\eta}_{Y|IM_1}(x) \cong E[\ln Y(x)] =$$

$$= \sum_{j=1}^{N_{IM_2}} E[\ln Y(x, z_j) | IM_1, IM_2]. \quad f_{IM_1|IM_2}(z_j | x) \qquad \text{Eq.3.20}$$

where $\hat{\eta}(\cdot)$ denotes the estimated median for the stripe response. For a selection consisting of N_T ground motion records the above expression can be expanded by dividing the chosen records into N_{IM_2} bins, in which each bin is represented by value, z_j. The $E[\ln Y(x, z_j)]$ is the estimated conditional mean (i.e., sample average) for the natural logarithm of response in each bin, represented by value,

z_j, for a given IM_1 value, x and $f_{IM_2|IM_1}(z_j \mid x)$ is the probability that IM_2 is equal to z (in bin j) given IM_1 equal to x (e.g. it can be obtained from disaggregation).

In a similar manner, the conditional variance of the natural logarithm of response for a given $IM_1=x$, can be expanded with respect to a candidate secondary intensity measure, IM_2, as:

$$\hat{\beta}^2_{\ln Y|IM_1}(x) \cong \sum_{j=1}^{N_{IM_2}} E[(\ln Y(x,z_j))^2 \mid IM_1, IM_2] \cdot f_{IM_1|IM_2}(z_j \mid x) - \qquad \text{Eq.3.21}$$
$$- (E[\ln Y \mid IM])^2$$

Here, $E[(\ln Y(x, z_j))^2|IM_1,IM_2]$ denotes the expected value estimated by the conditional sample average of the squares of the natural logarithm (i.e., the estimated second moment) of structural response to ground motions in each bin represented by the value z_j (for a given $IM_1 = x$).

As it was stated in the beginning of this work, an intensity measure IM_1 is sufficient if it renders the critical demand to capacity ratio or the damage measure considered conditionally independent of the ground motion characteristics, for a given intensity level (e.g., $IM_1=x$). The statistical equivalent to this statement is to establish that the conditional probability distribution for the critical demand to capacity ratio of the structure for a given intensity level is independent of other ground motion characteristics, namely:

$$f_{Y|IM_1}(x) = f_{Y|IM_1,IM_2}(x,z_j) \qquad \text{Eq.3.22}$$

for any z_j value.

The sufficiency criterion can be also "approximated" in terms of the (conditional) statistical moments of the response (e.g., conditional mean and variance) being independent of the ground motion characteristics. For example, a "first-order measure" of the sufficiency criterion can be obtained by

establishing that the first (conditional) moment of the response for a given IM_1 level, x, is independent of other ground motion characteristics:

$$E[\ln Y(x) \mid IM_1] = E[\ln Y(x, z_j) \mid IM_1, IM_2] \qquad \text{Eq.3.23}$$

for all z_j value.

For a lognormal random variable, the above equation can be written as the equality of the medians:

$$\ln \hat{\eta}_{Y \mid IM_1}(x) = E[\ln Y \mid (x, z_j)] \qquad \text{Eq.3.24}$$

If an *IM* is sufficient, it can be demonstrated that the two sides of equation 3.20 will be always equal (by substituting $\hat{\eta}_{Y \mid IM_1, IM_2}(x, z_j)$ by $\hat{\eta}_{Y \mid IM_1}(x)$ in the equation) and does not depend on the probability distribution $f_{IM_2 \mid IM_1}$:

$$\ln \hat{\eta}_{Y \mid IM_1}(x) = \sum_{j=1}^{N_{IM_2}} \ln \hat{\eta}_{Y \mid IM_1}(x) \cdot f_{IM_2 \mid IM_1}(z_j \mid x) =$$
$$= \ln \hat{\eta}_{Y \mid IM_1}(x) \cdot \sum_{j=1}^{N_{IM_2}} f_{IM_2 \mid IM_1}(z_j \mid x) \qquad \text{Eq.3.25}$$

The above conclusion is based on the fact that the sum of the fractions $f_{IM_2 \mid IM_1}(z_j \mid x)$ is equal to unity. A "second order measure" of sufficiency criterion can be expressed in terms of the (conditional) second moment of the response:

$$E[(\ln Y(x))^2 \mid IM_1] = E[(\ln Y(x, z_j))^2 \mid IM_1, IM_2] \qquad \text{Eq.3.26}$$

for all z_j value.

Similarly, it can be demonstrated that the two sides of equation 3.21 will always be equal, independent of $f_{IM_2|IM_1}(z_j \mid x)$, if the second-order approximation to sufficiency are established.

9.2. Accounting for Collapse Cases in Multiple-Stripe Analysis

When multiple-stripe analysis is performed for high *IM* levels, it happens quite often that the structural analysis cases do not yield meaningful values. This could either imply that the structure has lost its load bearing capacity or may simply signal a numerical in-convergence. Since both cases are characterized by very large damage measure values, they are both referred to, for simplicity, as the "collapse cases".

In this study the logistic regression is used in order take into account the collapse cases, that happen in the structural analysis for increasing level of IM_1. In order to explicitly take into account collapse cases the stripe response is divided into two parts, namely, the non-collapse and the collapse parts. As far as it regards the non-collapse part of the stripe response, one could proceed as described in the previous section. For example, the linear least squares can be applied to the non-collapse part in order to model the correlation between IM_1 and IM_2. Alternatively, it can be divided into different bins. The logistic regression [25] is applied to the collapse data in order to predict the probability collapse as a function of the second intensity measure IM_2, rather than estimating the probability of collapse simply as the fraction of records in an IM_1 stripe that cause collapse (in the latter case, probability of collapse will not depend on IM_2).

Using the indicator variable *C* to designate occurrence of collapse (*C* equals 1 if the record causes collapse and 0 otherwise), the following functional form is fitted:

$$P(C|IM_1 = x, IM_2 = z) = \frac{e^{a(x)+b(x)\cdot z}}{1+e^{a(x)+b(x)\cdot z}} \qquad \text{Eq.3.27}$$

where *a* and *b* are coefficients to be estimated for the stripe response at $IM_1=x$.

Using the total probability theorem the first term in the integrand of equation 3.4 can be expanded in this way:

$$P_{DM|IM_1,IM_2}(DM > y|x,z) = P_{DM|IM_1,IM_2}(DM > y|x,z,NC) \cdot$$

$$\cdot P(NC|IM_1 = x, IM_2 = z) + 1 \cdot P(C|IM_1 = x, IM_2 = z)$$

<div align="right">Eq.3.28</div>

where:

$$P(NC|IM_1 = x, IM_2 = z) = 1 - P(C|IM_1 = x, IM_2 = z)$$

<div align="right">Eq.3.29</div>

is the probability of not having collapses given $IM_1=x$ and $IM_2=z$.

The term $P_{DM|IM_1,IM_2}(DM > y|x,z,NC)$ may be estimated by a lognormal probability distribution whose mean and standard deviation are calculated using equations 3.20 and 3.21. Alternatively, in the case of a vector-valued **IM**, it can be calculated using linear least squares in order to estimate the mean and the standard deviation for the probability distribution $P_{DM|IM_1,IM_2}(DM > y|x,z,NC)$.

10. Numerical Results

Distinguished by number of analyses carried out, two alternative procedures are considered in this work: the cloud method and the multiple-stripe method.

10.1. Cloud Method

The cloud method is a procedure in which the structure is subjected to a set of ground motion records of different *IM* values: this method provides a "cloud" of response values from which statistical parameters of *DM* given *IM* can be estimated.

10.1.1. Record Selection A (Sel_A)

For record selection A (*Sel_A*) the primary *IM* used in this study in a scalar form is the peak ground acceleration (PGA), that can be regarded as a scale factor of the single spectrum of the selection of records, paired in vector form, with magnitude (M), since it can be regarded as a "shape factor" of the single spectrum.

In Figure 3.4a the results obtained using the cloud method for the PGA and Y data pairs are shown. As stated in advance, in order to establish sufficiency of the primary *IM* and the effectiveness of ground motion characteristic variables as additional regression variables, a graphical statistical tool known as the residual-residual plot is used. The main advantage of the residual-residual plots is that they offer visual means for judging the improvement caused by an additional regression variable. In Figure 3.4b the residual-residual plot related to the introduction of magnitude as additional intensity measure, and the p-values calculated for the hypotheses test are shown. Judging from both the *p*-value and the reported *b* value, a significant positive trend in the plot can be observed: this indicates that, as expected, the peak ground acceleration is not sufficient with respect to the magnitude. Figure 3.4c shows the results obtained by the cloud method adopting the vector intensity measure [PGA, M]. The multiple regression is used to predict the structural damage measure as a function of both peak ground acceleration and magnitude.
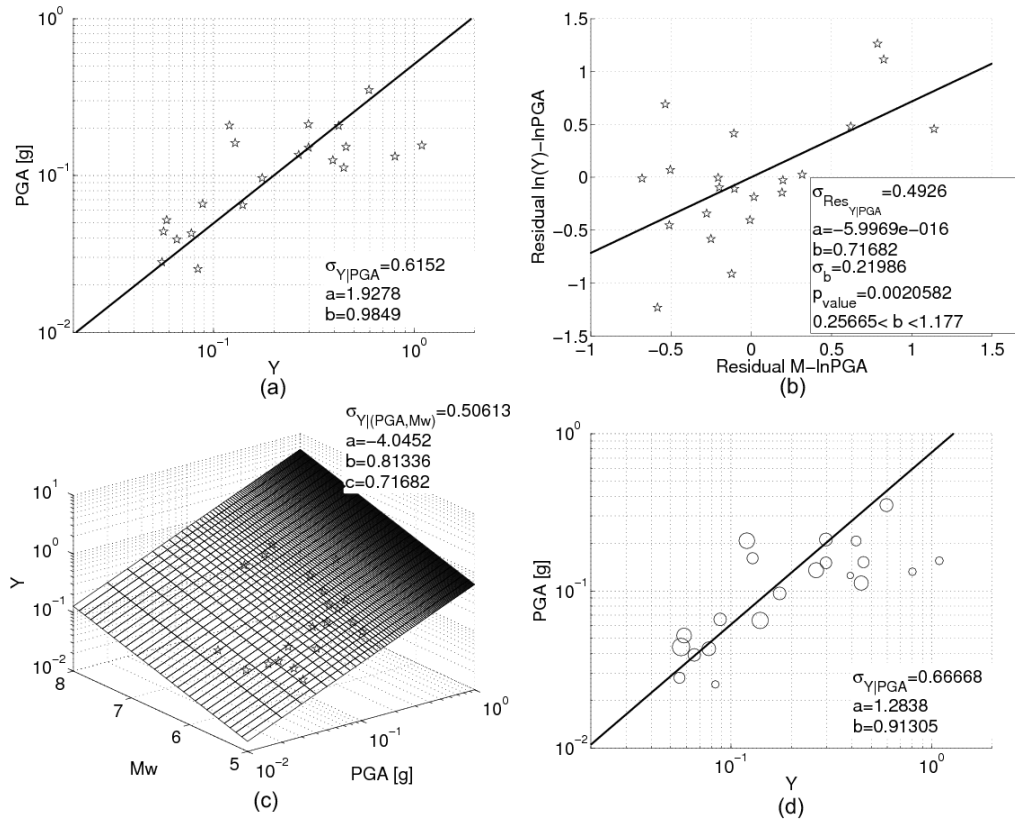
Figure 3.4. (a) Simple regression PGA-Y, *Sel_A*. (b) Residual-residual plot for magnitude as a second independent variable. (c) Multiple regression PGA-M-Y , *Sel_A*. (d) Weighted regression PGA-M-Y, *Sel_A*.

It would be interesting to study how the seismic risk, represented herein by the mean annual frequency of exceeding the structural damage measure, is affected by the weighed regression scheme. The results of weighted regression (Figure 3.4d) can be used in order to predict the conditional mean and standard deviation of the damage measure as a function of PGA; these parameters are then incorporated in equation 3.3 in order to calculate the structural fragility. The mean annual frequency of exceeding the structural damage measure can be calculated from equation 3.2 by integrating the structural fragility and the peak ground acceleration hazard curve (Figure 3.11b) (extracted from the site of

INGV for the coordinates of the site (lat. 40.915; lon. 14.78)). Moreover, the mean annual frequency of exceeding the damage measure Y has been calculated from equation 3.4 adopting the pair [PGA, M] as the vector-valued intensity measure and serves as a benchmark for judging if the weighted regression is helpful in adjusting for the dependence on magnitude. Figure 3.5 illustrates the results obtained by following the above-mentioned alternative methods. The thick line represents the mean annual frequency of exceeding the damage measure Y adopting the pair [PGA, M] as the intensity measure; the thin line represents the mean annual frequency of exceeding the damage measure Y using PGA as the intensity measure, and the dashed line represents the mean annual frequency of exceeding the damage measure Y using PGA as the intensity measure but adjusting for the dependence on magnitude by weighted regression.
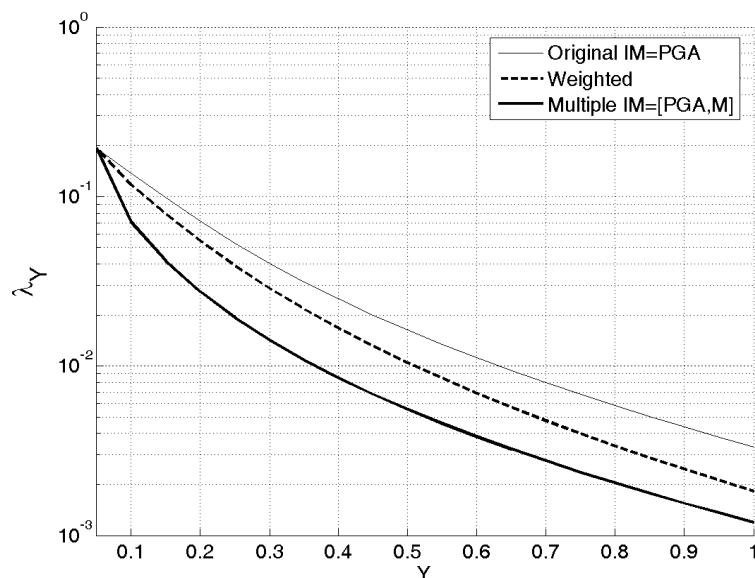
Figure 3.5. The mean annual frequency of exceeding the damage measure Y, cloud analysis, *Sel_A*.

It can be observed that the weighted regression manages to take into account some of the information provided by the secondary *IM* and its corresponding

mean annual frequency of exceeding Y ends up somewhere between those corresponding to the original cloud method and the multiple-regression, respectively. In other words, the weighting scheme is partially effective in taking into account the magnitude dependence in the prediction of seismic risk.

10.1.2. Record Selection B (Sel_B)

For record selection B (*Sel_B*) the primary *IM* used in this study in scalar form is the first-mode spectral acceleration. Similar to PGA, it can be regarded as a scaling factor for the spectrum of each ground motion record centered around the fundamental period of the structure. The first-mode spectral acceleration is paired in vector form, with the deviation from the ground motion prediction relationship ε, that can be regarded as an approximation to the "shape factor" of the single spectrum in a range of periods in the vicinity of the fundamental period of the structure. The results obtained using the cloud method in order to predict Y adopting $S_a(T_1)$ as the primary *IM* based on selection B are illustrated Figure 3.6a.

In order to establish the sufficiency of the primary *IM* and the effectiveness of ground motion characteristic variable ε as the secondary *IM*, the residual-residual plot is used. In Figure 3.6b the residual-residual plot related to the introduction of epsilon as additional *IM* is shown; the *p*-value obtained from hypotheses test is also indicated on the residual-residual plot. Judging from both the *p*-value and the reported sigma value, a statistically significant negative trend can be observed. This means that first-mode spectral acceleration is not sufficient with respect to the epsilon. Figure 3.6c shows the results obtained by the multiple-regression and adopting the vector $[S_a(T_1), \varepsilon]$ as the intensity measure. The results of the non linear dynamic analysis following the weighted cloud method and employing the seismic hazard disaggregation are shown in Figure 3.6d. The data pairs $(S_a(T_1), Y)$ are plotted by circles with diameters proportional to the corresponding weight assigned through the weighted regression scheme.

The alternative regression schemes (i.e., simple, weighted and multiple regression) are then used in order to estimate the conditional mean (of the

logarithm) and the conditional standard deviation (of the logarithm) of the structural damage measure Y as a function of the adopted *IM*. When using the simple and weighted regression schemes, the structural fragility is calculated from equation 3.3 for the scalar *IM*. In the case of multiple regression, the structural fragility is calculated from equation 3.5 and is conditional on both *IM*'s adopted.
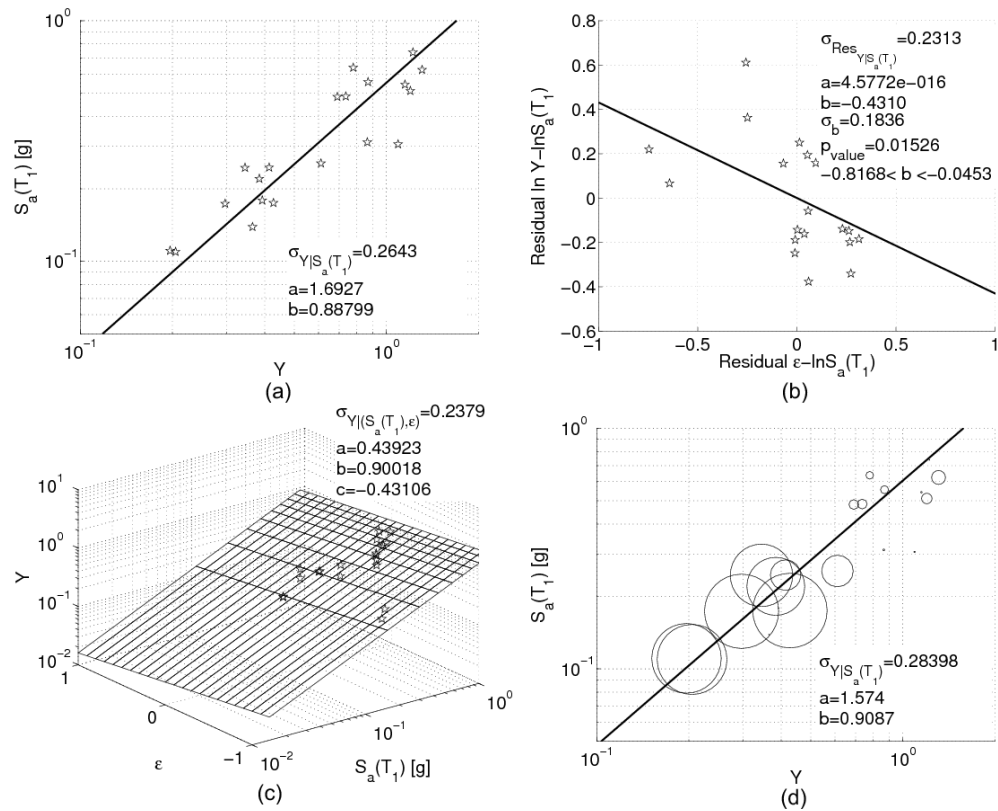
Figure 3.6. (a) Simple regression $S_a(T_1)$-Y, *Sel_B*. (b) Residual-residual plot for epsilon as a second independent variable. (c) Multiple regression $S_a(T_1)$-Y-ε, *Sel_B*. (d) Weighted regression $S_a(T_1)$- Y-ε, *Sel_B*.

Once the structural fragility is obtained, it is integrated numerically with the spectral acceleration hazard curve (Figure 3.13b) (extracted from the site of INGV for the coordinates of the site (lat. 40.915; lon. 14.78) and period equal

to 0.75 seconds) in order to calculate the mean annual frequency of exceeding the damage measure Y or the seismic risk curve. Figure 3.7 illustrates the seismic risk curve calculated using the above-mentioned alternative methods. It can be observed that the seismic risk curve calculated using the weighted regression manages to adjust partially for the dependence on epsilon. Obviously, the resulting improvement depends both on the spread of the epsilon values for the selected ground motion records and the ground motion prediction relationship used in the hazard/disaggregation analysis (Figure 3.3b).
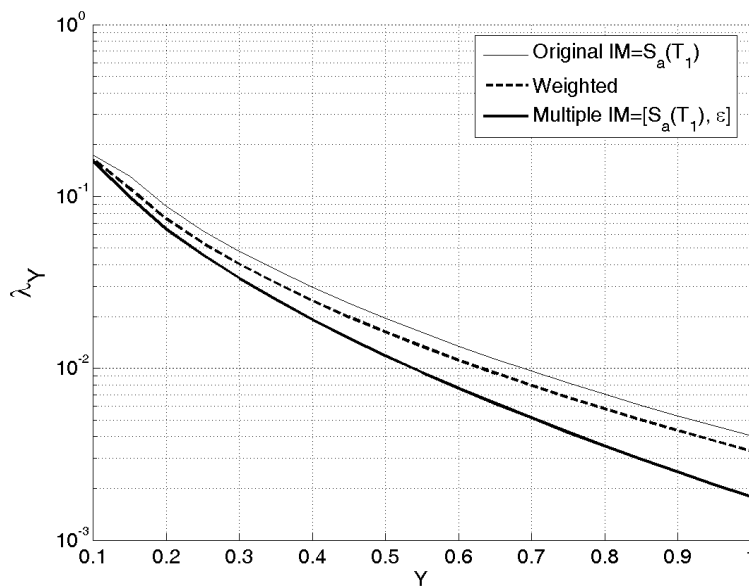
Figure 3.7. The mean annual frequency of exceeding the damage measure Y, cloud analysis, *Sel_B*.

The choice of epsilon as the secondary *IM* has been inspired by the fact that it acts as a proxy for spectral shape in the vicinity of the fundamental period of the structure. Therefore, it is interesting to investigate also the dependence of the damage measure Y given $S_a(T_1)$ on spectral acceleration at another period $T_2 \neq T_1$, $(S_a(T_2))$, in order to consider in an explicit way the shape of the elastic acceleration spectrum. The procedure followed for establishing the dependence of Y given $S_a(T_1)$), on $S_a(T_2)$ is similar to the one followed in order to

investigate the sufficiency of $S_a(T_1)$ with respect to ε. In the same manner, $S_a(T_2)$ is regarded as a second regression variable, and the residual-residual plots are used to study its efficiency in reducing the dispersion. It would be interesting to identify the period whose corresponding spectral acceleration is most efficient in predicting the structural damage measure conditional on the first-mode spectral acceleration. The efficiency of the spectral acceleration at a period, $T_2 \neq T_1$, as the second regression variable, has been studied from the point of view of the reduction in the standard error of the regression. This leads to finding an optimal period T_2 at which the dispersion is minimum, or in other words to the pair $[S_a(T_1), S_a(T_2)]$ that has maximum efficiency as an intensity measure.
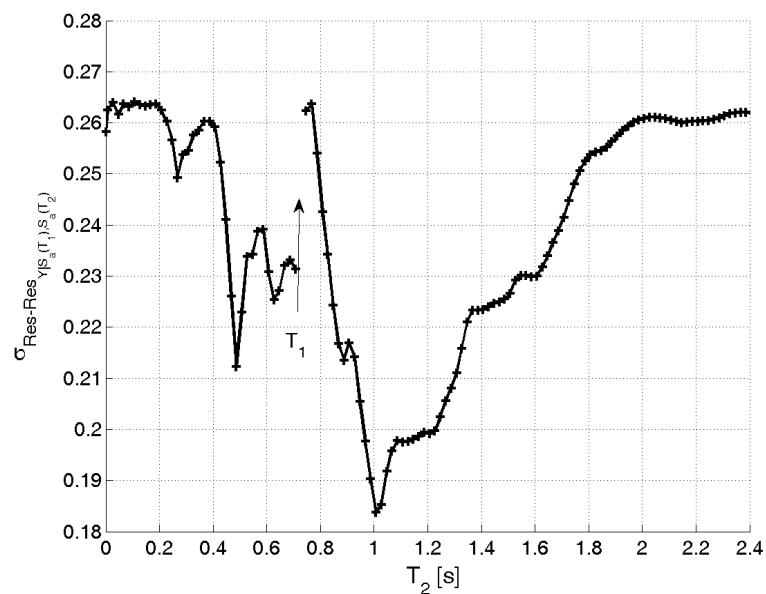
Figure 3.8. Sigma of the residual-residual plot for $S_a(T_2)$ as a second independent variable for predicting the structural response for different values of the period T_2.

The plot in Figure 3.8, illustrates the values for the sigma (dispersion measure) in the residual-residual regressions performed for a range of periods.

It can be observed that choosing the spectral acceleration at $T_2=1$ second leads to the maximum reduction in the residual-residual dispersion. The period

corresponding to the first mode of the structure is also marked on the figure. The efficiency demonstrated by T_2=1s in reducing the sigma of the residual-residual plot signals severe non linear behaviour in the structural elements resulting in the elongation of the period for the structure herein considered.

In order to characterize the joint probability distribution for the logarithm of the spectral accelerations at two periods T_1 and T_2, the mean and standard deviation values for both can be extracted from the ground motion prediction equation [26]. In order to completely specify the first and second moments for this pair of spectral values, one needs to evaluate the correlation between $\ln S_a$ values at the two periods. An empirically-determined relationship for such correlation is given by Inoue and Cornell [27]:

$$\rho_{\ln S_a(T_1),\ln S_a(T_2)} = 1 - 0.33\left|\ln(T_1/T_2)\right| \qquad 0.1s \leq T_1, T_2 \leq 4s \qquad \text{Eq.3.30}$$

Previous research has established that $\ln S_a(T_1)$ and $\ln S_a(T_2)$ are each marginally normally distributed [28]. Under the mild assumption that they are also jointly normally distributed, one can obtain the conditional mean of $\ln S_a(T_2)$, given $\ln S_a(T_1)$:

$$\mu_{\ln S_a(T_1)|\ln S_a(T_2)=x} = \mu_{\ln S_a(T_2)} + \rho_{\ln S_a(T_1),\ln S_a(T_2)} \cdot \sigma_{\ln S_a(T_2)} \left(\frac{x - \mu_{\ln S_a(T_1)}}{\sigma_{\ln S_a(T_1)}} \right) \qquad \text{Eq.3.31}$$

The conditional standard deviation of $\ln S_a(T_2)$ is given as:

$$\sigma_{\ln S_a(T_1)|\ln S_a(T_2)=x} = \sigma_{\ln S_a(T_2)} \sqrt{1 - \rho^2_{\ln S_a(T_1),\ln S_a(T_2)}} \qquad \text{Eq.3.32}$$

These statistics have been used in order to obtain the mean annual frequency of exceeding the critical component demand to capacity Y. The conditional

mean and standard deviation derived from equations 3.31 and 3.32 can be used in order to construct the conditional probability distribution $f(S_a(T_2)|S_a(T_1))$.

Figure 3.9a shows the results obtained by the cloud method and the introduction of spectral acceleration for $T_2 = 1s$ as the secondary *IM*, using the multiple regression.
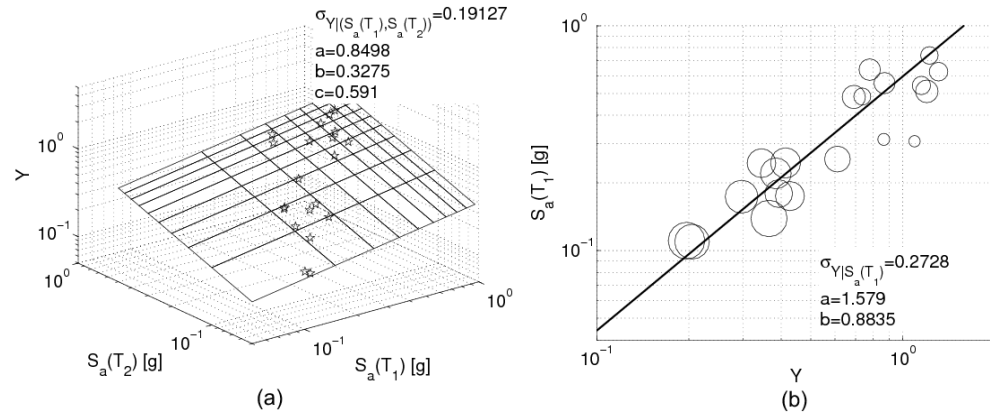
Figure 3.9. (a) Multiple regression $S_a(T_1)$-$S_a(T_2)$-Y, *Sel_B*. (b) Weighted regression $S_a(T_1)$-$S_a(T_2)$-Y, *Sel_B*.

Figure 3.9b illustrates the results of weighted regression analysis exploiting the additional information provided by the conditional probability distribution $f(S_a(T_2)|S_a(T_1))$. The $(S_{a,i}(T_1), Y_i)$ data pairs are plotted by circles with diameters proportional to the corresponding weight which is proportional to $f(S_a(T_{2i})|S_a(T_{1i}))$. The results of the weighted regression can be used in order to estimate the conditional mean and standard deviation of the damage measure based on which the structural fragility can be calculated from equation 3.3.

In a similar manner, the multiple regression results are used in order to estimate the mean and standard deviation conditional on both $S_a(T_1)$ and $S_a(T_2)$. These statistics can be incorporated in equation 3.5 in order to calculate the structural fragility. The resulting fragility based on the weighted regression is integrated numerically from equation 3.2 for a scalar *IM* with the spectral acceleration hazard curve (Figure 3.13b) in order to calculate the mean annual frequency of exceeding Y. The fragility obtained based on the multiple

regression is integrated with the spectral acceleration hazard in equation 3.4 for a vector *IM* in order to provide the seismic risk curve. Figure 3.10 illustrates the seismic risk curves calculated by following the alternative approaches just discussed.
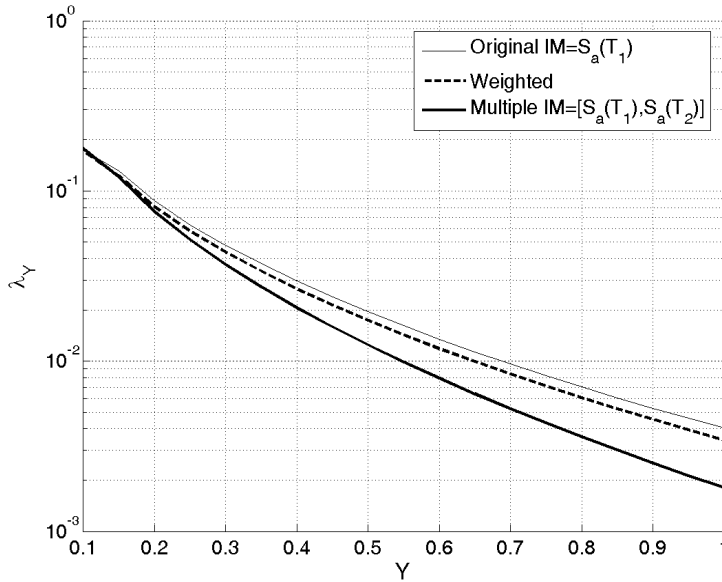
Figure 3.10. The mean annual frequency of exceeding the damage measure Y, cloud analysis, *Sel_B*.

It can be observed that there is only a small gain in information resulting from incorporating the correlation between the two spectral values inside the weighted regression scheme. The same as the case of $IM_2=\varepsilon$, the weights applied inside the weighted regression are quite sensitive to both interval covered by the $S_a(T_2)$ values of the selection of records and the characterization of $f(S_a(T_2)|S_a(T_1))$.

10.2. Multiple-Stripe Analysis

The results of multiple-stripe analysis are used in order to investigate the efficiency of the weighting scheme based on the information provided by

seismic hazard, in the prediction of the mean annual frequency of exceeding the damage measure Y and using the same intensity measures used in the cloud method.

10.2.1. Record Selection A (Sel_A)

Figure 3.11a illustrate the results of multiple-stripe analysis for the structure considered herein subjected to record selection A.
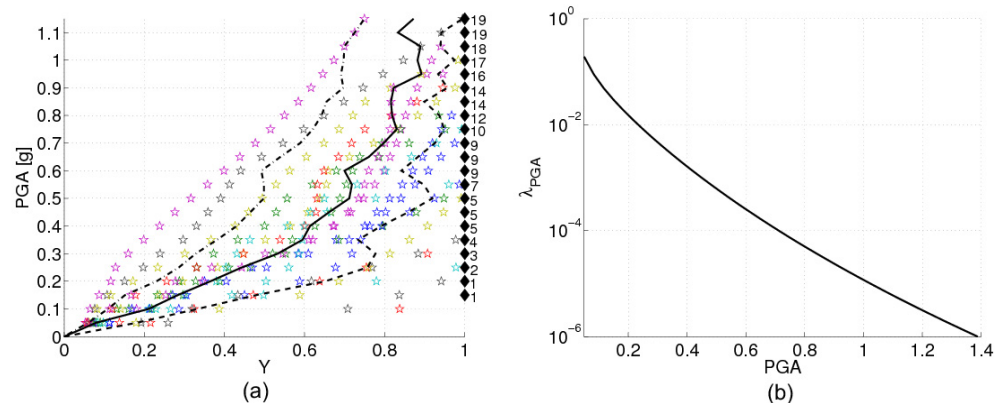
Figure 3.11. (a) Results of multiple stripe analysis for *Sel_A*. (b) Peak ground acceleration hazard curve.

The critical demand to capacity ratio Y (the stripe response) is calculated for increasing levels of PGA using the multiple-stripe method. The lines connecting the (counted) 16th, 50th and 84th percentiles of the stripe response at each IM level are also shown; numbers near black diamonds in Figure 3.11a indicate the number of collapse cases encountered for each level of PGA.

In Figure 3.11b the peak ground acceleration hazard curve (extracted from the site of INGV for the coordinates of the site (lat. 40.915; lon. 14.78)) is shown.

The statistics of the stripe response (i.e., mean and standard deviation of the logarithm) are calculated from equations 3.18 and 3.19 and incorporated in equation 3.3 in order to calculate the structural fragility. For the vector-valued intensity measure [PGA, M], a simple regression analysis is performed for the

stripe response, at each PGA level, on logarithm of the stripe response versus moment magnitude M. The regression results are then used in order to calculate the conditional mean and standard deviation of the logarithm of Y given PGA and M. These statistics are incorporated in equation 3.5 in order to calculate the structural fragility. Alternatively, the weighted multiple stripe analysis is used in order to weigh the stripe response based on the results of seismic hazard disaggregation or *f(M|PGA)*. The weighted statistics (mean and standard deviation of logarithm) for the stripe response are calculated from equations 3.20 and 3.21. The structural fragility can be calculated from Equation 3 for the scalar *IM* based on the weighted statistics. It should be mentioned that the presence of the collapse cases in the stripe response is accounted for by employing a logistic regression scheme as discussed previously.
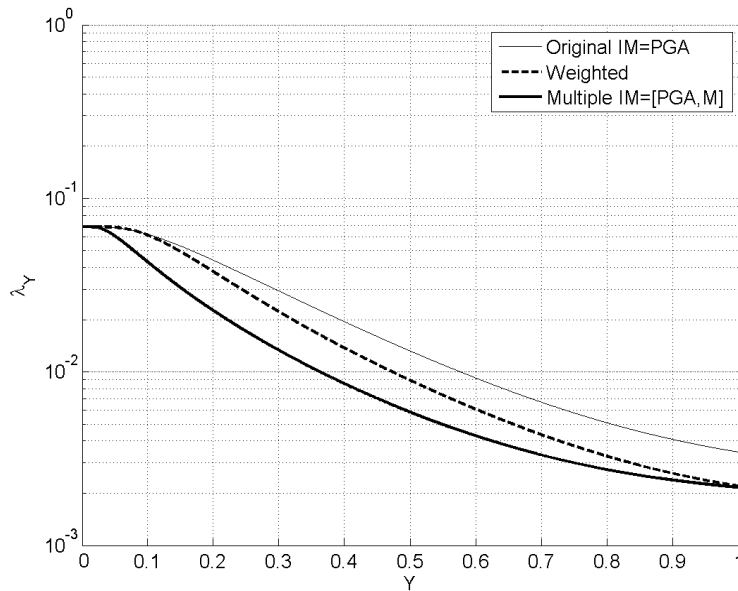
Figure 3.12. Hazard curves for the critical component demand to capacity Y, multiple-stripe analysis, *Sel_A*.

Through numerical integration of the structural fragility with the peak ground acceleration hazard curve, the seismic risk curves for the critical

component demand to capacity are calculated by employing the alternative methods discussed above (Figure 3.12).

Given the increased sophistication and computational effort associated with the multiple-stripe method compared to the cloud method, the position of the hazard curve calculated using the weighted method indicates that the weighting scheme for the stripes analysis is more effective in taking into account the magnitude dependence in the prediction of hazard for the critical component demand to capacity with respect to the curve obtained through the cloud method.

In other words, in the cloud method the efficiency of the weighted regression scheme depends strongly on the suite of ground motion records selected, since they are not scaled. Instead, when applying the stripes method, the ground motion records are scaled to successively increasing levels of PGA and can cover a more thorough range of the ground motion intensity.

10.2.2. Record Selection B (Sel_B)

Figure 3.13a illustrates the results of multiple-stripe analysis for the structure herein considered subjected to record selection B.
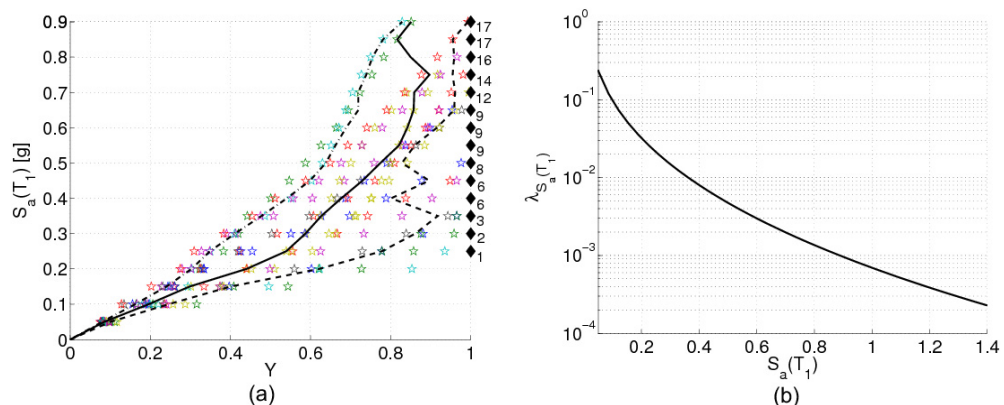
Figure 3.13. (a) Results of multiple stripe analysis for *Sel_B*. (b) Spectral acceleration hazard curve for T_1=0.75s.

The stripe response is obtained for increasing levels of $S_a(T_1)$. The lines connecting the (counted) 16th, 50th and 84th percentiles of the stripes are also shown in Figure 3.13a; numbers near black diamonds indicate the number of collapse cases for each level of $S_a(T_1)$.

In Figure 3.13b the spectral acceleration hazard curve (extracted from the site of INGV for the coordinates of the site (lat. 40.915; lon. 14.78) and period equal to 0.75 seconds) is shown.

Figure 3.14 illustrates the seismic risk curve for the critical component demand to capacity obtained by means of numerical integration and employing the alternative methods discussed in the previous section for record selection A, adopting $S_a(T_1)$ as the primary *IM* and epsilon as the secondary *IM*.
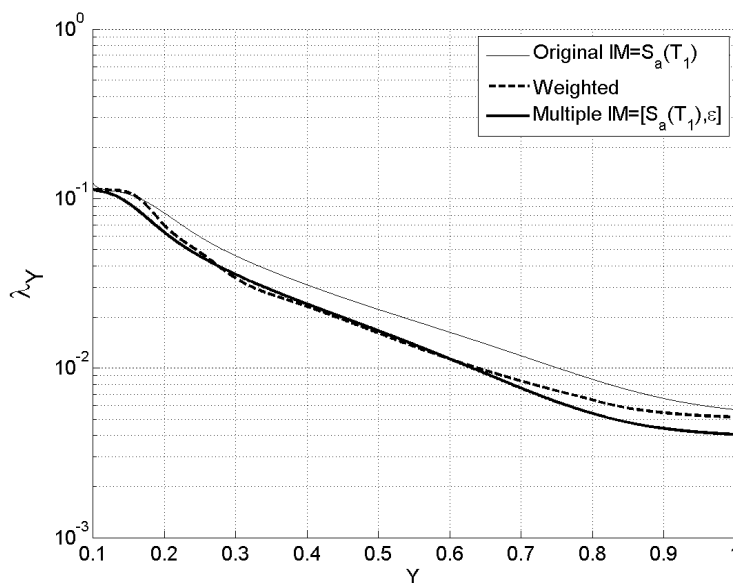
Figure 3.14. Hazard curves for the critical component demand to capacity Y, multiple-stripe analysis, *Sel_B*.

It can be observed that the weighted multiple-stripe, based on the additional information provided by seismic hazard disaggregation, manages to capture almost perfectly the dependence on epsilon. This can be attributed to the fact that the ground motion records are being scaled over the whole range of

possible $S_a(T_1)$ values; this may help in reducing the dependence on the particular selection of records employed. Furthermore, the pair of *IM*'s $S_a(T_1)$ and $S_a(T_2)$ are also studied in the framework of the multiple stripe analysis, for record selection B.

The conditional probability distributions $f(S_a(T_2)|$ $S_a(T_1))$ of spectral acceleration at $T=T_2$ given spectral acceleration at the fundamental period of the structure are illustrated in Figure 3.15; moreover, the histogram of the values of $S_a(T_2)$ of the record selection B is also shown in the bottom of the figure.
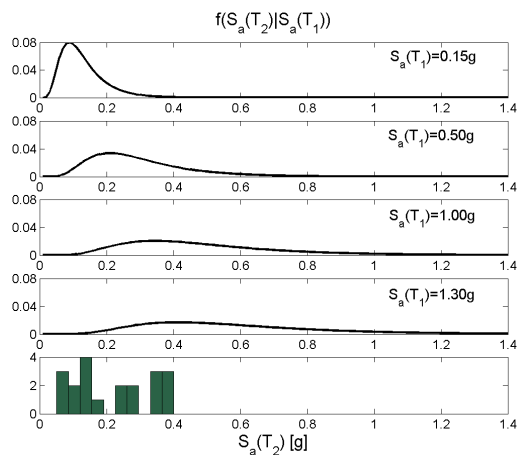
Figure 3.15. Conditional probability distribution of $S_a(T_2)$ given some values of $S_a(T_1)$ and histogram of $S_a(T_1)$ values for *Sel_B*.

Figure 3.16 illustrates the seismic risk curve for the critical component demand to capacity which is calculated through numerical integration of the structural fragility and the spectral acceleration hazard curve in Figure 3.13b, employing the alternative methods discussed previously. The procedure for obtaining the probability distribution $f(S_a(T_2)|S_a(T_1))$ is the same as that described for cloud method.
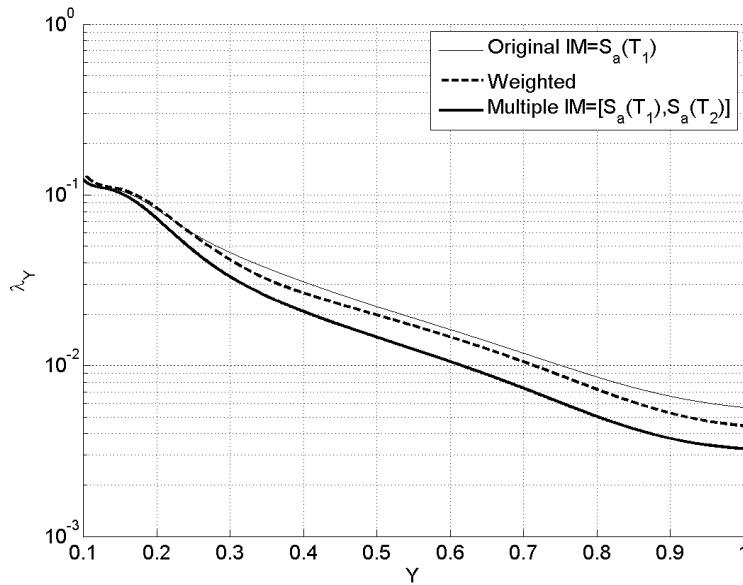
Figure 3.16. Hazard curves for the critical component demand to capacity Y, multiple-stripe analysis, *Sel_B*.

It can be observed that the weighted multiple-stripe analysis does not succeed in including the additional information provided by the secondary intensity measure $S_a(T_2)$. It may be noted from Figure 3.15, that the conditional probability distributions $f(S_a(T_2)|\ S_a(T_1))$ of spectral acceleration at $T=T_2$ given spectral acceleration at the fundamental period of the structure do not defer drastically from the histogram of the $S_a(T_2)$ values for selection B. Moreover, the conditional probability distributions seem to remain invariant for large values of $S_a(T_1)$. Therefore, the weighted stripe method leads to little improvement compared to the original stripes.

11.   Conclusions

In the framework of the probabilistic performance-based assessment of existing structures, in order to calculate the mean annual frequency of exceeding a specified damage level using non linear time-history analysis, it is useful to introduce an intermediate parameter, the ground motion intensity

measure *IM*, to relate the ground motion record characteristics to the structural performance. The intensity measure approach is appealing because it allows for (roughly speaking) decoupling the seismic hazard analysis and the structural fragility analysis.

The seismic hazard function, for the adopted *IM*, can be obtained from the results of site-specific probabilistic seismic hazard analysis or directly from the national seismic maps.

In order to estimate the structural fragility, depending on the amount of structural analysis, two alternative non-linear dynamic analysis procedures can be considered: the cloud method and the multiple-stripe method.

However, the approach based on the introduction of the intensity measure, assumes that structural response depends only upon the chosen *IM* parameter, and not on any other properties of the ground motion. This required condition is termed "sufficiency" and means that the structural response for a given *IM* is statistically independent of the ground motion characteristics. This hypothesis must be carefully verified since, if the sufficiency condition is not met, then the probability distribution for the damage measure will not only depend upon *IM*, but also upon the (other) properties of the records selected for analysis. Hence, in case the properties of the selected records do not reflect, in a realistic manner the records that the real structure will be subjected to, a biased estimate of structural response would be obtained. If the adopted *IM* is sufficient with respect to other ground motion characteristics, depending on the amount of structural analysis, both cloud and multiple-stripe methods can be implemented in order to evaluate structural fragility. In order to estimate the statistical properties of *DM* given *IM* by employing the cloud response, the linear least squares scheme can be applied. Instead, in the framework of multiple-stripes method, the statistical properties of each stripe response, can be evaluated based on the *DM* values calculated in response to the scaled suite of records for various *IM* levels.

One effective way to increase the sufficiency of an *IM*, is to introduce additional parameters, so that the resulting vector-valued **IM** would describe more completely the properties of the ground motion. In particular, a vector

intensity measure $\boldsymbol{IM}=[IM_1, IM_2]$ consisting of two parameters can be adopted; IM_1 represents the primary intensity measure and IM_2 represents the secondary intensity measure that strives to capture the ground motion characteristics not already described by IM_1. Also in the case of a bi-variate IM, both cloud and multiple-stripe methods can be implemented in order to evaluate the structural fragility. In the context of the cloud method, the two-variable linear least squares scheme can be used to estimate the statistical parameters for DM conditional on both IM_1 and IM_2. In the framework of multiple-stripe method the linear regression analysis can be employed on each stripe response in order to investigate the dependence on the secondary IM_2 parameter for each IM_1 level. A simple statistical and graphical tool known as the residual-residual plots is employed in this work in order to reveal possible dependence of the response DM conditional on the adopted primary IM, on a candidate secondary IM.

In the cases where sufficiency for the primary IM is not established, a weighting scheme based on the results of the seismic hazard analysis for the ground motion characteristic variable(s) can be implemented in the estimation of the structural fragility. This is to adjust for the dependence of the structural response, conditional on the adopted primary IM_1, on the candidate secondary IM_2. In the context of the cloud method the weighted regression scheme is applied to the cloud response, weighting each square residual term in relation to the conditional probability distribution $f(IM_2|IM_1)$, obtained through seismic hazard disaggregation. In the framework of the multiple-stripe analysis, an analogous weighting procedure was employed, in order to account for the information available on the correlation between IM_1 and a candidate IM_2, obtained through seismic hazard disaggregation. In this approach, the stripe response is discretized into into a set of IM_2 bins; each bin is then weighted by the probability $f(IM_2| IM_1)$ obtained from seismic hazard analysis..

The conditional probability distributions for magnitude given peak ground acceleration $f(M|PGA)$ and for epsilon of the ground motion prediction relation given the spectral acceleration at first mode, $f(\varepsilon|S_a(T_1))$ have been calculated

through the disaggregation of the seismic hazard for the site of the case-study structure using the Bayesian probabilistic framework.

The implication of using the weighting scheme has been studied in terms of seismic risk represented herein by the mean annual frequency of exceeding the critical component demand to capacity ratio (Y), using both cloud and multiple-stripe methods. In order to evaluate the efficiency of the weighting scheme the seismic risk curve obtained was compared with the curves obtained by adopting the scalar primary IM_1 and the vector valued $\mathbf{IM}=[IM_1, IM_2]$.

In particular, as scalar primary IM's, the peak ground acceleration PGA and the spectral acceleration at the first mode $S_a(T_1)$ were considered. The weighting scheme was applied to adjust for the magnitude-dependence of the structural response conditional on PGA. Alternatively, considering $S_a(T_1)$ as the primary IM, the weighting scheme was used to adjust for the *epsilon*-dependence of the structural response conditional on $S_a(T_1)$. Finally, the weighting scheme is used to take into account the spectral shape-dependence of the structural response conditional on $S_a(T_1)$ at a period $T_2 \neq T_1$, ($S_a(T_2)$). The same pairs of intensity measures were also considered as vector-valued $\mathbf{IM}$. The seismic risk curves calculated by adopting the vector-valued IM's were used to benchmark the efficiency of the weighting scheme.

Among all the analysed cases, it is observed that the weighting scheme manages to take into account some of the information provided by the secondary IM and its corresponding mean annual frequency of exceeding Y ends up somewhere between those obtained adopting the scalar primary IM and the vector-valued $\mathbf{IM}$ consisting of the primary and the secondary intensity measures, respectively. However, the weighting scheme proves much more efficient for multiple-stripe analysis compared to the cloud analysis. This can be attributed to the fact that, the multiple-stripe analysis spans over a wider range of ground motion intensity levels and therefore proves less sensitive to the selection of ground motion records compared to the cloud method. On the other hand, the success of the weighting scheme for the cloud method depends on the selection of records. In general, it can be observed that the weighted scheme enhances the assessment of the mean annual frequency of exceeding a

specified damage level for the structure considered herein and allows a more accurate estimation of the structural response with a limited number of analyses.

12.   References

[1]   Iervolino I., Maddaloni G., Cosenza E. (2008). "Eurocode 8 compliant real record sets for seismic analysis of structures", *Journal of Earthquake Engineering*, 12(1): 54–60.

[2]   Iervolino I., Maddaloni G., Cosenza E. (2009). A note on selection of time-histories for seismic analysis of bridges in Eurocode 8. *Journal of Earthquake Engineering.* (in press)

[3]   Bazzurro P., Cornell C.A., (1998), Disaggregation of seismic hazard, *Bulletin of the Seismological Society of America*, 89**(2)**:501-520, April 1999.

[4]   Jalayer, F., and Cornell, C. A. Alternative Nonlinear Demand Estimation Methods for Probability- Based Seismic Assessments, *Earthquake Engineering and Structural Dynamics*, **38**(8), 951-972, 2009.

[5]   Luco N. and Cornell C.A.. Structure-Specific Scalar Intensity Measures for Near-Source and Ordinary Earthquake Ground Motions, *Earthquake Spectra*, Volume 23, Issue 2, pp. 357-392 May 2007.

[6]   Iervolino I., Cornell C.A. (2005). Record selection for nonlinear seismic analysis of structures. *Earthquake Spectra*, **21**(3):685-713.

[7]   Tothong, P., and Luco, N., 2007. Probabilistic seismic demand analysis using advanced ground motion intensity measures, *Earthquake Eng. Struct. Dyn.* **36**, 1837–1860.

[8]   Baker J.W, Cornell C.A. A vector-valued ground motion intensity measure consisting of spectral acceleration and epsilon. *Earthquake Engineering & Structural Dynamics*, 34:1193-1217, 2005.

[9]   McGuire RK. *Seismic Hazard and Risk Analysis*. Earthquake Engineering Research Institute; First Edition, August 2004.

[10] Vamvatsikos D, Cornell CA. Incremental dynamic analysis, *Earthquake Engineering and Structural Dynamics*, **31**(3), 491-514, 2001.

[11] Baker J.W. Probabilistic structural response assessment using vector-valued intensity measures. *Earthquake Engineering & Structural Dynamics*, 36 **(13)** 1861-1883, 2007.

[12] Cordova, P. P., Deierlein, G. G., Mehanny, S. S. F., and Cornell, C. A., 2000. Development of a two-parameter seismic intensity measure and probabilistic assessment procedure, *Proceedings of the 2nd U.S.-Japan Workshop on Performance-Based Seismic Design Methodology for Reinforced Concrete Building Structures*, PEER Report 2000/10, Pacific Earthquake Engineering Research Center, University of California, Berkeley.

[13] Jalayer, F., Franchin, P. and Pinto, P.E. (2007), A Scalar Decision Variable for Seismic Reliability Analysis of RC Frames, *Special issue of Earthquake Engineering and Structural Dynamics on Structural Reliability*, Vol. 36 (13): 2050-2079, June 2007.

[14] Ditlevsen O, Masden H. *Structural Reliability Methods*, June 1996; John Wiley & Sons Inc.

[15] Scott MH, GL Fenves. Plastic hinge integration methods for force-based beam-column elements, *Journal of Structural Engineering, ASCE*, 132**(2)**:244-252, February 2006.

[16] Mander J.B., Priestley M.J.N., Park R., Theoretical stress-strain model for confined concrete, *Journal of Structural Engineering*, vol.114, n.8, August 1988, pp.1804-1826.

[17] Ordinanza del Presidente del Consiglio dei Ministri (OPCM) n. 3431, Ulteriori modifiche ed integrazioni all'ordinanza del Presidente del Consiglio dei Ministri n. 3274 del 20 marzo 2003. Gazzetta Ufficiale della Repubblica Italiana n. 107 del 10-5-2005 (Suppl. Ordinario n.85), 2005.

[18] Sabetta F, Pugliese A. Estimation of response spectra and simulation of non-stationary earthquake ground motions. *Bulletin of the Seismological Society of America*, 86**(2)**:337-352, April 1996.

[19] CEN, European Committee for Standardisation TC250/SC8/ [2003] "*Eurocode 8: Design Provisions for Earthquake Resistance of Structures, Part 1.1: General rules, seismic actions and rules for buildings*," PrEN1998-1.

[20] Meletti C. and Valensise G., Zonazione sismogenetica ZS9 – Rapporto Conclusivo, March 2004.

[21] Shome N., and Cornell C.A. (1999). Probabilistic seismic demand analysis of non-linear structures. *Report No. RMS-35, Stanford University*, Stanford, CA.

[22] Luco N., (2002) Probabilistic seismic demand analysis, SMRF connection fractures, and nearsource effects, *Stanford University*, Stanford, CA, 260 pp.

[23] Rice J. A., (1995) *Mathematical Statistics and Data Analysis*, Belmont, CA: Duxbury/Wadsworth.

[24] Jalayer F. *Direct Probabilistic Seismic Analysis: Implementing Non-linear Dynamic Assessments*, Ph.D. Thesis, Department of Civil and Environmental Engineering, Stanford, CA, March 2003.

[25] Neter J., Kutner M. H., Nachtsheim C. J. and Wasserman W., (1996). *Applied linear statistical models*, (McGraw-Hill, Boston).

[26]   Baker, J.W. (2005). Vector-Valued Ground Motion Intensity Measures for Probabilistic Seismic Demand Analysis, Ph.D. Thesis, *Stanford University*; Stanford, California. 321p.

[27]   Inoue T. and Cornell C.A., 1990. Seismic hazard analysis of multi-degree-of-freedom structures, Reliability of Marine Structures, *RMS-8, Stanford*, CA, 70 pp.

[28]   Abrahamson, N. A. (2000). State of the practice of seismic hazard evaluation, GeoEng 2000, Melbourne, Australia, 19–24 November 2000, 659-685.

Chapter IV

An Efficient Bayesian Method for Taking into Account the Modelling Uncertainties in the Evaluation of Structural Reliability

1.   Introduction

In a previous work (Jalayer et al. 2008 [1]), summarized in chapter II, the authors have implemented a Bayesian probabilistic framework for a case-study existing structure in order to both characterize the uncertainties in the material properties and structural detailing and also to update the structural reliability by employing the results of in-situ tests and inspections. In this chapter a proposal for applying the results of structural analysis for a small sample of structural modeling realizations in the Bayesian probabilistic framework is presented. This method can provide interval parameter estimations necessary for evaluation the structural reliability. The structural reliability assessments based on the small-sample interval estimates can be also implemented inside the time-history analysis procedures using a set of ground motion records in order to take into account the uncertainty in the ground motion representation.

2.   The Methodology

The Bayesian framework for inference is used in order to obtain robust estimates for the structural reliability and its standard deviation based on small-sample simulations of structural modelling parameters. This methodology represents a simple alternative to large sample simulations like those discussed in chapter II. However, in order to benchmark this simplified alternative method, the results of large sample simulations reported in the previous chapter are used.

If the probability of failure is described by an analytic probability distribution with parameters χ (e.g., median and standard deviation of the lognormal distribution) denoted by $P(F|\chi)$, given the set of parameters $\underline{\theta}$ that represent all the uncertain parameters considered in the problem, the expected value (or the robust estimate) for the probability of failure, given a set of values Y for the structural performance index, can be expressed as:

$$E[P(F \mid D)] = \int_{\Omega} P(F \mid \chi) p(\chi \mid D) d\chi \qquad \text{Eq. 4.1}$$

where $p(\chi \mid D)$ is the posterior probability distribution for the set of parameters χ given the data D and Ω is the space of possible values for χ. In a similar way, the robust variance for the probability of failure can be calculated as:

$$\sigma_{P(F|D)} = E[P(F \mid D)^2] - E[P(F \mid D)]^2 \qquad \text{Eq. 4.2}$$

2.1.   The Vector of Uncertain Parameters

It is assumed that the vector $\underline{\theta}$ represents all the uncertain parameters considered in the problem. The vector $\underline{\theta}$ can include the uncertainties in the mechanical properties of the materials, in the structural construction details

(a.k.a., *defects*) and in the representation of the ground motion uncertainty. One of the main characteristics of the construction details is that possible deviations from the original configurations are mostly taken into account in those cases leading to undesirable effects. This explains why the uncertainties related to construction details are also referred to as the *structural defects*.

2.2.   The Characterization of the Uncertainties

Three types of uncertainties are considered herein, namely, the uncertainty in the material mechanical properties, the uncertainties in the structural detailing parameters and the uncertainty in the ground motion input.

The parameters identifying the prior probability distributions for the material mechanical properties (concrete strength and the steel yielding force) have been based on the values typical of the post world-war II construction in Italy ([2,3]); the adopted probability distributions are the same reported in table 2.2 of chapter II.

The prior probability distributions for the structural detailing parameters are defined based on qualitative prior information coming from judgment and prior experience [1]; the adopted prior distributions are the same reported in table 2.3 of chapter II.

A set of 30 ground motion records are chosen from the European Strong-motion Database or ESD[7] for soil type B in order to take into account the record-to-record variability. The spectral acceleration at the fundamental period of the case study structure is considered as the ground motion intensity measure (*IM*).

2.3.   The Structural Performance Index

When only the structural modeling uncertainties are considered, the definition of structural capacity in this work is based on the limit state of severe damage as proposed by the Italian Code (OPCM [4], NTC [5,6]). That is, the

---

[7] http://www.isesd.cv.ic.ac.uk/ESD/Database/Database.htm

onset of critical behavior in the first element, characterized by member chord rotations larger than 3/4th of the corresponding ultimate chord rotation capacity. The structural demand is characterized by the intersection of the code-based inelastic design spectrum and the static pushover curve transformed into that of the equivalent SDOF system (capacity spectrum method, [7], Appendix C). As an index for the global structural performance, the ratio of structural demand to capacity is used [8].

When the ground motion uncertainty together with the modeling uncertainties are taken into account, the structural performance index is characterized based on the concept of cut-sets [9] in structural reliability. A structural cut-set is defined as a set of structural components that, once all of them have failed, they can transform the whole structure or part of it into a mechanism. Among the set of all possible cut-sets, the critical cut-set is the one that first forms a global mechanism. Therefore, the performance index is taken as the demand to capacity ratio of the strongest component of the weakest cut-set.

In this work, three types of global mechanism are considered: (a) ultimate rotation capacity in the columns (b) formation of soft stories (c) shear failure in the columns (Appendix E).

The component yield rotation, ultimate rotation and shear capacities are calculated according to the new Italian Unified Code (NTC, [5,6]) (Appendices B and E).

It should be noted that the structural performance in both cases signals failure when it is greater than unity and signals no structural failure when it is less than or equal to unity.

2.4.   The Effect of Uncertainty on Structural Risk Assessment

It can be argued that the particular realization of the vector of median material mechanical properties for the structure without defects (original design) would lead to approximately the median value for the distribution of the structural performance variable for the structure. This stems from the invariance property of the median and other percentiles under strictly

monotonic functions. However, the structural fragility analysis may not be characterized as a strictly monotonic function (i.e., different realizations of the vector of uncertain parameters could lead to the same value for the structural performance index). Nevertheless, it is presumed that the invariance properties might be better conserved for the median which has equal probability of being exceeded or not. However, the same property may not be quite as useful when also the structural defects are being considered. That is, it is more difficult to form the vector of median values for the parameters characterizing the construction details. In other words, the vector of median values is not going to correspond to the original design specifications.

As mentioned before, the structural model reflecting the original design configurations characterize the best-case in the set of all possibilities regarding structural defects. This leads to the conclusion that the median structural performance index for the structure with defects is going to be larger than the median for the structural performance index for the original structure (without defects).

3.   A Closed-Form Solution for Structural Reliability

The structural reliability or the probability of failure in the case of a structure with modeling uncertainties (no uncertainty in the ground motion) can be expressed by a Lognormal cumulative density function (CDF) as following:

$$P(Y(\underline{\theta}) > y) = 1 - \Phi\left(\frac{\log y - \log \eta_Y}{\beta_Y} \right) \qquad \text{Eq.4.3}$$

where Φ is the Gaussian cumulative distribution function, Y is the structural performance index and η_Y and β_Y are the median and the standard deviation (of the logarithm) for the probability distribution of the structural performance index (the parameters χ in equation 4.1).

3.1.   Uncertainty in Structural Materials

If only the uncertainty in material properties is being considered, $\eta_Y = \eta_{U1}$ (U_1 indicate the uncertainty related only to material properties) and the median can be approximated using a single structural analysis, where $\underline{\theta}$ is taken to be equal to vector of median material properties and without defects (values of structural details parameter corresponding to original design). The median value for the structural performance variable can be calculated as:

$$\eta_{Y(\underline{\theta})} \approx Y(\eta_{\underline{\theta}})$$ Eq.4.4

Supposing that the effect of uncertainties in the material properties is described by a Lognormal probability distribution, the best estimate value for $\beta_Y = \beta_{U1}$ can be calculated from the following formula using the Bayesian inference [7]:

$$p(\beta|Y) = k \cdot \beta^{-(n+1)} \cdot e^{-\frac{ns^2}{2\beta^2}}$$

$$k = \frac{(ns^2)^{n/2}}{2^{(n/2)-1} \cdot \Gamma(n/2)}$$ Eq.4.5

where the data Y is the structural performance measure evaluated for the set of n different realizations of the vector of uncertain parameters $\underline{\theta}$ related only to the mechanical properties of the materials (values of structural details parameter corresponding to original design). The best estimate for β_{U1} can be taken as the maximum likelihood estimate or the 84% percentile for the posterior probability distribution for β.

3.2.   Taking into Account Uncertainty in Structural Details

In order to take into account the effect of the uncertainty in structural detailing (indicated in the following with U_2), it is assumed that the median for

the posterior probability distribution is going to increase. Therefore, the effect of the uncertainties in the structural detailing on structural performance index can be expressed by a Lognormal probability distribution with median equal to $\eta_Y = \eta_{U2}$ and standard deviation equal to β_{U2}. Again using Bayesian inference, the posterior probability distribution for median and standard deviation can be written as:

$$p(\eta, \beta | Y) = k \cdot \beta^{-(n+1)} \cdot e^{-\frac{vs^2 + n(\log(\eta) - \overline{\log Y})^2}{2\beta^2}}$$

$$k = \sqrt{\frac{n}{2\pi}} \left[\Gamma\left(\frac{v}{2}\right) \right]^{-1} \left(\frac{vs^2}{2}\right)^{v/2}$$

Eq.4.6

where $Y = \{Y_1, \ldots, Y_n\}$ is the vector of n different realizations of the structural performance index, $v = n - 1$ and $\overline{\log Y} = \sum \log Y / n$. The best-estimate values for the median and standard deviation can be calculated either as the maximum likelihood pair for the posterior probability distribution function or based on a given (e.g., 84%) confidence contour.

It should be mentioned that the data Y is gathered by calculating the structural performance measure for the set of n realizations of the structural model generated by different realizations of both material mechanical properties and structural detailing parameters.

It should be noted that equation 4.6 is general and applicable also to the case in which only the uncertainty in structural materials properties are taken into account; in fact equation 4.5 is a special case of equation 4.6 assuming the median η is known.

3.3.   Taking into Account Uncertainty in Ground Motion Representation

The structural reliability in the presence of modeling uncertainties and uncertainties in the representation of the ground motion can be calculated from the following Lognormal CDF:

$$P(Y(\underline{\theta}) > y|S_a) = 1 - \Phi\left(\frac{\log y - \log \eta_{Y|S_a}}{\beta_{U_T}}\right)$$

Eq.4.7

where $\beta_{U_T} = \sqrt{\beta_{Y|S_a}^2 + \beta_{U_1}^2 + \beta_{U_2}^2}$ is the standard deviation for the probability distribution of the structural performance index and $\eta_{Y|Sa}$ is the median for the probability distribution of the structural performance index.

The terms $\beta_{Y|Sa}$, β_{U1} and β_{U2} represent the effect of the uncertainty in the ground motion representation, the uncertainty in the material properties and the uncertainty in structural details, respectively. It should be noted that is assumed that the probability distributions for these different types of uncertainty are independent.

The equation 4.7 yields the structural fragility that then has to be integrated with the hazard function for the spectral acceleration S_a, or for another adopted *IM*, in order to obtain the hazard function for the structural performance variable Y (the seismic risk curve).

Suppose that a selection of n ground motion records are used to represent the effect of ground motion uncertainty on the structural performance index. Let $S_{a,i}$ and Y_i represent the spectral acceleration and the performance index for the ground motion record i, respectively. The data pairs (Y, S_a) is gathered by calculating the structural performance measure for the set of n ground motion records applied at the structural model generated by different realizations of material mechanical properties and structural detailing parameters. The posterior probability distribution for standard deviation can be calculated as:

$$p(\beta_{UT}|Y,S_a) = \Gamma\left(\frac{\nu}{2}\right)^{-1} \cdot \left(\frac{\nu s^2}{2}\right)^{\frac{\nu}{2}} \cdot \beta_{UT}^{-(\nu+1)} \cdot e^{-\frac{\nu s^2}{2\beta_{UT}^2}}$$

Eq.4.8

where $vs^2 = \sum_{i=1}^{n}\left(\log Y_i - a - b\log S_{a,i}\right)^2$, that is the sum of the square of the residual for a linear regression (chapter III) of logY and logSa, $v = n - 2$ and a and b are the regression coefficients equal to:

$$a = \frac{\sum \log Y_i \sum \log S_{a,i}^2 - \sum \log S_{a,i} \sum \log Y_i \log S_{a,i}}{n\sum \log S_{a,i}^2 - \left(\sum \log S_{a,i}\right)^2}$$

$$b = \frac{n\sum \log Y_i \log S_{a,i} - \sum \log S_{a,i} \sum \log Y_i}{n\sum \log S_{a,i}^2 - \left(\sum \log S_{a,i}\right)^2}$$

Eq.4.9

The joint posterior probability distribution for the coefficients of the linear regression can be calculated as:

$$p(\omega|Y,S_a) = k\left[1 + \frac{(\omega - \hat{\omega})^T X^T X (\omega - \hat{\omega})}{vs^2}\right]^{-\frac{v+1}{2}}$$

$$k = \frac{\Gamma\left(\dfrac{n}{2}\right)\sqrt{n\sum \log S_{a,i}^2 - \left(\sum \log S_{a,i}\right)^2}}{vs^2\Gamma\left(\dfrac{1}{2}\right)^2\Gamma\left(\dfrac{n}{2} - 1\right)}$$

Eq.4.10

which is a *bivariate t-distribution* where X is a nx2 matrix whose first column is a vector of ones and is second column is the vector of log $S_{a,i}$; ω is the 2x1 vector of regression coefficients a and b.

The median and the standard deviation for the probability distribution for $Y|S_a$ can be taken equal to the maximum likelihood estimates $\eta_Y = a \cdot S_a^b$ and $\beta_{Y|S_a} = s$. The robust estimates for the expected value and the standard deviation of the failure probability can be obtained from equation 4.1 and 4.2 based on the product of the posterior probability distribution $p(\beta_{UT}|Y, S_a)$ and $p(\omega|Y, S_a)$, evaluated through equation 4.8 and 4.10 respectively, assuming that

they are independent; so in presence of modeling uncertainties and uncertainties in the representation of the ground motion the vector of parameters χ in equation 4.1 is equal to $\chi = (\omega, \beta_{UT}) = (\log a, b, \beta_{UT})$.

4.   Numerical Results

The methodology presented in the previous section is applied to the case study existing structure. In order to validate the simplified alternative method, the results of large sample simulations reported in chapter II are used.

4.1.   The Structural Reliability given the Design Spectrum

The probability distribution for the structural performance index *Y,* in the presence of uncertainty in material properties, is calculated in the work briefly discussed in chapter II [1] using the Monte Carlo simulation with $N_{sim} = 500$ samples.
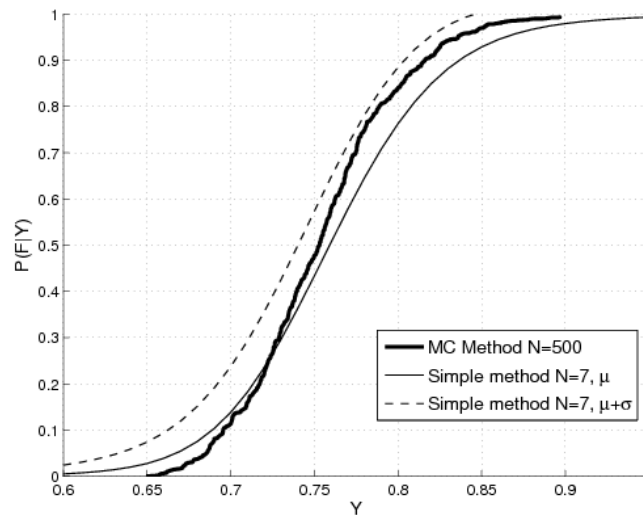
Figure 4.1: The structural fragility taking into account the uncertainties in the material properties, *N*=7.

The structural fragility is plotted in Figure 4.1 against the structural performance index Y in solid lines.

The data Y used for updating the probability distribution as in equation 4.6 has been obtained using Monte Carlo simulation with $N = 7$ samples. The result is plotted in Figure 4.1 in tiny solid line. In a similar manner, the robust standard deviation for the fragility curve is plotted in dashed lines in Figure 4.1.

It can been observed that with only 7 samples a confidence interval can be constructed for the fragility curve which contains the fragility curve obtained based on Monte Carlo simulation with 500 samples.

Figure 4.2 illustrates the same set of results based on a dataset of structural response for $N = 20$ model realizations.
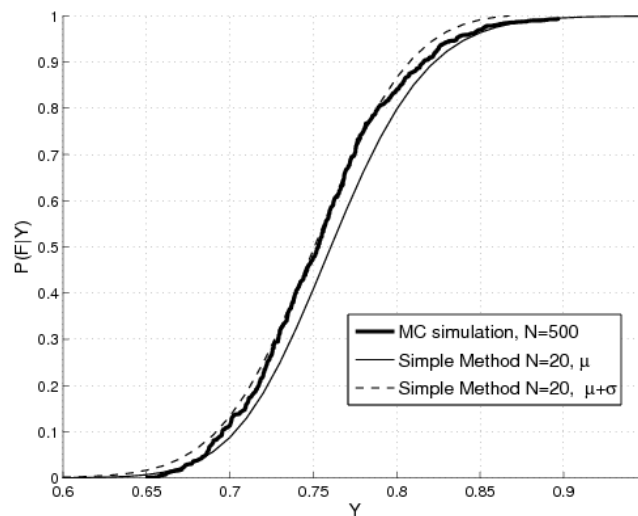
Figure 4.2: The structural fragility taking into account the uncertainties in the material properties, *N*=20.

It can be observed that the confidence interval based on a sample size of $N = 20$ narrows down with respect to the one based on $N = 7$.

The posterior probability distribution for β_Y is plotted in Figure 4.2 for both $n = 7$ and $n = 20$ simulations, using equation 4.6.
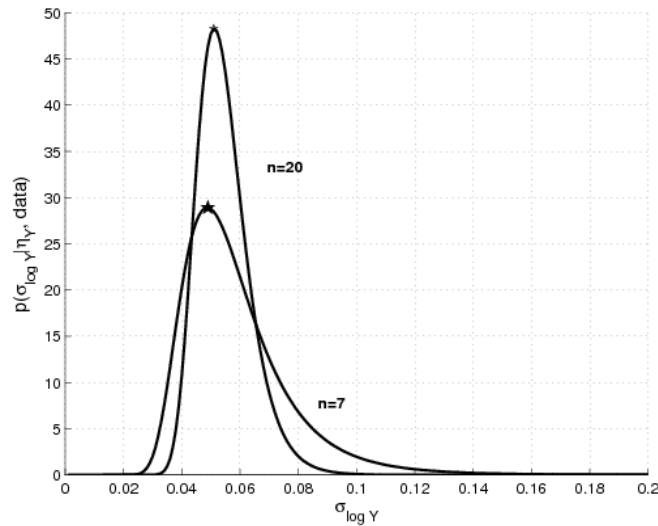
Figure 4.3: The probability distribution for β_Y.

The standard deviation is taken equal to the maximum likelihood estimator (MLE) shown in the figure for both cases. It can be seen that increasing the sample size reduces the width of the posterior distribution without a significant change in the MLE.

The probability distribution for the structural performance index Y in the presence of both uncertainties in the material properties and in the structural detailing parameters is calculated using the Subset Simulation and using $N = 400$ samples [1]. The fragility curve derived based on the results of Subset Simulation (the best-estimate) is plotted in Figure 4.4 in thick solid line. On the other hand, the robust estimate for the fragility curve is again calculated from equations 4.1 and 4.3 employing the joint posterior distribution calculated from equation 4.6 based on a data of $N = 20$ samples.

It should be noted that the $N = 20$ samples are generated using Monte Carlo simulation taking into account both uncertainties in the material properties and uncertainties in structural detailing.

The robust estimate for the fragility using the simple method (based on small-sample simulation) is plotted in Figure 4.4 in tiny solid line.

The expected value plus standard deviation for the simple method is also shown in Figure 4.4 in dashed lines.
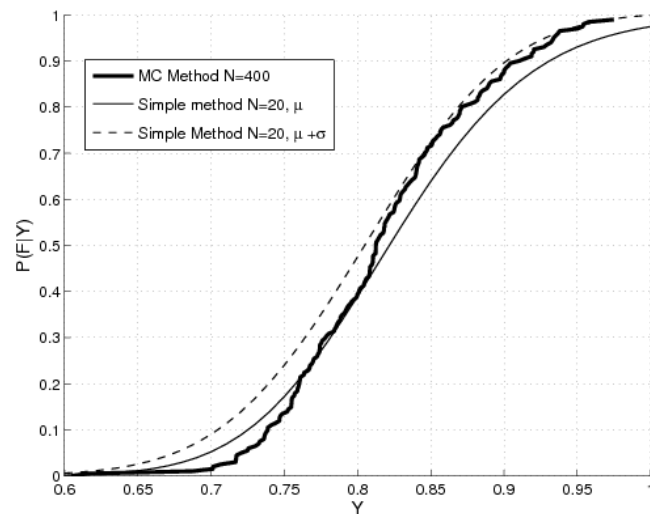
Figure 4.4: The structural fragility taking into account the uncertainties both in material properties and the structural detailing

It can be observed that the confidence interval constructed using the simple method roughly contains the Subset Simulation result.

4.2. The Structural Reliability taking into account the Ground Motion Uncertainty

Table 4.1 shows the list of ground motion used in order to take into account the record-to-record variability. As mentioned previously a set of 30 ground motion records are chosen from the European Strong-motion Database or ESD[8] for soil type B ($400 \leq Vs \leq 600$ m/s), with moment magnitude between 5.3 to 7.2 and the epicentral distance between 7 and 87km.

---

[8] http://www.isesd.cv.ic.ac.uk/ESD/Database/Database.htm

Table 4.1. The list of 30 selected ground motion records

Record	M_w	Fault Mechanism	Vs30 [m/s]	ED [km]	FD [km]	PGA [g]	$S_a(T_1)$ [g]
Valnerina	5.8	normal	?	23	21	0.04	0.03
Friuli, Italy-02	5.9	reverse	412	18	18	0.21	0.08
Preveza	5.4	thrust	?	28	7	0.14	0.10
Umbria	5.6	normal	546	19	19	0.21	0.02
Lazio Abruzzo	5.9	normal	?	36	28	0.07	0.05
Etolia	5.3	thrust	405	20	12	0.04	0.01
Kyllini	5.9	strike slip	490	14	11	0.15	0.15
Irpinia, Italy-01	6.9	normal	600	15	18	0.13	0.30
Potenza	5.8	strike slip	494	28	29	0.10	0.08
Ano Liosia	6.0	normal	411	20	9	0.16	0.06
Adana	6.3	strike slip	?	39	30	0.03	0.05
South Iceland	6.5	strike slip	?	15	10	0.21	0.13
Patras	5.6	strike slip	665	30	?	0.05	0.02
Friuli	6.5	thrust	?	42	34	0.06	0.22
Campano Lucano (o.c.1)	6.9	normal	472	48	33	0.11	0.25
Campano Lucano (o.c.1)	6.9	normal	529	16	13	0.16	0.31
Kalamata (o.c.1)	5.9	normal	486	10	0	0.22	0.48
Kalamata (o.c.1)	5.9	normal	399	11	0	0.24	0.48
Umbria Marche (o.c.1)	6.0	normal	546	11	1	0.52	0.56
Umbria Marche	6.0	normal	450	38	27	0.09	0.17
South Iceland (o.c.1)	6.5	strike slip	?	7	6	0.63	0.54
Duzce 1 (o.c.1)	7.2	oblique	662	26	13	0.13	0.18
Friuli	6.5	thrust	?	87	71	0.07	0.12
Campano Lucano (o.c.2)	6.9	normal	472	48	33	0.14	0.26
Campano Lucano (o.c.2)	6.9	normal	529	16	13	0.18	0.31
Kalamata (o.c.2)	5.9	normal	486	10	0	0.30	0.63
Kalamata (o.c.2)	5.9	normal	399	11	0	0.27	0.51
Umbria Marche (o.c.2)	6.0	normal	546	11	1	0.46	0.64
South Iceland (o.c.2)	6.5	strike slip	?	7	6	0.51	0.74
Duzce 1 (o.c.2)	7.2	oblique	662	26	13	0.16	0.14

For each ground motion record a different realization of the vector $\underline{\theta}$ of the structural modelling parameters is considered.

The structural performance index Y is calculated based on the concept of the critical cut-set [9] considering both the rotation and the shear capacity in the sections. It turns out the shear failure in columns dominates and the regression coefficients are calculated from equation 4.7 as $a = 1.1366$ and $b = 0.24$.

The posterior probability distribution for the standard deviation is calculated from equation 4.8; in Figure 4.5 is shown the obtained distribution by which it can be observed that the MLE is equal to $\beta_{Y|Sa} = 0.10$.
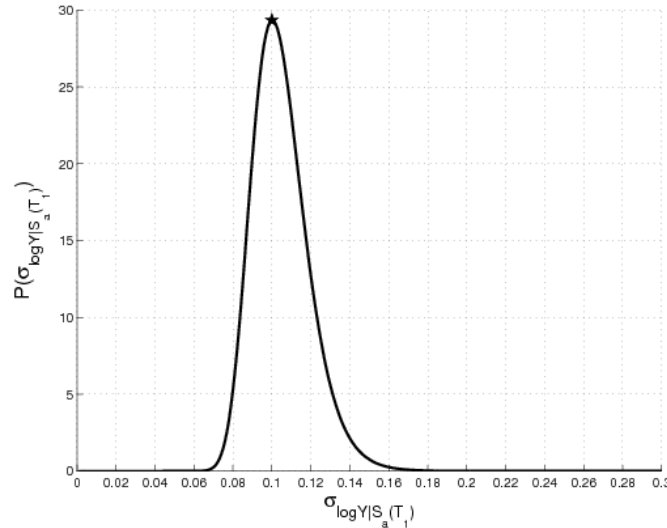
Figure 4.5: The probability distribution for $\beta_{Y|Sa}$.

The joint posterior probability distributions for *a* and *b* is obtained from equation 4.10; the coefficients of regression and their posterior probability distributions are calculated in two cases: (a) based on the set of 30 ground motion records not considering the modeling uncertainties, and (b) based on the set of 30 ground motion but generating realizations of structural model using Monte Carlo simulation taking into account both the uncertainties in the material properties and the uncertainties in the structural detailing. In both cases, the robust estimate and the standard deviation of the structural fragility are calculated from equations 4.1 and 4.2 employing the probability of failure from equation 4.7 and the product of the posterior probability distributions for the coefficient of regression and the standard deviation from equations 4.10 and 4.8, respectively.

The expected value for the probability of failure in case (a) is plotted in Figure 4.6 in tiny solid line. Moreover, in the same figure, the expected value

plus standard deviation for the probability of failure in case (a) is plotted in tiny dashed line.
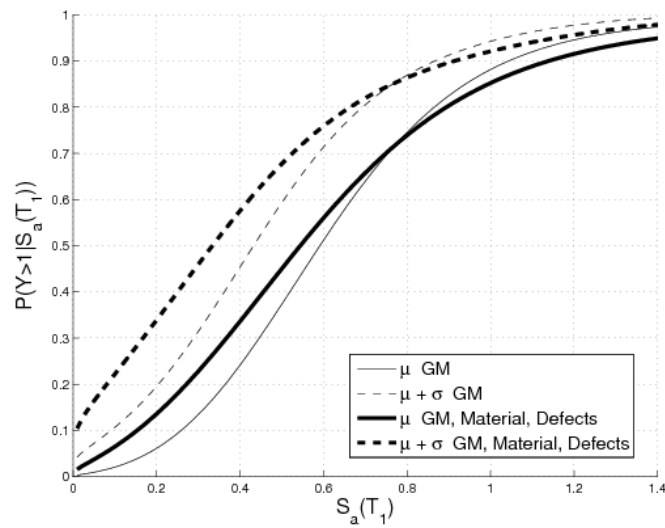
Figure 4.6: Robust estimate for the failure probability taking into account the record-to-record variability considering or not modeling uncertainties

The robust failure probability and the standard deviation are plotted respectively in the same figure with thick solid line and dashed line also considering case (b). From the confidence intervals obtained for the failure probability in case (a) and case (b), it can be observed that the presence of structural modeling uncertainties leads to a significant increase in the probability of failure. This confirms that the structural modeling uncertainties can be quite significant in the existing buildings.

5.   Conclusions

In this chapter a method is presented for robust interval estimation of the structural reliability taking into account the modeling uncertainties in existing RC buildings.

This method employs small sample structural analysis results in a Bayesian inference framework leading to posterior probability distributions for the median and standard deviation for the structural performance index.

The posterior probability distributions for the statistical parameters can be used to obtain a robust confidence interval for the probability of failure. The robust confidence interval is obtained by calculating the posterior (robust) expected value and the standard deviation of the probability of failure based on the posterior probability distribution(s).

It should be noted that the best-estimates for parameters of interest are not necessarily the maximum likelihood point estimates; they could also be interval estimates reflecting the significant uncertainty in parameter estimation due to small data sample sizes.

The results are presented in two cases, (a) for a specific representation of the ground motion uncertainty, (b) considering the record-to-record variability in ground motion.

In case (a) for which the results of extensive simulations were already available, the small-sample methods succeeded in reproducing the structural fragility curves.

In case (b), the fragility curves obtained using the small-sample inferences, make it possible to compare the influence of structural modeling uncertainties to that of the ground motion representation. They reconfirm the importance of taking into account the uncertainty both in the material properties and structural detailing in the structural reliability evaluations for an existing building.

It is demonstrated how the Bayesian framework for inference can be implemented, together with both static and dynamic analysis method, for providing confidence intervals for the structural reliability.

6.   References

[1]   Jalayer F, Iervolino I, Manfredi G. Structural modeling uncertainties and their influence on seismic assessment of existing RC structures. Under Review *Structural Safety* 2008.

[2]   Verderame GM, Manfredi G, Frunzio G. Le proprietà meccaniche dei calcestruzzi impiegati nelle strutture in cemento armato realizzate negli anni 60. *X Congresso Nazionale \L'ingegneria Sismica in Italia"*, Potenza e Matera, 9-13 Settembre 2001a [in Italian].

[3]   Verderame GM, Stella A, Cosenza E. Le proprietà meccaniche degli acciai impiegati nelle strutture in cemento armato realizzate negli anni '60. *X Convegno Nazionale L'Ingegneria Sismica in Italia"*, Potenza e Matera 9-13 Settembre 2001b [in Italian].

[4]   Ordinanza del Presidente del Consiglio dei Ministri (OPCM) n. 3519 (2006). Criteri per l'individuazione delle zone sismiche e la formazione e l'aggiornamento degli elenchi delle medesime zone. *Gazzetta Ufficiale della Repubblica Italiana* 108, 2006 (*in Italian*).

[5]   MIN.LL.PP, DM 14 gennaio, *Norme Techniche per le Costruzioni*. Gazzetta Ufficiale della Repubblica Italiana, 29, 2008 (*in Italian*).

[6]   MIN.LL.PP, DM 14 gennaio, *Istruzioni per l'applicazione delle Norme Techniche delle costruzioni*. Ministero della Infrastruttura, 29, 2008 (*in Italian*).

[7]   Fajfar, P. "Capacity spectrum method based on inelastic demand spectra", *Earthquake Engineering and Structural Dynamics*; 28:979–93, 1999.

[8]   Jalayer F, Franchin P, Pinto PE. A scalar damage measure for seismic reliability analysis of RC frames. *Earthquake Engineering and Structural Dynamics*. 36:2059-2079, 2007.

[9]   Ditlevsen O, Masden H. *Structural Reliability Methods*, June 1996; John Wiley & Sons Inc.

[10]   Box GEP, Tiao GC. Bayesian Inference in Statistical Analysis. *Wiley Classics Library Edition*, 1992.

Chapter V

An Alternative Performance–Based Safety–Checking Format

1.   Introduction

A fully probabilistic method coupled with non-linear dynamic analysis would be the best method in order to incorporate all relevant sources of uncertainties in the assessment of existing RC structure; however pragmatism oblige the adoption of a simplified format, calibrated on the fully probabilistic method, able to put the engineer in the condition to approach the problem by incorporating the uncertainties of different nature in the assessment procedure [1].

This chapter focuses on the assessment of structural reliability for different knowledge levels employing a simple method with a format similar to the *Load-Resistance Factor Design* (LRFD) [2] suitable for code implementation.

The results obtained with the simple method employed herein are confronted and supported by the results obtained through probability-based methods consisting of standard Monte-Carlo simulation (chapter II) and the efficient simulation-based method (chapter IV).

For each knowledge level, the effect of tests and inspections is included by employing the Bayesian updating framework.

The Bayesian framework for probabilistic inference seems to be a perfect vehicle for taking into account the results of tests and inspection in updating the structural model.

In chapter II has been briefly discussed a previous work by Jalayer et al. 2008 [3] in which the authors demonstrate how the simulation methods based on Bayesian updating can be used to both update the structural reliability and the probability distribution for the modeling parameters, in the presence of test and inspection results. However, the application of the simulation schemes requires a large number of structural analyses and there seems to be a need for less computationally intensive methods for updating the structural model and structural reliability. Thus, the efficient Bayesian simulation-based method for robust estimation of structural reliability, described in details in chapter IV, has been adopted. This method exploits a relatively small number of structural analyses in order to yield the *robust reliability* for the structure. The term robust refers to the fact that the reliability is calculated taking into account all possible structural models and their relative plausibilities.

In this chapter a probabilistic and performance-based approach is proposed as an alternative to the confidence factor approach for code-based recommendations; this format is already adopted in the American Department of Energy Guidelines DOE-1020 [4] and in SAC-FEMA guidelines [5,6,7,8].

This LRFD-like simplified approach leads to an analytic closed-form solution which compares the factored demand against factored capacity with a specified confidence level for various knowledge levels.

For seismic assessment using static analyses, an analogous formulation can be adopted which yields the structural performance parameter corresponding to a certain confidence.

2.   The Knowledge Levels

Recent codes such as Eurocode 8 (EC8, [9]) seem to synthesize the effect of structural modeling uncertainties in the confidence factors (CFs) that are applied to mean material property values. The CFs are classified and tabulated as a function of discrete knowledge levels (KLs) acquired based on the results

of specific in-situ tests and inspections. The code approach based on the CF seem to provide a level of conservatism in the assessment of existing buildings, reducing mean material property values.

The KLs are determined based on the amount of tests and inspections performed on the building (see Table I.2. of the introduction)

In this chapter four distinct knowledge levels are taken into consideration. The first knowledge level, referred to as KL_o describes the state of the knowledge about the structure before the in-situ tests and inspections are performed. The other three knowledge levels KL_1, KL_2 and KL_3 are characterized based on the Eurocode recommendations, respectively, limited, extended and comprehensive levels of knowledge.

3.   The Methodology

In this section a methodology for taking into account the sources of modeling uncertainties in the probabilistic performance assessment of existing RC buildings is presented.

It should be mentioned that since this research effort mainly focuses on the code-based procedure involving the application of confidence factors, the uncertainties in the capacity models are not taken into account. This is because the Eurocode 8 [9] takes into account the uncertainty in the capacity model separately by applying a less-than-unity safety factor (γ_{el}).

3.1.   Load and Resistance Factor Design Framework

The design/assessment of a structure depends upon predicted loads and the structure's capacity to resist them. Both loads and structural capacity have various sources and levels of uncertainty.

Engineers have historically compensated for these uncertainties by using experience and subjective judgment. On the other hand, these uncertainties can be quantified using probability-based methods aimed at achieving specific performance objectives.

The intention of LRFD has been to separate uncertainties in loading from uncertainties in resistance and then to use procedures from probability theory to ensure a prescribed margin of safety.

Figure 5.1 shows probability density functions (PDFs) for load effect, Q, and resistance, R.
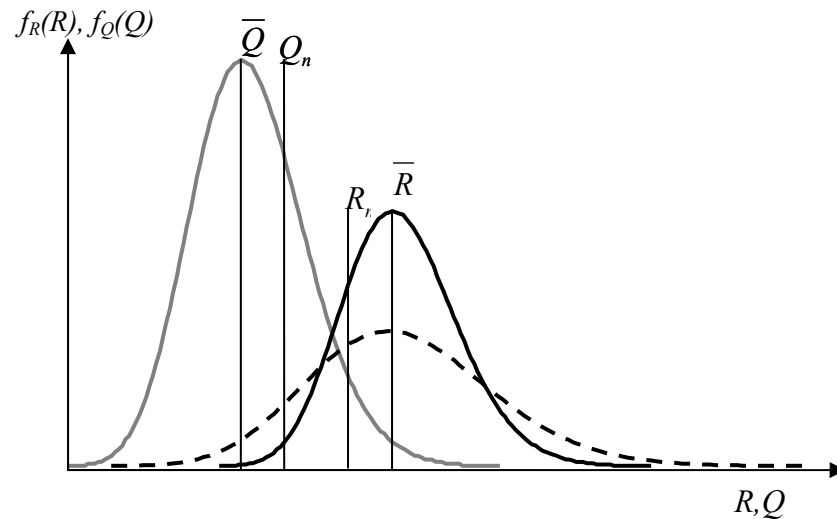
Figure 5.1: Probability density functions for load effect, Q, and resistance, R.

Since failure is defined as the load effect exceeding the resistance, the probability of failure ($P_f = P [R < Q]$) is related to the extent to which the two probability density functions overlap (although not simply to the area of overlap).

In LRFD, partial safety factors are applied separately to characteristic central values for load and resistance. Resistance is reduced and loads are increased, by multiplying the corresponding characteristic (or nominal) values by factors called strength (resistance) and load factors, respectively. Using this approach, the factored (i.e., reduced) strength of a structure must be larger than a linear combination of the factored (i.e., increased) loads. The nominal values

(e.g., the nominal strength, R_n) are those calculated by the specific calibrated design method and are not necessarily the means ($\overline{R}$ and $\overline{Q}$).

Then, for a given structure design based on the application of resistance and load factors, the probability of failure, that is, the probability that the factored loads exceed the factored resistances, should be smaller than the prescribed value.

The importance of the LRFD format lies in the fact that the load and resistance factors are related to the uncertainty in load and resistance. Therefore, a factor of safety that is calculated as the ratio of factored resistance to factored load, already includes the effect of uncertainties (Figure 5.1), as opposed to a safety that is calculated as the ratio of median resistance to median load.

3.2.   Demand and Capacity Factor Design Framework

As a proposal alternative to the confidence factor approach for code-based recommendations, a probabilistic and performance-based approach, adopted in the American Department of Energy Guidelines DOE-1020 [4] and in SAC-FEMA guidelines [5,6,7,8], is revised. This LRFD-like simplified approach leads to an analytic and closed-form solution which compares the factored demand against factored capacity.

$$FD \leq FC \qquad\qquad\qquad Eq.5.1$$

The factored demand and capacity are respectively equal to median demand D and median capacity C multiplied by some factors.

$$D \cdot \gamma \leq C \cdot \phi \qquad\qquad\qquad Eq.5.2$$

The magnifying demand factors γ and the de-magnifying capacity factors ϕ take into account all sources of uncertainty, such as record-to-record (ground

motion) variability, structural modeling uncertainty and the uncertainty in the capacities. This approach, that is also known as the *Demand and Capacity Factor Design* (DCFD) [10] for its similarity with the LRFD (AISC, LRFD Code) [2], takes into account the overall effect of the various types of uncertainties on a global structural performance parameter.

The alternative proposals discussed herein can all be implemented in order to estimate the parameters within the DCFD framework for safety checking of existing buildings for various knowledge levels.

In this section the adopted DCFD format is briefly described starting from the most general case that also includes the uncertainty in ground motion representation employing non-linear dynamic analysis, in particular the cloud method presented in chapter III. However an alternative performance-based safety-checking format is also presented herein employing non-linear static analysis.

3.2.1. DCFD and PBEE Frameworks

Adopting the probabilistic performance-based assessment described in chapter II (PBEE), a probabilistic performance objective can be expressed by ensuring that the MAF (mean annual frequency) λ_{LS} of structural demand D reaching or exceeding structural capacity C_{LS} for a limit state is smaller than or equal to a tolerable annual frequency P_0:

$$\lambda_{LS} = \lambda\left(D > C_{LS}\right) \le P_0 \qquad\qquad \text{Eq.5.3}$$

where λ_{LS} is also referred to, more briefly, as the limit state probability and/or failure probability[9]. It should be noted that the demand and capacity terms appearing in the performance objective are global variables.

---

[9] For an event with very small probability of occurrence, such as a strong earthquake, the numerical value of MAF of occurrence and the probability of occurrence in one year are very close.

In the framework of DCFD the performance objective in equation 5.3 is represented in the following form:

$$FD(P_0) \leq FC \qquad\qquad \text{Eq.5.4}$$

where $FD(P_0)$ is the factored demand at the allowable probability level P_0 and FC is the factored capacity [11].

The structural performance parameter is the one adopted in all the other chapters, that is the critical demand to capacity ratio denoted as Y. As stated previously, this ratio assumes the value of unity on the verge of the limit state function. By adopting this structural performance parameter, the structural reliability can be expressed as the probability that Y assumes a value greater than unity:

$$P_f = P(Y > 1) \qquad\qquad \text{Eq.5.5}$$

Introducing the critical demand to capacity ratio Y, the performance objective in equation 5.3 is expressed as:

$$\lambda(Y > 1) \leq P_0 \qquad\qquad \text{Eq.5.6}$$

Consequently the performance objective in equation 5.4 is expressed as:

$$FY(P_0) \leq 1 \qquad\qquad \text{Eq.5.7}$$

Under the assumption that:

1) the spectral acceleration hazard is described as a power-law function of the spectral acceleration level (the chosen *IM*):

$$\lambda_{S_a}\left(S_a\right) = k_0 \cdot S_a^{-k} \qquad\qquad \text{Eq.5.8a}$$

2) the critical demand to capacity ratio can be expressed as:

$$Y = \eta_{Y|S_a} \cdot \varepsilon_{Y|S_a} \qquad\qquad \text{Eq.5.8b}$$

where it is assumed that the median is a power-law function of the spectral acceleration level ($\eta_{Y|S_a} = a \cdot S_a^b$) and that $\varepsilon_{Y|S_a}$ is described by a unit-median Lognormal PDF with fractional standard deviation equal to $\beta_{Y|S_a}$.

than the performance objective in equation 5.7 can be derived as:

$$\eta_{Y|S_a^{P_0}} \cdot e^{\frac{1}{2}\frac{k}{b}\beta^2_{Y|S_a^{P_0}}} \le 1 \qquad\qquad \text{Eq.5.9}$$

where $\eta_{Y|S_a^{P_0}}$ and $\beta_{Y|S_a^{P_0}}$ are median and fractional standard deviation of the critical demand to capacity ratio at a spectral acceleration equal to $S_a^{P_0}$ which has mean annual frequency of exceedance equal to P_0.

It should be noted that the expression in the first term of the equation 5.9 is based on a property of the lognormal variables, where the expected value of a lognormal variable is equal to its median times the exponential of half of the squared standard deviation [12].

The performance objective in equation 5.9 compares the factored critical demand to capacity ratio at allowable probability P_0 against unity.

A single variable ε_{UC} is employed to represent the (global) effect of component modelling uncertainties on the fragility curve and it is assumed that ε_{UC} is Lognormal with unit median and fractional standard deviation β_{UC}.

An extended formulation of the DCFD format in the presence of structural modelling uncertainties can be derived by assuming that the median critical demand to capacity ratio can be expressed as follows:

$$\eta_{Y|S_a} = \eta_{Y|S_a,\varepsilon_{UC}=1} \cdot \varepsilon_{UC} \qquad\qquad \text{Eq.5.10}$$

where $\eta_{Y|S_a,\varepsilon_{UC}=1}$ is the median critical demand to capacity ratio for a given S_a and under the assumption that there is no capacity modelling uncertainty.

It should be noted that it is assumed that the uncertain variable ε_{UC} representing the global effect of modelling uncertainty is independent of the S_a level.

The DCFD performance objective in terms of the critical demand to capacity ratio in the presence of capacity modelling uncertainty can be derived as:

$$\eta_{Y|S_a^{P_0},\varepsilon_{UC}} \cdot e^{\frac{1}{2}\frac{k}{b}\beta^2_{Y|S_a^{P_0}}} \cdot e^{\frac{1}{2}\frac{k}{b}\beta^2_{UC}} \leq 1 \qquad\qquad \text{Eq.5.11}$$

3.2.2. Non-Linear Static Analysis

In the case of static analyses, the capacity spectrum method (CSM) [13] is used to obtain the global demand to capacity ratio (Appendix C). Moreover, at the onset of the limit state, the shear capacity of the structural components is also verified by calculating the shear demand to capacity ratio for the structural components (Appendix E). The overall structural performance parameter is finally taken as the larger between the critical shear component demand to capacity ratio and the overall demand to capacity ratio derived from CSM.

The expected value for the critical demand to capacity ratio can be calculated from the following (assuming that Y is described by a Lognormal distribution):

$$\eta_Y \cdot e^{\frac{1}{2}\beta^2_Y} \leq 1 \qquad\qquad \text{Eq. 5.12}$$

where η_Y is the median and β_Y is the standard deviation of the logarithm for the probability distribution for the structural performance parameter *Y*. The parameter β_Y represents the overall effect of uncertainties on the probability distribution for the structural performance parameter.

In other words, the inequality in equation 5.12 is checks whether the expected (mean) value for the structural performance parameter is less than or equal to unity. Alternatively, one can calculate a given percentile %x of the structural performance parameter *Y* and check to see whether it is less than or equal to unity:

$$\eta_Y \cdot e^{\Phi^{-1}(x)\beta_Y} \leq 1 \qquad\qquad \text{Eq. 5.13}$$

where $\Phi^{-1}(x)$ is the inverse Gaussian cumulative density function (CDF) for percentile x.

3.2.3. Non-Linear Dynamic Analysis

In the case of dynamic analyses, the *cut-set* [14] concept in reliability theory is employed to find the critical component demand to capacity ratio that takes the structure closer to the onset of the limit state. This critical demand to capacity ratio corresponds to the strongest component of the weakest structural mechanism [11]:

$$Y = \min_l \max_j \frac{D_{lj}}{C_{lj}} \qquad\qquad \text{Eq. 5.14}$$

where l is the structural mechanism index considered and j is the component index within l^{th} mechanism. In this case the mechanisms considered involve the ultimate chord rotation in the components, the formation of global mechanisms (e.g., soft story and beam mechanisms) and the component shear capacity.

When the uncertainty in the ground motion representation (the record-to-record variability) is considered, the DCFD formulation is expressed as:

$$\eta_Y(P_o) \cdot e^{\frac{1}{2}\frac{k}{b}(\beta^2_{Y|S_a} + \beta^2_{UC})} \leq 1 \qquad \text{Eq. 5.15}$$

where P_o is an acceptable threshold for structural failure probability and $\eta_Y(P_o)$ is the median structural performance parameter corresponding to the acceptable probability P_o. The terms $\beta_{Y|Sa}$ and β_{UC} represent the effect of record-to-record (Ground Motion) variability and structural modeling uncertainties, respectively, on the total dispersion in the structural performance parameter given spectral acceleration. In the same manner as the static case, the inequality in equation 5.7 can be verified with a certain %x confidence:

$$\eta_Y(P_o) \cdot e^{\frac{1}{2}\frac{k}{b}\beta^2_{Y|S_a}} \leq e^{-\Phi^{-1}(x)\sqrt{\beta^2_{Y|S_a} + \beta^2_{UC}}} \qquad \text{Eq. 5.16}$$

where $\Phi^{-1}(x)$ is the inverse Gaussian cumulative density function (CDF) for percentile x.

3.3.   Characterization of the Uncertainties for KL$_0$

It is assumed that the vector $\underline{\theta}$ represents all the uncertain parameters considered in the problem.

Typically, the uncertainties present in a seismic assessment problem can be classified in different groups, namely, the uncertainties in the representation of the ground motion, the modeling uncertainties, associated with the structural finite element model and the component capacity models, and the uncertainties

in the structural modeling parameters. As stated in the previous chapters this work focuses on the uncertainty in the structural modelling parameters related to the available information on the characteristics of existing buildings. This is the type of uncertainty that is believed to be addressed implicitly by the application of confidence factors. Two groups of structural modeling uncertainties are considered, the uncertainty in the mechanical property of materials and the uncertainty in the structural construction details.

3.2.1. Materials

The parameters identifying the prior probability distributions for the material mechanical properties (concrete strength and the steel yielding force) have been based on the values typical of the post world-war II construction in Italy [15,16]. The parameters that are used to define the Lognormal probability distributions for the material properties are the same adopted in the previous chapter and reported in chapter II, Table 2.2.

3.2.2. Structural Details

One of the main characteristics of the construction details is that possible deviations from the original configurations are mostly taken into account in those cases leading to undesirable effects. This justifies why the uncertainties related to construction details are usually referred to as the *structural defects*.

The prior probability distributions for the structural detailing parameters can be defined based on qualitative prior information coming from expert judgment or based on *ignorance* in the extreme case [3]. Table 5.1 shows (for illustrative purpose only) the example specifications used to construct the prior probability distributions for the structural detailing parameters.

Table 5.1. The uncertainties in details (systematic).

Defects	Distribution	Type
Insufficient anchorage (beams)	Uniform [0.50,1]	Systematic over floor
Error in diameter (columns)	Uniform [0.7697,1]	Systematic over floor and section type
Superposition (columns)	Uniform [0.75,1]	Systematic over floor
Errors in configuration (columns)	Uniform [0.75,1] [0.67,1]	Systematic over floor and section type
Absence of a bar (beams)	Uniform [0.70,1] [0.69,1] [0.60,1]	Systematic over floor and section type
Stirrup spacing (beams typeI)	Uniform [15cm, 30cm]	Systematic
Stirrup spacing (beams typeII)	Uniform [20cm, 35cm]	Systematic
Stirrup spacing (columns)	Uniform [20cm, 35cm]	Systematic

It should be noted that, since the focus of this work is on the procedure for seismic assessment given the knowledge level, the prior probability distribution characteristics shown in Table 5.1 are merely for illustrative purposes. Therefore, a thorough characterization of the prior probability distributions for the structural defects is out of the scope of this work. Later on, in the next chapter, it is shown how the prior probability distributions for construction details can be characterized based on qualitative and collective expert opinion.

Anyway, Table 5.1 shows a list of possible defects, their probability distribution and correlation characteristics. For the construction details regarding the rebar, the uncertain parameter is a less-than-unity factor which will be applied to the steel area. That is why the maximum value for the uncertain parameters related to longitudinal rebar defects is equal to unity.

3.2.3. Ground Motion

In order to take into account the uncertainty in the representation of the ground motion, the same set of 30 ground motion records chosen from the European Strong-motion Database or ESD[10] for soil type B ($400 < V_s < 600$ m/s) adopted in the previous chapter are used (moment magnitude between 5.3 to 7.2 and the epicentral distance between 7 and 87 km).

The acceleration spectra for the original (unscaled) selected records are plotted in Figure 5.2 together with to code spectrum defined by Eurocode for the site of interest.
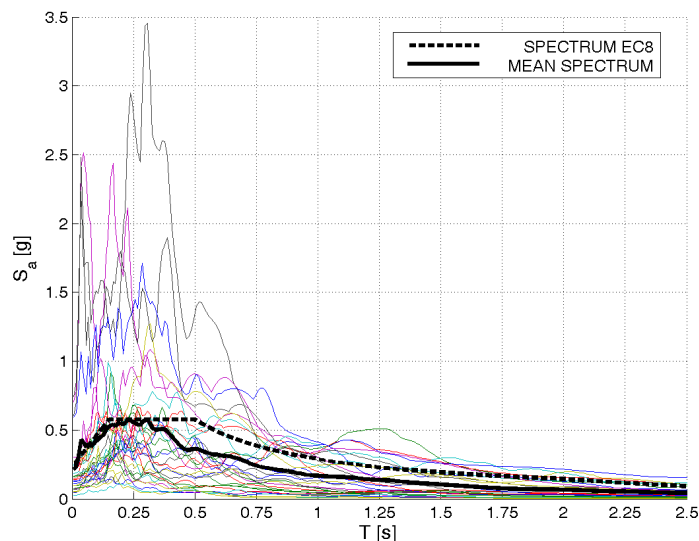
Figure 5.2. Acceleration spectra (30 records, unscaled).

---

[10] http://www.isesd.cv.ic.ac.uk/ESD/Database/Database.htm

3.4.   Updating the Probability Distribution

The probability distributions for the structural modeling parameters can be updated employing the Bayesian framework for inference.

It is assumed that the material properties are homogeneous across each floor or construction zone. Therefore, the material property value assigned to each floor can be thought of as an average of the material property values across the floor/zone in question. The results of tests and inspections for each floor can be used to update the probability distribution for the mean material property across the floor. Figure 5.3 illustrates an example where the test results for concrete strength have all verified the nominal value (f_c = 165 kg/cm^2) for different levels of knowledge. It can be observed that the updated curve has the same median but has its dispersion reduced as the amount of data increases. In the following the updating procedure for the concrete strength f_c is demonstrated; however, the exact same procedure is applied for steel yielding strength f_y.

Let $D = \{D_i : i = 1 : N\}$ denote the set of data available for the concrete strength for a given construction zone. Assuming that the data measurements contain no errors[11], the updated probability distribution for mean concrete strength across the floor can be calculated using the Bayes formula:

$$p(f_c \mid D) = \frac{p(D \mid f_c) p(f_c)}{\int p(D \mid f_c) p(f_c) df_c}$$

Eq. 5.17

---

[11] The consideration of measurement errors can also be implemented in the Bayesian updating procedure. For example for a given data measurement denoted by $\hat{D}$, the probability distribution for $\hat{D}$ given the exact value D can be denoted by $p(\hat{D} \mid D)$. Therefore, the likelihood for data measurement $\hat{D}$ given the mean concrete strength f_c is known can be calculated as: $p(\hat{D} \mid f_c) = \int p(\hat{D} \mid D) p(D \mid f_c) dD$, (assuming that the measurement error does not depend on f_c).

where, *p(f_c)* denotes the prior probability distribution for the mean concrete strength across the construction zone. For example, in this case it can refer to the characterization of the uncertainty in concrete strength before the tests are conducted for the knowledge level KL_o; that is the lognormal distribution described in Table 5.3.

Table 5.3. Probabilistic characterization of the mechanical property of RC.

Variable	Distribution	Mean [kg/cm^2]	COV
f_y	LogNormal	165	0.15
f_c	LogNormal	3200	0.08

Moreover, assuming that the data are independent, the likelihood $p(D|f_c)$ can be written as:

$$p(D \mid f_c) = \prod_{i=1}^{N} p(D_i \mid f_c) \qquad \text{Eq. 5.18}$$

The likelihood functions $p(D_i \mid f_c)$ are also assumed to be lognormal probability distribution with median value equal to f_c and standard deviation of the logarithm equal to the value tabulated in Table 5.3.

Figure 5.3 illustrates the probability distribution of the mean concrete strength value across the construction zone for the knowledge levels, KL_o, KL_1, KL_2 and KL_3 based on the extreme hypothesis that all the test results confirm the nominal (median) value.

It should be mentioned that such an extreme hypothesis is considered for the purpose of parameter studies on the effect of test results. Otherwise, the methodology is general with respect to the outcome of the test results. It can be observed from the figure that standard deviation for the updated probability distribution for each knowledge level decreases across increasing knowledge levels while the median value remains invariant.
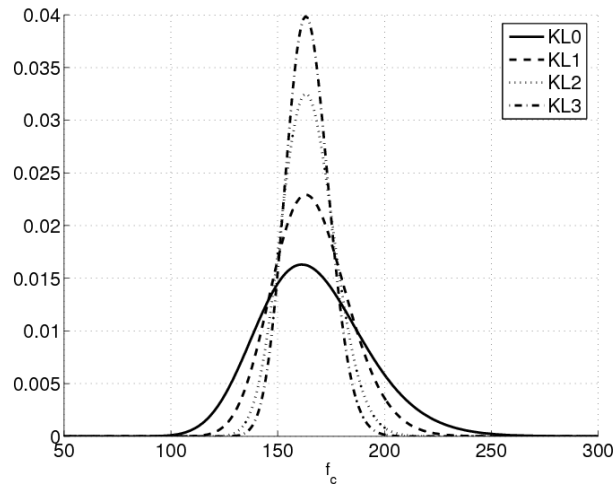
Figure 5.3. The prior and the updated probability distributions for concrete for different knowledge levels.

With regard to the structural detailing parameters, a slightly different approach is employed. Assuming that the probability of not having a construction defect in a member is equal to f, the probability distribution for f can be updated using the test results. If the test results indicate that of n cases observed n_d of them demonstrate a defect, the probability distribution for f can be also updated according to the Bayes formula:

$$p(f \mid D) = \frac{p(D \mid f)p(f)}{\sum_f p(D \mid f)p(f)} \qquad\qquad \text{Eq. 5.19}$$

where $p(f)$ is the prior probability distribution for f and $p(D|f)$ is the likelihood function for the data D given the value of f.

In the absence of prior information it can be assumed that $p(f)$ is a uniform distribution from 0 to 1. Use can be made of expert judgment and experience in order to limit the lower and the upper bounds for the defect probability f. The likelihood function can calculated using the binomial distribution:

$$p(D\,|\,f) = \binom{n}{n_d}(1-f)^{n_d}\,f^{\,n-n_d} \qquad\qquad \text{Eq. 5.20}$$

Figure 5.4 illustrates the prior probability distribution for the spacing between the shear reinforcement together with updated distribution based on the extreme hypothesis that all of the test results verify the design value (s = 15 cm).
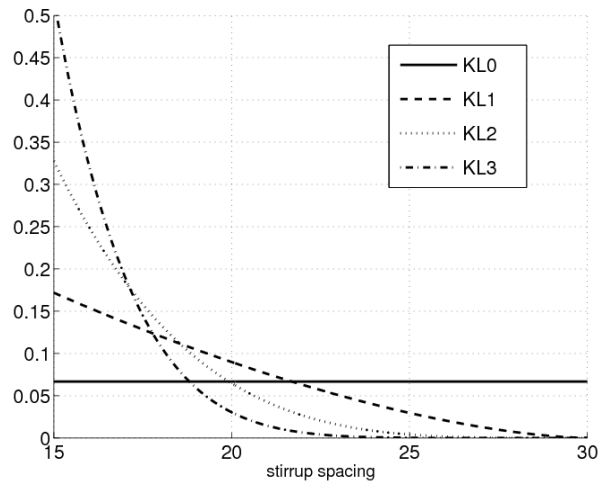
Figure 5.4. The uniform prior and the updated probability distribution for the distance between shear reinforcement.

It can be observed that the consideration of the test data focuses more narrowly the probability distribution around the design value.

Figure 5.5 displays the prior distribution on the anchorage effectiveness factor.
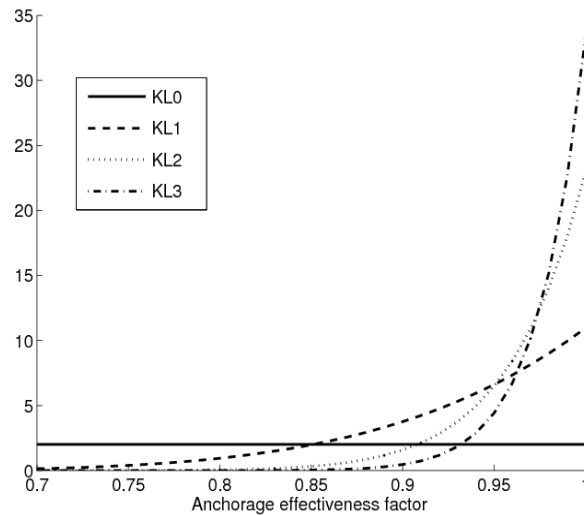
Figure 5.5. The uniform prior and the updated probability distribution for the anchorage effectiveness factor.

The figure also shows the updated probability distributions after the test results for the three knowledge levels verify the design value (i.e., effectiveness factor equal to unity).

The same as the probability distribution for stirrup spacing, it can be observed that, across the increasing knowledge levels, the probability distributions become more and more focused around the nominal value.

3.5.   Using the Efficient Method for Estimating the Robust Reliability

The efficient Bayesian method presented in chapter IV is in this chapter implemented in order to estimate the robust reliability of the case study structure [17].

As stated previously, if the probability of failure is described by an analytic probability distribution with parameters χ (e.g., median and standard deviation of the lognormal distribution) denoted by $P(F|\chi)$, given the set of parameters, the expected value (or the robust estimate) for the probability of failure, given a set of values Y for the structural performance index, can be expressed as:

$$E[P(F \mid D)] = \int_{\Omega} P(F \mid \chi) p(\chi \mid D) d\chi \qquad \text{Eq. 5.21}$$

where $p(\chi \mid D)$ is the posterior probability distribution for the set of parameters χ given the data D and Ω is the space of possible values for χ. In a similar way, the robust variance for the probability of failure can be calculated as:

$$\sigma_{P(F\mid D)} = E[P(F \mid D)^2] - E[P(F \mid D)]^2 \qquad \text{Eq. 5.22}$$

In particular, the structural reliability or the probability of failure in the case of a structure with modeling uncertainties (no uncertainty in the ground motion) can be expressed by a Lognormal CDF:

$$P(Y(\underline{\theta}) > y) = 1 - \Phi\left(\frac{\log y - \log \eta_Y}{\beta_Y}\right) \qquad \text{Eq.5.23}$$

in which the vector of parameter χ, indicated in equation 5.21 is formed by $\{\eta_Y, \beta_Y\}$.

Using Bayesian inference, the posterior probability distribution for median and standard deviation based on data Y can be written as [18]:

$$P(\eta_Y, \beta_Y \mid Y) = k\beta_Y^{-(n+1)} \exp\left(-\frac{vs^2 + n(\log\eta_Y - \overline{\log Y})^2}{2\beta^2_Y}\right)$$

$$k = \sqrt{\frac{n}{2\pi}} \Gamma(v/2)^{-1}\left(\frac{vs^2}{2}\right)^{v/2} \qquad \text{Eq. 5.24}$$

where $Y=\{Y_1, ..., Y_n\}$ is the vector of n different realizations of the structural performance index, $v=n-1$, $\overline{\log Y}$ is the mean value for $\log Y$ and ns^2 is sum of

the squares of the deviations from the mean value. The expected value and the standard deviation for the probability of failure can be calculated from equations 5.21 and 5.22 based on the posterior probability distribution $p(\chi|D) = p(\eta_Y, \beta_Y|Y)$ in equation 5.24. Otherwise, the best-estimate values for the median and standard deviation can be calculated either as the maximum likelihood pair for the posterior probability distribution function or based on a given (e.g., 84%) confidence level.

The structural reliability in the presence of modeling uncertainties and uncertainties in the representation of the ground motion can be calculated from the Lognormal CDF:

$$P(Y(\underline{\theta}) > y \mid S_a) = 1 - \Phi\left(\frac{\log y - \log \eta_{Y|S_a}}{\beta_{UT}} \right)$$

$$\beta^2{}_{UT} = \beta^2{}_{Y|S_a} + \beta^2{}_{UC}$$

<div align="right">Eq. 5.25</div>

where $\eta_{Y|Sa}$ is the median for the probability distribution of the structural performance index and β_{UT} is the standard deviation for the probability distribution of the structural performance index. The terms $\beta_{Y|Sa}$ and β_{UC} represent the effect of the uncertainty in the ground motion representation, the uncertainty in the material properties and the structural details, respectively. It should be noted that equation 5.25 yields the structural fragility; after integrating it with the hazard function for the spectral acceleration, or for another adopted *IM*, the hazard function for the structural performance variable *Y* (the seismic risk curve) can be obtained.

Suppose that a selection of *n* ground motion records are used to represent the effect of ground motion uncertainty on the structural performance index. Let $S_{a,i}$ and Y_i represent the spectral acceleration and the performance index for the ground motion record *i*, respectively. The posterior probability distribution for standard deviation can be calculated as:

$$P(\beta_{UT} \mid Y) = \Gamma(\nu/2)^{-1} \left(\frac{\nu s^2}{2} \right)^{\nu/2} \beta_{UT}^{-(\nu+1)} \exp(\frac{-\nu s^2}{2\beta^2_{UT}})$$

<div align="right">Eq. 5.26</div>

The data pairs (Y, S_a) are gathered by calculating the structural performance measure for the set of n ground motion records applied at the structural model generated by different realizations of material mechanical properties and structural detailing parameters. The terms νs^2 is equal to the sum of the square of the residuals for a linear regression of $\log Y$ on $\log S_a$ and a and b are the regression coefficients. The joint posterior probability distribution for the coefficients of the linear regression $\omega = (\log a, b)$ can be calculated as:

$$P(\omega \mid Y, S_a) = k \left[1 + \frac{(\omega - \hat{\omega})^T X^T X (\omega - \hat{\omega})}{\nu s^2} \right]^{-\frac{\nu+1}{2}}$$

$$k = \frac{\Gamma\left(\dfrac{n}{2}\right) \sqrt{n \sum \log S^2_{a,i} - (\sum \log S_{a,i})^2}}{\nu s^2 \Gamma\left(\dfrac{1}{2}\right)^2 \Gamma\left(\dfrac{n}{2} - 1\right)}$$

<div align="right">Eq. 5.27</div>

which is a *bivariate t-distribution* where X is a $n \times 2$ matrix whose first column is a vector of ones and its second column is the vector of $\log S_{a,i}$ and ω is the 2×1 vector of regression coefficients $\log a$ and b. The median and the standard deviation for the probability distribution for $Y|S_a$ can be taken equal to the maximum likelihood estimates $\eta_Y = a S_a^b$ and $\beta_{Y|Sa} = s$. The robust estimates for the expected value and the standard deviation of the failure probability can be obtained from equations 5.21 and 5.2 by substituting the product of the posterior probability distributions $p(\omega|Y,S_a)$ and $p(\beta_{UT}|Y,S_a)$ in equations 5.27 and 5.26, assuming they are independent. $\chi = (\omega, \beta_{UT}) = (\log a, b, \beta_{UT})$.

4.   Application to the Case-Study Structure

The methodology presented in this section is applied to the case study existing structure.

4.1.   Non-Linear Static Analysis

When only the structural modeling uncertainties are considered, the definition of structural capacity in this work is based on the limit state of severe damage as proposed by the Italian Code [19,20,21]. That is, the onset of critical behavior in the first element, characterized by member chord rotations larger than 3/4th of the corresponding ultimate chord rotation capacity. The structural demand is characterized by the intersection of the code-based inelastic design spectrum and the static pushover curve transformed into that of the equivalent SDOF system [13] (Appendix C). As an index for the global structural performance, the ratio of structural demand to capacity is used [11].
The component yield rotation, ultimate rotation and shear capacities are calculated according to the new Italian Unified Code [20,21] (Appendices B and E).

4.1.1.   Calculation of the Structural Fragility

The structural fragility curve for the structure under study can be calculated by employing the efficient Bayesian method described above based on the structural performance parameter for static analyses for a set of 20 Monte Carlo (MC) realizations of the structural model. These realizations take into account the uncertainties in the material properties and the structural defects. The probability distributions for the uncertain parameters are updated according to the increasing knowledge levels. Thus, for each knowledge level, the 20 realizations of the structural model are generated from the (updated) probability distributions corresponding to the KL's and based on the results of tests and inspections. Since the results of tests and inspections available for the structure in question did not exactly match the EC8 [9] criteria, the test results used herein are simulated assuming that all the inspections performed verify the

original design values. Figure 5.6 demonstrates the robust fragility curves (the probability of failure for a given value of Y) obtained.

The robust fragility for knowledge levels KL_1, KL_2 and KL_3 is calculated as the expected value of the structural fragility in equation 5.23, given that its median and standard deviation are known from equation 5.21, where the joint probability distribution for median and standard deviation is given in equation 5.24. For each knowledge level, also the standard deviation in the robust fragility estimate is calculated from equation 5.22.
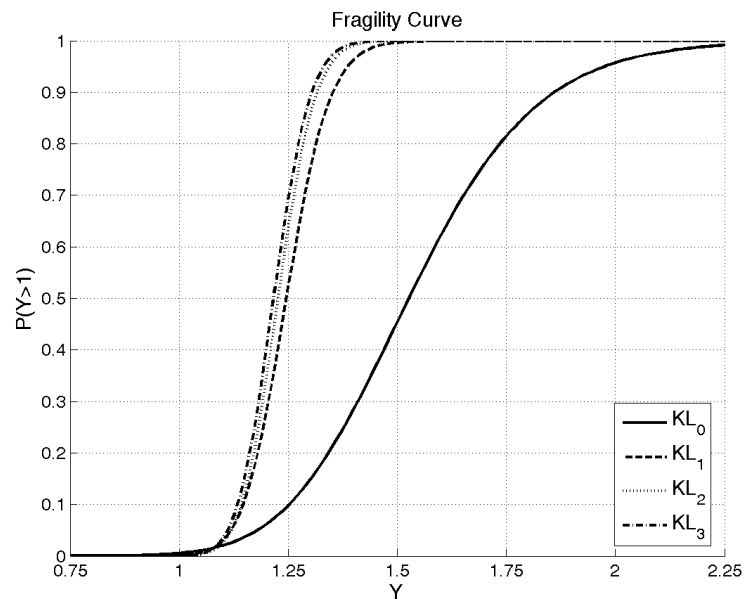
Figure 5.6. The structural fragility curves for the knowledge levels KL_o, KL_1, KL_2 and KL_3. (hp1: 100% verified).

It can be observed that the upon increasing knowledge levels both the median and the dispersion in the fragility curves (β_Y and η_Y in equation 5.12) decrease as the test results all verify the nominal values. However, it can be immediately verified that the structure does not verify the criteria in equation

5.12 in none of the knowledge levels. That is, because the median η_Y is already greater than unity[12].

Figure 5.7 shows the plus/minus one standard deviation confidence interval for the robust fragility curves for each knowledge level together with the structural performance parameter obtained applying the confidence factors specified in the code for each knowledge level (the vertical lines).
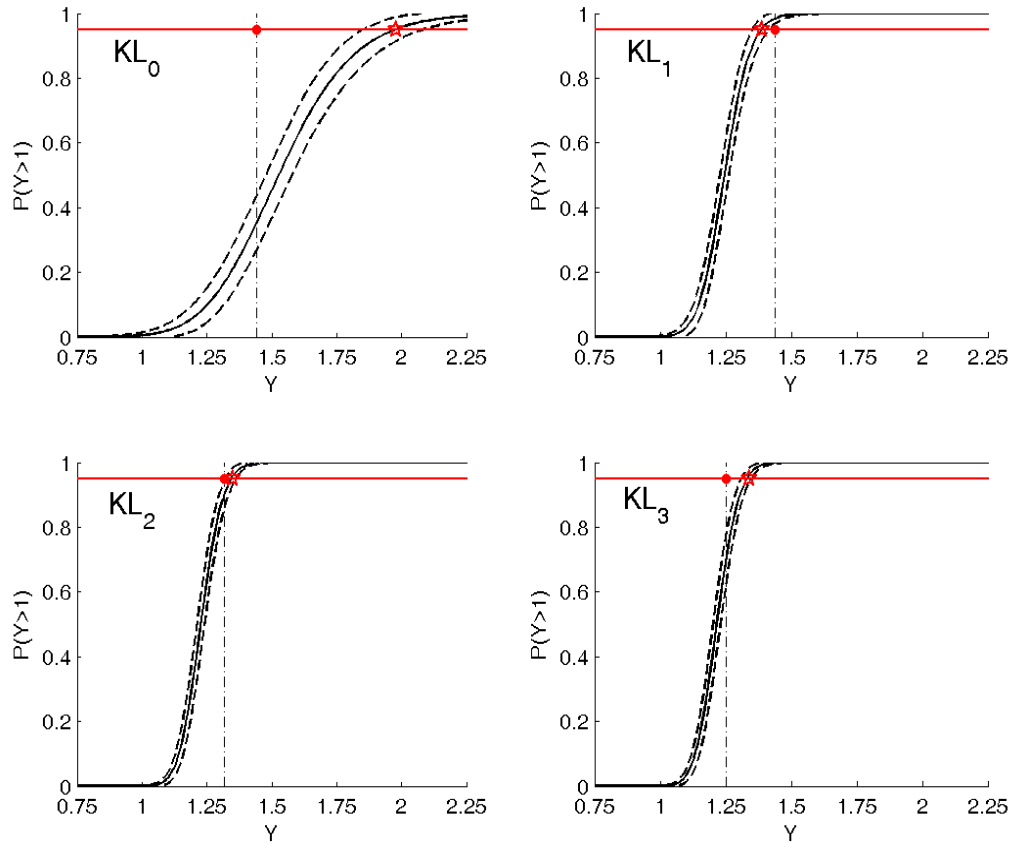
Figure 5.7 The plus/minus standard deviation interval structural fragility curves for the knowledge levels KL_0, KL_1, KL_2 and KL_3

---

[12] This is due to the fact that the structural components do not verify against shear, a typical problem for existing reinforced concrete structures not designed for seismic loading.

An alternative definition of the CF can be composed based on the global performance of the structure by obtaining the structural performance parameter that has a specific (say 95%) probability of not being exceeded [3]. The horizontal lines in the figure illustrate the %95 confidence level and the star illustrate the structural performance parameter that has %95 probability of not being exceeded. Comparing this alternative confidence-based definition to the values obtained by applying the code procedure for knowledge levels KL_1, KL_2 and KL_3, we can observe that the two definitions agree reasonably well and that the code-based values are slightly conservative. However, code-based value for KL_1 remains significantly non-conservative with respect to the prior robust fragility curve at KL_o that is before applying the test results.

Obviously, this conclusion is drawn based on the hypothesis that the test results all verify the nominal values.

In fact, in the following the robust fragility curves and their corresponding plus/minus standard deviation confidence intervals are obtained also based on two other alternative hypotheses.

The first alternative hypothesis states that none of the test results confirm the nominal value; the resulting robust fragility curves are shown in Figure 5.8 for the three knowledge levels.
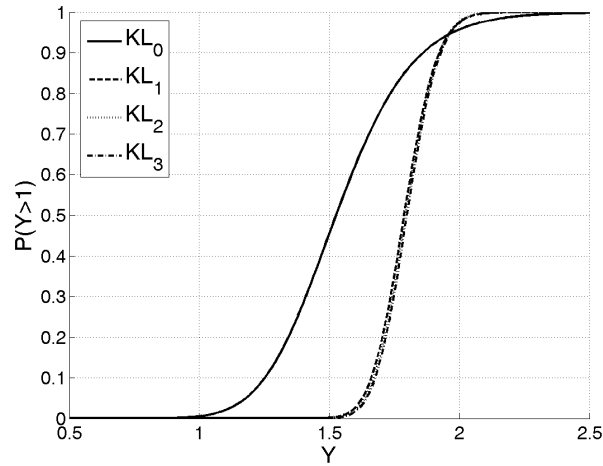
Figure 5.8. The structural fragility curves for the knowledge levels KL_o, KL_1, KL_2 and KL_3 (hp2: 0% verified).

The second alternative hypothesis states that only %50 of the test results verify the nominal value. The resulting robust fragility curves are shown in Figure 5.9 for the three knowledge levels.
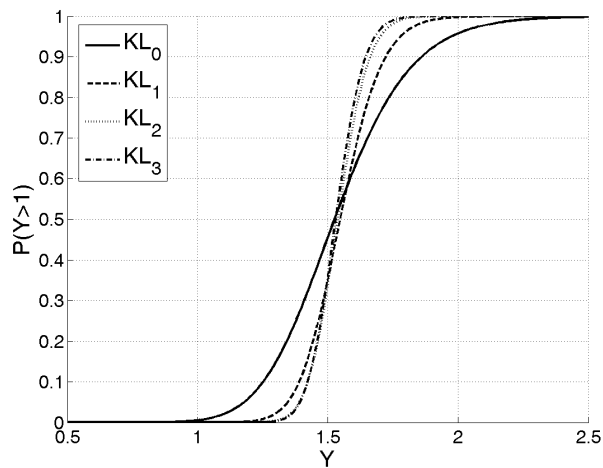
Figure 5.9. The structural fragility curves for the knowledge levels KL_o, KL_1, KL_2 and KL_3 (hp3: 50% verified).

Comparing figures 5.6, 5.8 and 5.9 it can be observed that the standard deviation of the fragility curves corresponding to each knowledge level remains invariant with respect to the test results while the median value significantly changes.

It should be mentioned that these are simplified hypotheses regarding the outcome of the tests assuming that the percentage of not verifying the test results is constant throughout all types of defects in the structure.

4.1.2. Verification of results using the standard Monte Carlo simulation

The results shown in the previous section are verified by reiterating the reliability assessments for the knowledge levels using the standard Monte Carlo simulation. For the prior knowledge level KL_0, 500 realizations of the vector of uncertain parameters are simulated based on the prior probability distribution before implementing the test results. For knowledge levels KL_1, Kl_2 and KL_3, given the reduced dispersion in the corresponding updated probability distributions, 200 simulation realizations are performed at each level.

Figure 5.10 illustrate how the fragility curves calculated based on MCS compare with the plus/minus one standard deviation interval provided by employing the efficient method described in chapter IV.
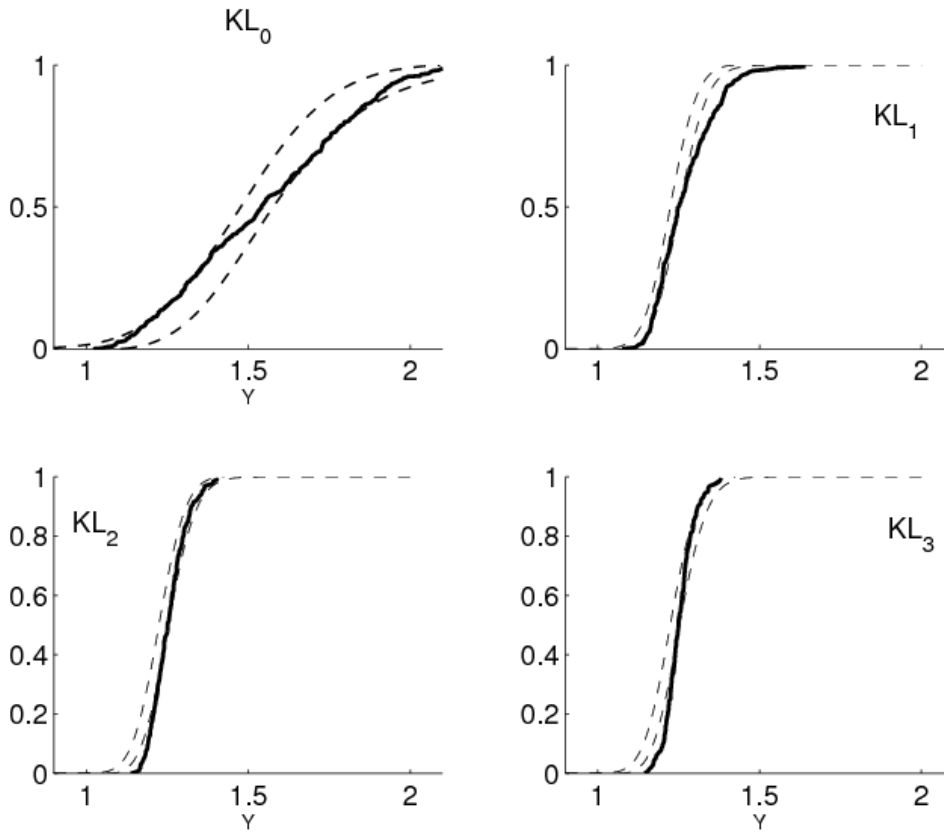
Figure 5.10. The approximate code-based hazard curves for the knowledge levels KL_o, KL_1, KL_2 and KL_3.

4.2.   Non-Linear Dynamic Analysis

When the ground motion uncertainty together with the modeling uncertainties are taken into account in this work, the structural performance index is characterized based on the concept of cut-sets in structural reliability [14].

Three types of global mechanism are considered herein: (a) ultimate rotation capacity in the columns (b) formation of soft stories (c) shear failure in the columns (Appendices B and C).

4.2.1. The Code-Based Method

It is shown previously in this work how applying the CF's can be viewed from the stand-point of overall structural performance using the non-linear static analyses. In a similar way, it can be shown how applying CF's can influence the structural performance in the dynamic case.

A set of 7 records are chosen from European Ground motion database or ESD[13]; they are all main-shock recordings and include only one of the horizontal components of the same registration. The soil category on which the ground motions are recorded is stiff soil (400 m/s < V_{s30} < 700 m/s) which is consistent with the soil-type for the site. The earthquake events have moment magnitude between 5.4 and 6.5, and closest distances ranging between 16km and 71km.
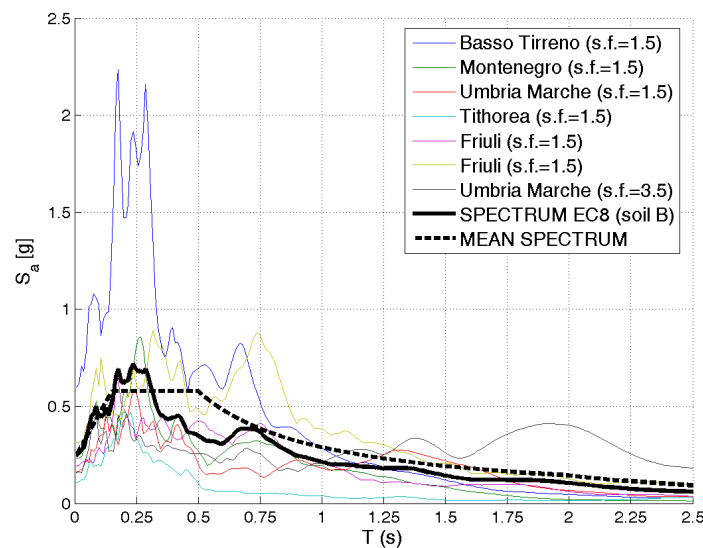
Figure 5.11. Scaled acceleration spectra.

---

[13] http://www.isesd.cv.ic.ac.uk/ESD/Database/Database.htm

In order to have a set compatible with the code-specified spectrum (EC8) the suite of records has been scaled. In Figure 5.11 the scaled spectra with corresponding scaled factors are plotted.

For each CF specified in the code, the structural performance variable for the set of records is calculated for a structural model (without defects) with material properties divided by that CF.

The structural performance variable is related to the spectral acceleration using linear regression with conditional median and standard deviation (of the logarithm) equal to $\eta_{Y|Sa}$ and $\beta_{Y|Sa}$. The structural fragility is calculated from equation 5.15 setting β_{UC} equal to zero. Finally, the structural fragility is integrated with the spectral acceleration hazard curve (extracted from the site of INGV for the coordinates of the site (lat. 40.915; lon. 14.78), period equal to 0.75) in order to calculate the mean annual probability of exceeding a specific value for the structural performance parameter.

The resulting risk curves for the structural critical demand to capacity ratio corresponding to different values of CF are plotted in Figure 5.12.
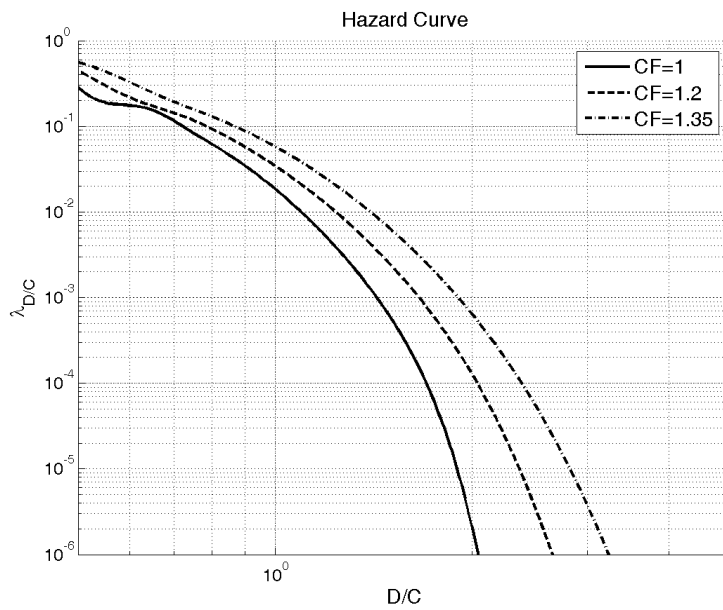
Figure 5.12. Hazard curves obtained following the CF approach for the knowledge levels KL_o, KL_1, KL_2 and KL_3.

It should be noted that dispersion in these hazard curves reflects only the record-to-record variability.

4.2.2. Calculation of the Structural Reliability

The structural hazard curve for increasing levels of knowledge is calculated in this stage by integrating the robust fragilities and the spectral acceleration hazard curve at the site of the structure.

For each level of knowledge, the robust fragility is calculated from equations 5.21, 5.25, 5.26 and 5.27 using a set of 30 MC realizations of the structural model. At each knowledge level the robust hazard curve (i.e., the mean annual rate of exceeding the structural performance parameter) is calculated as the expected value of the hazard curve given that the median and the standard deviation for the structural fragility curve calculated from equation 5.25 are known. The median value for the fragility curve is estimated by employing the linear least squares as a function of the spectral acceleration at the fundamental mode of the structure. The joint probability distribution for the linear least squares coefficients is calculated from equation 5.27 and the probability distribution for the standard deviation of the fragility curve is calculated from equation 5.26 based on the results of a small set of 30 Monte Carlo simulations. The standard deviation as it can be seen in equation 5.25 can be calculated as the square root of the sum of squares of two parts representing the effect of ground motion uncertainty denoted by $\beta_{Y|S_a}$ and the structural modelling uncertainty denoted by β_{UC}.

The set of MC realizations for each KL are generated based on the corresponding (updated) probability distributions. The suite of 30 records are the same adopted in chapter IV.

The resulting hazard curves are plotted in solid lines in Figure 5.13 knowledge levels KL_o, KL_1, KL_2 and KL_3. For each knowledge level, the hazard curve obtained by following the code procedure and applying the corresponding confidence factors is plotted in dashed lines. The horizontal line

in each sub-figure represents the allowable probability level, here 10% probability of exceedance in 50 years.

It can be shown [12] that calculating the left-hand side of equation 5.3 for a given acceptable probability P_o is equivalent to finding the value corresponding to P_o from the hazard curve for structural performance parameter. It can be readily observed that for an acceptable probability of P_o=0.002 or 10% in 50 years, the structure does not verify for none of the KL. The intersection of the admissible level with the code-based and robust hazard curves are shown with circles and stars respectively.

It can be observed that, unlike the static case, the code-based method is not conservative with respect to the robust fragility estimate. However, there is a reasonable agreement between the two methods.
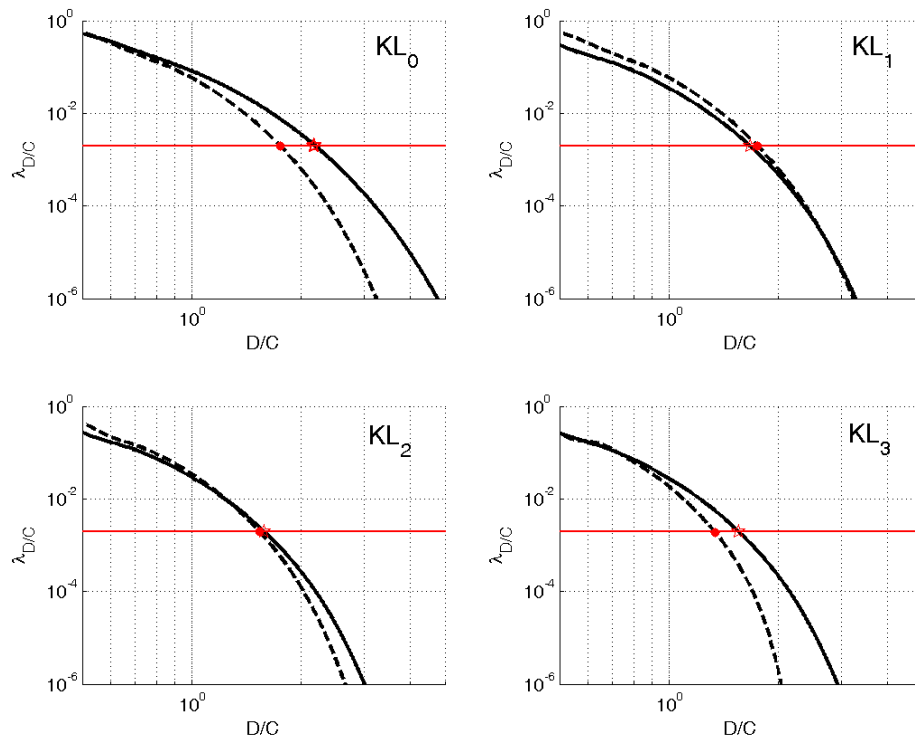
Figure 5.13. The robust hazard curves (solid) and the hazard curves based on the CF approach (dashed) for the knowledge levels KL_o, KL_1, KL_2 and KL_3.

5.   Code-Based Implementation of the Alternative Performance-Based Safety-Checking Format

Having calculated the structural reliability for different knowledge levels taking into account the structural modelling uncertainties, now the questions remains as to how such calculation can affect the code-based procedures. That is, how to formulate code-based performance-based assessments considering different sources of uncertainty. This section proposes a performance-based safety-checking format that accounts in an approximate way for both the amount and the outcome of in-site tests.

In the case of static analyses, the SAC-FEMA [6,7] formulation in equation 5.13 to obtain the *x* percentile of the structural performance parameter can be re-written as following:

$$\widehat{Y} \cdot \gamma \cdot e^{\Phi^{-1}(x)\beta_Y} \leq 1 \qquad\qquad \text{Eq. 5.28}$$

where γ is a bias factor and β_Y is the standard deviation of the robust fragility curve. $\widehat{Y}$ represents the structural performance parameter calculated based on the median material properties based on the test results and nominal values for the structural detailing parameters. The bias factor γ (usually larger-than-unity) represent the factor that once multiplied by the nominal value $\widehat{Y}$ leads to the median value η_Y.

Tables 5.4 and 5.6 outline the parameters β_Y and γ values for the three knowledge levels considered for the case study structure and based on static analyses. The three columns represent the three simplified hypotheses adopted previously regarding the outcome of the test results.

Table 5.7 outline these parameters for the knowledge level KL_o before the tests are preformed.

It can be observed that based on the prior distributions considered herein, considering the structural modeling uncertainties can affect the structural reliability up to %15. Considering the hypothesis that %100 of the test results

verify the nominal values, it can be observed that the bias factors are very close to one.

Table 5.4. Table of values for β_{UC} (uncertainty in the material properties and structural details).

		100% verified	50% verified	0% verified
SPO	KL_1	0.0641	0.0835	0.0586
	KL_2	0.0527	0.0616	0.0556
	KL_3	0.0531	0.0554	0.0527
DYN	KL_1	0.0800	0.0868	0.1142
	KL_2	0.0393	0.0635	0.0742
	KL_3	0.0216	0.0472	0.0682

Table 5.5. Table of values for β_{UT} (include the uncertainty in the ground motion representation).

		100% verified	50% verified	0% verified
DYN	KL_1	0.1784	0.1816	0.1938
	KL_2	0.1643	0.1717	0.1759
	KL_3	0.1609	0.1663	0.1735

Table 5.6. Table of values for γ.

		100% verified	50% verified	0% verified	**CF**
SPO	KL_1	0.9933	1.2343	1.4255	**1.35**
	KL_2	0.9782	1.2272	1.4294	**1.20**
	KL_3	0.9701	1.2206	1.4349	**1.00**
DYN	KL_1	1.0984	1.3306	1.4698	**1.35**
	KL_2	1.0521	1.3046	1.4812	**1.20**
	KL_3	1.0362	1.2632	1.4953	**1.00**

Table 5.7. Table of values for KL_0.

		γ	β_{UC}
SPO	KL_0	1.5245	0.1455
DYN	KL_0	1.3342	0.1783

Likewise, when the uncertainty in the ground motion representation (the record-to-record variability) is considered, the formulation in equation 5.16 can be re-written as:

$$\widehat{Y} \cdot \gamma \cdot e^{\frac{1}{2}\frac{k}{b}\beta_{Y|S_a}^2} \le e^{\Phi^{-1}(x)\sqrt{\beta_{Y|S_a}^2 + \beta_{UC}^2}}$$ Eq. 5.29

where γ is a bias factor and β_{UC} represent the over-all effect of structural modeling uncertainties. $\widehat{Y}$ represents the structural performance parameter calculated based on the median material properties obtained from the test results and nominal values for the structural detailing parameters.

$\widehat{Y}$ is calculated by performing linear least squares as a function of the first-mode spectral acceleration based on the set of 7 records. The bias factor γ (usually larger-than-unity) is a factor that once multiplied by the nominal value $\widehat{Y}$ leads to the median value for the structural performance parameter calculated using the maximum likelihood estimates for the regression coefficients obtained from the probability distribution in equation 5.27.

Table 5.4 and 5.6 tabulate the γ and β_{UC} for different knowledge levels and test outcomes based on non-linear time-history analyses. The same coefficients for the KL_0 knowledge level are listed separately in Table 5.7.

The tables reported in this section are classified based on the type of analysis, level of knowledge and the outcome of the test results. These tables, once calculated for representative classes of structures and periods of construction, can be employed, in lieu of more thorough probability-based methods, for performance-based assessment of existing buildings.

It should be noted that comparing the results shown in Table 5.4 and Table 5.5, there is a significant increase in the value of the dispersion of the structural fragility considering also the uncertainty in the ground motion representation. This emphasizes the importance of considering the uncertainties in the representation of the ground motion in the code-based procedure.

6.   Conclusions

Quantifying the uncertainty in the structural modeling parameters related to the level of knowledge about an existing structure is one of the main challenges in seismic performance assessment of existing buildings. The discrete

knowledge levels (KL) defined by the code leave significant room for interpretation. In other words, the code-based definition for KL does not lead to a unique configuration of tests and inspections. Moreover, it is not clear which level of structural reliability does the application of the confidence factors guarantee. Hence, with the emerging of performance-based design and life-cycle cost analysis in earthquake engineering, there seems to be a need for a code-based method that bridges the different knowledge levels to structural reliability and probabilistic structural performance assessment.

Intuitively speaking, the relation between the confidence factors and the knowledge levels seems to be highly dependent on the results of in-situ tests and inspections. Therefore, it is necessary to adopt a general probabilistic framework for updating the probability distribution for the uncertain parameters based on the test results. The Bayesian framework for inference seems to be perfectly suitable for this end; as it can sequentially incorporate the incoming tests and inspection results without discarding any prior information available.

The uncertain parameters considered include the material properties, the construction detailing parameters and, in the case of the dynamic analyses, the uncertainty in the ground motion representation. For each knowledge level, the probability distributions for the uncertain parameters are updated using the Bayesian updating frame work.

In the absence of test results abiding exactly with the code prescriptions, an idealized situation is considered in which all of the test results verify the original design values. Obviously, the methodology presented is general with respect to the outcome of the test and inspections.

The uncertain parameters are divided in groups (emulating various homogenous construction zones). It is assumed that the uncertain parameters belonging to distinct groups are fully un-correlated and only the uncertain parameters inside a given group can be correlated. It should be noted that decisions on possible groupings of the uncertain parameters can affect significantly the global performance assessment of the structure.

It is observed that for increasing knowledge levels, the estimates for the structural performance tend to get very close. This is while the structural performance parameters corresponding to the confidence factors tend to remain fairly distinct.

The approximate code-based method manages to provide reasonable estimates of the structural performance. However, it is not guaranteed that it would remain conservative with respect to the probability-based estimates as is the case of the assessments performed using the non-linear time-history analyses.

As a final note particular to the case-study considered, it should be mentioned that the critical value for the structural performance variable is almost always governed by the shear failure in structural components. This is a typical problem for the existing reinforced concrete structures designed only for the gravity loads.

In the context of a code-based performance-based assessment approach, different classes of existing buildings can be identified and analyzed. The prior probability distributions for the structural modeling uncertainties can be classified and tabulated based on the surveys of expert opinion and experience. It is important to identify those uncertain parameters that affect the structural response in a dominant way (e.g., the material properties, the stirrup spacing). These prior probability distributions are going to be updated based on the results of tests and inspections. The updated probability distributions are constructed for various KL's, based on special cases of tests and inspection results.

Finally, for different classes of structures and different levels of knowledge (and a few special cases of inspection results), the best-estimate values for the parameters defining the adopted safety-checking format and/or structural fragility can be tabulated.

It should be addressed that when tackling the problem of performance assessment of existing buildings, it is important to lay out a range of methods. In this manner, the suitable method can be selected as a function of the importance of the structure and the level of precision desired. For instance, in

the case of strategic buildings, it would be useful to recommend some relatively simple and approachable methods suitable for case-specific estimation of the parameters defining the safety checking format and/or structural fragility.

7. References

[1] Franchin P., Pinto P. E., Pathmanathan R., Assessing the adequacy of a single confidence factor in accounting for epistemic uncertainty, Convegno RELUIS *"Valutazione e riduzione della vulnerabilità sismica di edifici esistenti in cemento armato"*, Roma 29-30 maggio 2008.

[2] AISC. Manual *of Steel Construction Load and Resistannce Factor Design.* Second Edition, American Institute of Steel Construction Inc., Chigaco, IL, 1994.

[3] Jalayer F., Iervolino I., Manfredi G., "Structural modeling uncertainties and their influence on seismic assessment of existing RC structures", submitted to *Structural Safety*, 2008.

[4] Department of Energy (DOE), 1994. *Natural Phenomena Hazards Design and Evaluation Criteria for Department of Energy Facilities*, DOE-STD-1020-94, U.S. Department of Energy, Washington, D.C.

[5] Federal Emergency Management Agency (FEMA), 2000. *Recommended Seismic Design Criteria for New Steel Moment-Frame Buildings,* FEMA-350, SAC Joint Venture, Washington, D.C.

[6] Federal Emergency Management Agency (FEMA), 2000. *Recommended Seismic Evaluation and Upgrade Criteria for Existing Welded Steel Moment-Frame Buildings*, FEMA-351, SAC Joint Venture, Washington, D.C.

[7] Federal Emergency Management Agency (FEMA), 2000. *Recommended Post-Earthquake Evaluation and Repair Criteria for Welded Steel Moment-Frame Buildings*, FEMA-352, SAC Joint Venture, Washington, D.C.

[8] Federal Emergency Management Agency (FEMA), 2000. *Pre-Standard and Commentary for the Seismic Rehabilitation of Buildings*. FEMA 356, Washington, D.C.

[9] CEN, European Committee for Standardisation TC250/SC8/ [2003] "*Eurocode 8: Design Provisions for Earthquake Resistance of Structures, Part 1.1: General rules, seismic actions and rules for buildings,*" PrEN1998-1.

[10] Cornell, C. A., Jalayer, F., Hamburger, R. O., and Foutch, D. A., (2002), The probabilistic basis for the 2000 SAC/FEMA steel moment frame guidelines, *ASCE Journal of Structural Engineering*, Vol. 128, No.4, pp. 526-533.

[11]   Jalayer F, Franchin P, Pinto PE. A scalar damage measure for seismic reliability analysis of RC frames. *Earthquake Engineering and Structural Dynamics*. 36:2059-2079, 2007.

[12]   Jalayer, F., Cornell, C. A. (2008), "Alternative Nonlinear Demand Estimation Methods for Probability-Based Seismic Assessments", *Early View Earthquake Engineering and Structural Dynamics,* 2008.

[13]   Fajfar, P. Capacity spectrum method based on inelastic demand spectra, *Earthquake Engineering and Structural Dynamics*; **28**:979–93, 1999.

[14]   Ditlevsen O, Masden H. *Structural Reliability Methods*, June 1996; John Wiley & Sons Inc.

[15]   Verderame, G.M., Manfredi, G., Frunzio G., Le proprietà meccaniche dei calcestruzzi impiegati nelle strutture in cemento armato realizzate negli anni '60, X Congresso Nazionale *"L'ingegneria Sismica in Italia"*, Potenza-Matera 9-13 settembre 2001a.

[16]   Verderame, G.M., Stella, A., Cosenza, E., Le proprietà meccaniche degli acciai impiegati nelle strutture in cemento armato realizzate negli anni '60, X Convegno Nazionale *"L'Ingegneria Sismica in Italia"*, Potenza e Matera 9-13 Settembre 2001b.

[17]   Jalayer F., L. Elefante, Iervolino I., Manfredi G., "Small-Sample Bayesian Inference for Estimation of Structural Modeling Uncertainty Parameters in Seismic Assessment of Existing RC Buildings", *ICOSSAR09 Conference*, 2009.

[18]   Box, G.E.P. and Tiao, G.C., *Bayesian Inference in Statistical Analysis*, Wiley Interscience, 1992.

[19]   Ordinanza del Presidente del Consiglio dei Ministri (OPCM) n. 3431, Ulteriori modifiche ed integrazioni all'ordinanza del Presidente del Consiglio dei Ministri n. 3274 del 20 marzo 2003. Gazzetta Ufficiale della Repubblica Italiana n. 107 del 10-5-2005 (Suppl. Ordinario n.85), 2005.

[20]   CS..LL.PP, DM 14 gennaio, *Norme Techniche per le Costruzioni*. Gazzetta Ufficiale della Repubblica Italiana, **29**, 2008a (*in Italian*).

[21]   CS.LL.PP, DM 14 gennaio, *Istruzioni per l'applicazione delle Norme Techniche delle costruzioni*. Ministero della Infrastruttura, **29**, 2008b (*in Italian*).

Chapter VI

How to Characterize Prior Probability Distribution for Structural Details: a Survey for Professional Engineers

1. Introduction

Developing prior distributions is undoubtedly the most controversial aspect of any Bayesian analysis [1,2]. Considerable care should be taken when selecting priors and the process by which priors are selected must be documented carefully. This is because inappropriate choices for priors can lead to incorrect inferences.

There are two types of priors: informative and non-informative (or "reference") [3] define a non-informative prior as one that provides little information relative to the analyzed experiment. Informative prior distributions, on the other hand, summarise the evidence about the parameters concerned from many sources and often have a considerable impact on the results.

Using informative prior distributions allows the incorporation of information available to analysts from the literature and in light of their experience. However, using informative priors is not a trivial task because their subjective nature.

Uniform priors are generally chosen when non-informative priors are needed, as it has been used in chapter V for structural details. However, given the versatility of the Bayesian updating framework in incorporating prior information, it is important to characterize prior probability distributions for construction details based on qualitative and collective information coming from experts in the field.

In relation to the probability distributions related to construction details, a survey for professional engineers has been prepared in order to be able to characterize these prior distributions in relation to expert opinion; the survey is presented in this chapter together with the preliminary results obtained by interviewing a small sample of professionals in order to test it.

2.   The Survey for Professional Engineers

In the framework of the alternative performance-based safety-checking format proposed in the previous chapter, the prior probability distributions for the structural modeling uncertainties can be classified and tabulated based on various surveys of expert opinion and experience.

One of the main characteristics of the construction details is that possible deviations from the original configurations are mostly taken into account in those cases leading to undesirable effects. This justifies why the uncertainties related to construction details are usually referred to as the *structural defects*.

In this section the steps followed for the development of the survey for professional engineers relative to the uncertainty in structural details are briefly summarized.

- First of all it is necessary to identify those modeling uncertainties that affect the structural response in a dominant way. Obviously these choices is always related to the level of sophistication that is adopted for the finite element model of the structure under assessment.

- Once a source of uncertainty related to structural details is identified it is necessary to determinate a quantifiable parameter or variable that is representative for the identified source of uncertainty.

- Then, it is necessary to assign a reasonable interval of values that the identified quantifiable parameter can assume. In this phase, the professional engineer can also indicate the most plausible value of the quantifiable parameter, in relation of her/his experience, in the assigned interval.

- Moreover for each source of uncertainty identified and its corresponding quantifiable parameter it is necessary to investigate its systematic nature. This serves in identifying the zone in which the parameter is going to be modelled as constant.

The compiling of the survey is anonymous, but two questions are included in order to have some information about the engineer's professional experience. First, the engineer has to state the professional association he belongs to, in order to consider the engineering practice typical of the reference province in which he operates.

Name	(facultative field)
Surname	(facultative field)
Affiliation	(facultative field)
Professional Association	(required field)

Furthermore a question related to the number of RC structures that the professional has designed, super-visioned and/or evaluated before and after 1976, is included.

RC buildings constructed before 1976	# designed or super-visioned	
	# evaluated or assessed	
RC buildings constructed after 1976	# designed or super-visioned	
	# evaluated or assessed	

This additional information can be used in order to weight the results of each compiled survey in relation to the experience of the engineer.

It should be noted that the chosen reference year 1976 is related to the first Italian code in which the National Earthquake framework for classifying national seismic hazard with special technical requirements for seismic zones was established: the Legge 2/2/1974, n. 64 [4], *"Provvedimenti per le costruzioni con particolari prescrizioni per le zone sismiche"*.

The questions have been grouped in relation to the specific source of uncertainty which they are related to. In the following, different sources of uncertainties considered are reported together with the relative questions inserted in the survey.

1)   Concrete cover

1.1	If the original documents indicates a value of the concrete cover δ (Figure 1) equal, for example, to cm 3, in your experience, what is the value of concrete cover that you expect to find in the existing structure?

Figura 1

1) < 1 cm	2) 1cm
3) 2 cm	4) 3 cm
5) 4 cm	6) >4 cm

1.2	Do you believe that this range is applicable to the entire structure or the evaluation should be repeated for different areas of the building (eg, those made with the same cast of concrete) or for each single structural component?

1) entire structure	2) cast of concrete
3) single structural component	

2)   Bars anchorage

2.1	In the original documents it is indicated that the anchor to be used is a hook. Among 100 hooks, in your experience, how many of them are well done in the existing structure? That is, how many of them are closed with an angle larger then 150 ° (Figure 2, A) ?		
	Figura 2		
	1) 100	3) 50	5) 10
	2) 80	4) 20	6) 0
	Among the hooks that are not properly closed, how many are closed with an angle between 90 ° and150° (Figure 2, B)?		
	1) 100	3) 50	5) 10
	2) 80	4) 20	6) 0

2.2	Do you believe that the previous answer is relative to the entire structure, to a single cast of concrete or to each single structural component?	
	1) entire structure	2) cast of concrete
	3) single structural component	
2.3	In the original documents an anchoring length of cm 25 is shown. In your experience, what is the value of the anchoring length you expect to find in the existing structure?	
	1) 10 cm	3) 15 cm
	2) 20 cm	4) 25 cm

2.4	Do you believe that this value is applicable to the entire structure, to a single cast of concrete or to each single structural component?	
	1) entire structure	2) cast of concrete
	3) single structural component	

3)   Stirrups

3.1	Among 100 stirrups inspected in an existing RC structure, how many, in your experience, have not been tied properly? (Figure 3)		
	Figura 3 [5,6]		
	1) 0	3) 25	5) 75
	2) 10	4) 50	6) 100

3.2	In the original documents it is indicated that in a beam of length equal to 4 m 26 stirrups have been installed. In your experience, how many stirrups are actually present in this beam in the existing structure?	
	1) ≤ 8	2) 10
	3) 12	4) 16
	5) 20	6) 26

3.3	In your experience, with reference to the previous query, do you expect to find the stirrups placed with regular spacing?	
	1) Yes	2) No

3.4	The original documents indicate that in a beam of length equal to 4 m 26 stirrups have been installed. How many stirrups do you expect to find in cm 50 of the beam near the supports?	
	1) 2	2) 3
	3) 4	4) 6
	and how many in a meter of beam span?	
	1) 2	2) 3
	3) 4	4) 6

3.5	Do you believe that this value is applicable to the entire structure, to a single cast of concrete or to each single structural component?	
	1) entire structure	2) cast of concrete
	3) single structural component	

3.6	Among 10 beam-column joints of the existing structure, in your experience, how often the stirrup in the beam-column connection may be absent?	
	1) ≤ 2	2) 4
	3) 6	4) 8
	5) 10	

3.7	In the case of absence of stirrup in the beam-column connection, how far away from the connection do you believe to find the first stirrup?	
	1) 2 cm	2) 5 cm
	3) 10 cm	4) 20 cm

3.8	The original documents indicate that in a meter of a 3 m long column 20 stirrups have been installed. In your experience, how many stirrups are actually present in a meter of column in the existing structure?	
	1) 6	2) 10
	3) 16	4) 20

3.9	In your experience, with reference to the previous question, do you expect to find the stirrups placed with regular space?	
	1) Yes	2) No

3.10	The original documents indicate that in a 3 m long column 20 stirrups have been installed. How many stirrups do you believe to find in 50 cm of the column corresponding to the lower end?	
	1) 2	2) 3
	3) 4	4) 5
	5) 6	6) ≥ 7

3.11	Do you believe that this value is applicable to the entire structure, to a single cast of concrete or to each single structural component?	
	1) entire structure	2) cast of concrete
	3) single structural component	

4) Reinforcing bars

4.1	The original documents indicate that in order to reinforce a specified storey in the structure two different types of reinforcement diameters ϕA and ϕB, with ϕA <ϕB (e.g., ϕ12 and ϕ14) have been used.
	Do you believe it is possible that in a beam reinforced with straight longitudinal bars of diameter ϕA and ϕB, the two diameters have been confused?
	1) Yes / 2) No
	Do you believe it is possible that in a beam reinforced with straight longitudinal bars of diameter ϕA and bent longitudinal bars of diameter ϕB, the two diameters have been inverted?
	1) Yes / 2) No
	Do you believe it is possible that in a column reinforced in a direction with bars of diameter ϕA and in the other direction with bars of diameter ϕB, reinforcement in the two directions have been reversed?
	1) Yes / 2) No

4.2	Assuming that the original documents indicate that in order to reinforce a certain level of the structure 50 reinforcing bars of diameter ϕA and 50 of diameter ϕB have been used, with ϕA < ϕB. Which is the total number of reinforcing bars of diameter ϕA do you expect to find in the existing structure?
	1) 35 ϕA / 2) 45 ϕA
	3) 55 ϕA / 4) 65 ϕA
	5) 75 ϕA / 6) 85 ϕA

4.3	In your experience which one of the following may have been the cause of error in arranging the bars in the above-mentioned cases?
	1) Lack of attention on the part of the carpenter
	2) Unavailability of a bar diameter during construction
	3) Economic reasons
	4) Other (specify)

4.4	The outline of beam reinforcement at the vicinity of support, obtained from the original documents is shown in Figure 4.
	Figura 4
	Do you believe it is possible to find a number of bent longitudinal bars smaller than the number indicate in the documents?
	1) Yes / 2) No
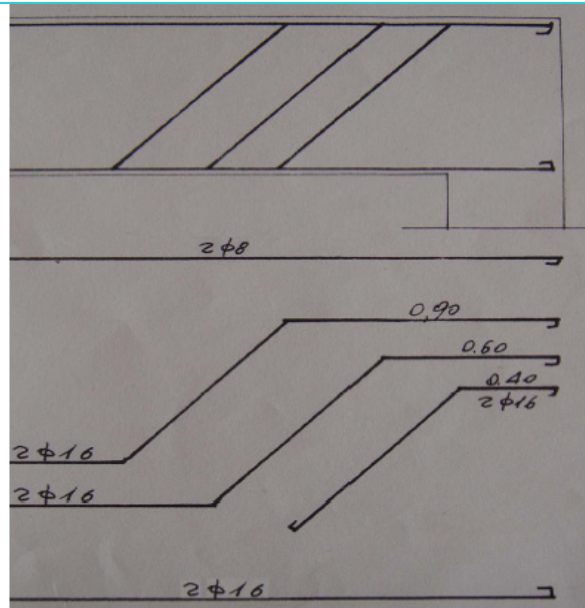
| 4.5 | Do you believe that this possibility depends on the bent longitudinal bars' length? |
| | 1) Yes / 2) No |

4.6	Among 10 beam sections whose reinforcement in the vicinity of support is specified Figure 4, in your experience, in how many of them one bent longitudinal bar would be missing with respect to what specified in the original documents?	
	1) 0	2) 1
	3) 2	4) 5
	5) 7	6) 10

4.7	Do you believe that it is possible that the missing shaped bars are more than one?	
	1) Yes	2) No

5)   Column superposition length

5.1	In your experience, do the original documents normally indicate the overlapping length of the reinforcement of the columns between successive levels?	
	1) Yes	2) No

5.2	If the original documents indicate a superposition length of 100 cm for an interstory height of 3 m, what is the value of the superposition length that you expect to find in the existing structure?	
	1) 10 cm	2) 25 cm
	3) 50 cm	4) 60 cm
	5) 75 cm	6) 100 cm

5.3	In your experience, if the original documents do not indicate the superposition length for columns, for an interstory height of 3 m, what is the value of the superposition length that you expect to find in the existing structure?	
	1) 10 cm	2) 25 cm
	3) 50 cm	4) 60 cm
	5) 75 cm	6) 100 cm

6) Rebar configuration

6.1	In the original documents of a structure with a rectangular plan shown in Figure 5, it is indicated that the rectangular column shown in the figure, oriented in the direction Y, is reinforced with six reinforcing bars of the same diameter.
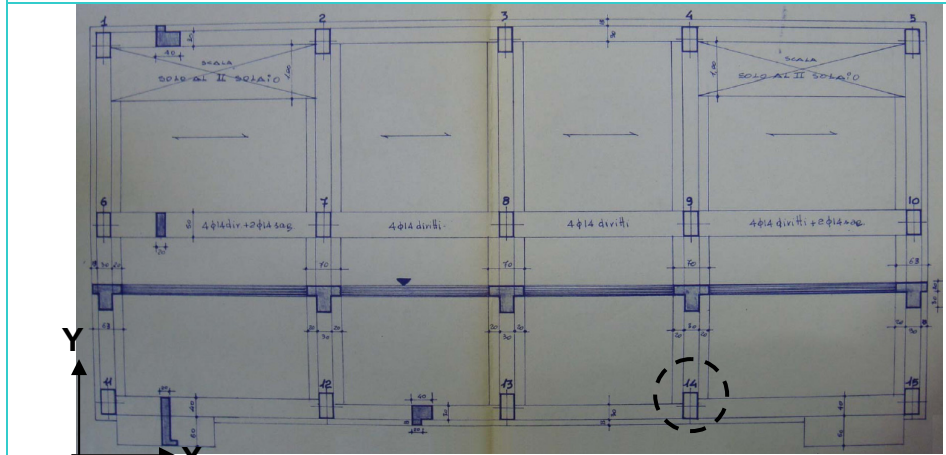
Figura 5

What is the rebar configuration you expect to find in the existing structure (Figure 6)?
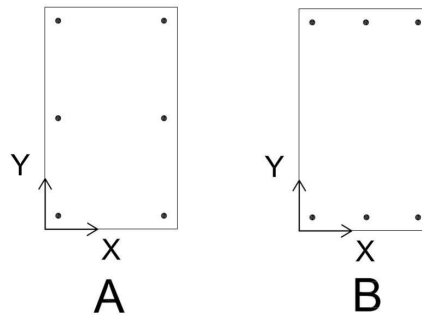
Figura 6

1) A   2) B

7)   Geometrical properties of structural elements

7.1	The original documents of a structure indicate that the cross section of a beam with a length equal to 4 m is characterized by a width of 40 cm and a height of 60 cm. In your experience, what is the actual size of the base of the beam width in the existing structure?	
	1) ≤ 30 cm	2) 35 cm
	3) 38 cm	4) 40 cm
	5) 43 cm	6) ≥ 45 cm
	And what is the actual size of the beam height in the existing structure?	
	1) ≤ 50 cm	2) 55 cm
	3) 58 cm	4) 60 cm
	5) 63 cm	6) ≥ 65 cm

7.2	The original documents of a structure indicate that a column with a height of 3 m, has a square cross section of 40 cmx40 cm. In your experience, what is the actual dimension of the side of the column section in the existing structure?	
	1) ≤ 30 cm	2) 35 cm
	3) 38 cm	4) 40 cm
	5) 43 cm	6) ≥ 45 cm

Moreover, in the survey few other questions have been included in order to leave the opportunity to the professional engineers to suggest other type of structural defects that they may have encountered in their professional experience.

8.1	Have you encountered in your professional experience, other types of "defects", not reported in this survey?	
	1) Yes	2) No
	If so, can you describe the "defect" type.	
	1) "defect" type	
	2) "defect" type	
	3) "defect" type	

8.2	Can you indicate, for each type of described "defect", a range of values that the parameter associated with the "defect" may assume? How often it is possible to find such a "defect" in 10 inspections directly operated on the existing structure.		
	1)	Range	
		Revealed in 10 inspections	
	2)	Range	
		Revealed in 10 inspections	
	3)	Range	
		Revealed in 10 inspections	

8.3	Please indicate any additional comments in space provided below.

3.   Preliminary Results

As mentioned before, the scope of this survey is to obtain a comprehensive database in order to classify and to characterize prior probability distributions for structural details in existing RC structures. In fact, based on the results obtained from the database, it is possible to draw the histograms of the parameter or variable representing the considered type of "defect". In the next step, a probability distribution can be fitted to the histogram.

Some preliminary results obtained by interviewing a small number of professionals are presented in this section.

It should be noted that this pilot small-sample survey has been developed in order to test the questionnaire before a large scale distribution. In fact, the survey has been modified and updated after processing the results of the pilot survey.
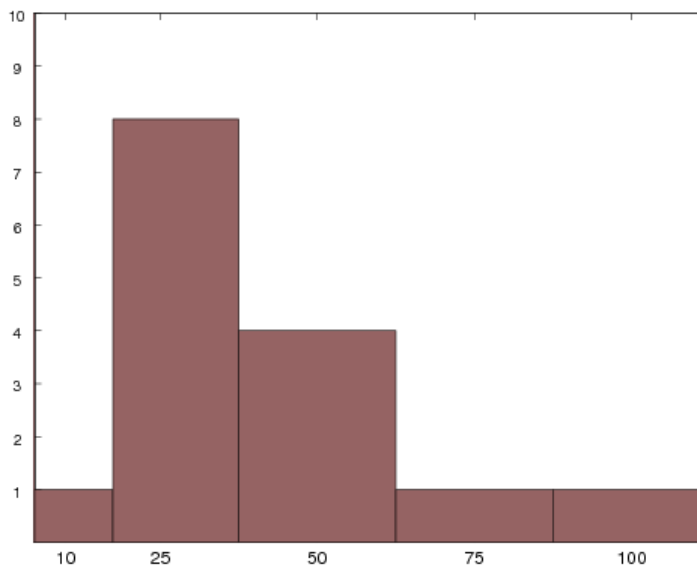
Figure 6.1 Histogram obtained from a small sample of answers gathered to the following question: Within 100 stirrups inspected in an existing RC structure how many, in your experience, have not been tied properly?

In Figure 6.1 the histogram obtained by employing the results of the small-sample survey in relation to the closure of the stirrups is shown.

In Figure 6.2, the histogram obtained from the answers to the question related to stirrup spacing in a beam element of an existing RC structure is shown.
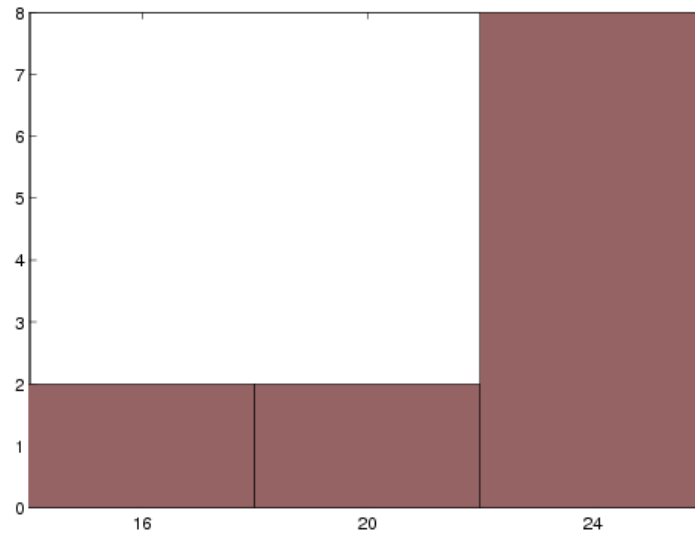
Figure 6.2 Histogram obtained from the engineer answers gathered to the following question: In the original documents it is indicated that in a beam of length equal to 4 m 24 stirrups have been inserted. In your experience, how many stirrups are actually present in the beam of the existing structure?

It should be noted that, like in many other questions of the survey, it is suppose that the analyst has access to the original documents of the existing structure. The scope of the survey is to evaluate, in relation to the analysts' experience, the variability of the construction details actually present in the existing structure.

In Figure 6.3, the histogram obtained based on the answers to the question related to the regularity of the stirrup spacing in the beam elements is shown.
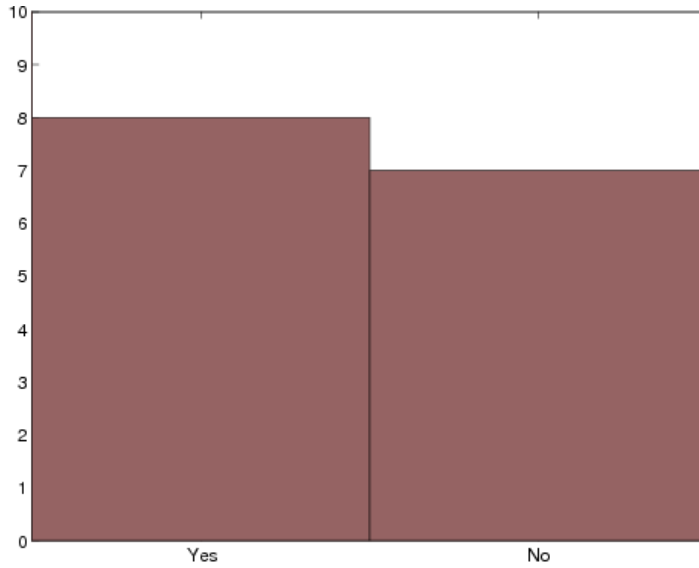
Figure 6.3 Histogram obtained from the answers to the question: With reference to the previous
question, do you expect to find the stirrups placed
with regular spacing?

As mentioned in the previous section, the engineer needs also to respond to the question of whether the information provided with the previous answers (in relation to the number of stirrups present in a beam of 4 m long and the regularity of their spacing) is systematic or not. In particular if the information is related to the single structural element analyzed or is systematic for the cast of concrete o for the entire structure. The resulting histogram is shown in Figure 6.4.
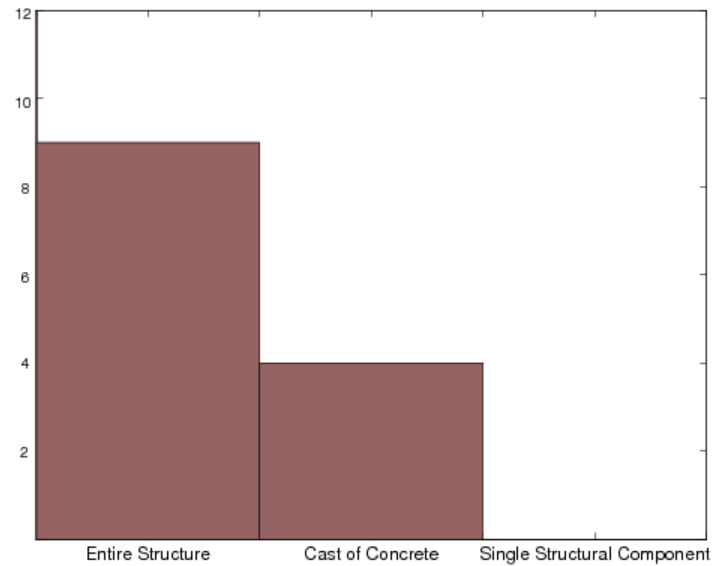
Figure 6.4 Histogram obtained from the answers to the question: Do you believe that this value is applicable to the entire structure, or the assessment should be repeated for different zones of the building (eg. those made with the same cast of concrete) or for each singular structural component?

It has to be noted that the preliminary results presented herein are corresponding to an earlier version of the survey. The survey included in the previous section is the final version.

4.   References

[1]   Lindley, D.V. 1983. Theory and practice of Bayesian statistics. *The Statistician* **32**, 1-11..

[2]   Walters, C.[J.] and D. Ludwig. Calculation of Bayes posterior probability distributions for key population parameters. *Can. J. Fish. Aquat. Sci.* **51**, 713-722.

[3]   Box, G.E.P. and Tiao, G.C., *Bayesian Inference in Statistical Analysis*, Wiley Interscience, 1992.

[4]   Legge 2 febbraio 1974 n. 64, "*Provvedimenti per le costruzioni con particolari prescrizioni per le zone sismiche*" (*in Italian*).

[5]   Santarella L. "*Il cemento armato – Le applicazioni alle costruzioni civili ed industriali*", Edizione Hoepli 1968.

[6]   Pagano M. "*Teoria degli edifici - Edifici in cemento armato*", Napoli, Edizione Liguori 1968.

Conclusions

This thesis focuses on the seismic assessment of existing RC buildings, with particular attention to the various sources of uncertainty that are involved in this problem.

A significant part of the total seismic risk in Italy, evaluated in economic terms, comes from the various type of damages endured by the existing buildings. This is the case for several other European countries in which the average service life for buildings is larger than that of countries like the United States. Therefore, management of existing building stock is a major concern in such regions.

As a result, more recent European seismic guidelines (EC8, OPCM, NTC) pay particular attention to seismic assessment of existing structures, which is distinguished from that of the new construction by lack of information about both the original features and the current state of building in consideration. Therefore, the assessment of existing RC structures is strongly affected by uncertainties in structural modeling, which may be comparable with those related to the representation of the ground motion.

Recent European codes seem to summarize the effect of these uncertainties in the so-called confidence factors that are applied to mean material properties, in order to allow for a certain level of conservatism when performing seismic assessment of an existing structure. This leads to using material strength values smaller then those determined based on available knowledge. The confidence factors are defined depending on the level of knowledge acquired for the

structure on the basis of specific test (destructive and non-destructive) and in-situ inspection results.

Although the confidence factors are applied to the properties of materials, the uncertainties in structural modeling are not limited to them and include also other structural detailing parameters (e.g., reinforcement detailing, cover thickness, etc.) entering into the seismic assessment problem. The variations in structural detailing parameters can prove quite significant to the extent that they may change the eventual structural collapse mechanism.

Moreover, the code definition of knowledge levels leaves considerable room for interpretation. In fact, the code indications does not lead to a unique configuration of tests and inspections. Furthermore, it is not clear what is the level of safety provided by the application of the confidence factors.

It seems intuitive that the relationship between the confidence factors and knowledge levels should be dependent on the result of tests and in-situ inspections. There seems to be a need for procedures which incorporate the test results and other relevant available information in order to update both the probability distribution for the modeling parameter and the structural reliability.

Therefore in this thesis an in depth discussion of how to handle different sources of uncertainty involved in an assessment problem has been presented, with specific attention to the problem of existing RC buildings.

The Bayesian framework for inference seems to be particularly suitable for this purpose, because allows to put in the sequence of test and inspection results without losing any prior information available.

In this thesis, three alternative proposals for performance assessment of existing reinforced concrete buildings using static non-linear analysis and dynamic time-history analysis are discussed, each involving increasing levels of analysis effort. Table C.1 outlines these methods and an estimated number of structural analyses they may require.

Table C.1. Alternative methods and the corresponding required number of analyses

Method	# of Analyses
Monte Carlo	200-500
Efficient Bayesian Method	20-30
The Code-based format	1

The most computationally demanding method is the standard Monte Carlo simulation method, that estimate the structural reliability by generating different realizations of the uncertain structural modeling parameters (i.e., different structural model realizations). Using a Bayesian updating algorithm, it is possible to update the structural fragility in relation to the available tests and inspections. This method has allowed to compare the results obtained for the case-study structure, in terms of global structural performance, with the code definitions of confidence factors and to formulate an alternative definition of the confidence factor.

An efficient simulation-based Bayesian method, that allows the robust estimation of the structural fragility with a small number of analysis has been developed and presented. The effectiveness of this method is verified by comparing the obtained results with those related to the standard Monte Carlo simulation method. It is observed, upon comparison with the Monte Carlo simulation results, that the efficient simulation-based method provides sufficiently accurate confidence intervals for the structural fragility in the static case.

As an alternative to the confidence factors, a probabilistic safety-checking format based on simplifying assumptions and adopted by the SAC-FEMA guidelines is discussed. This format can take into account the uncertainties in structural modeling and the uncertainties in the representation of the ground motion. The parameters for the structural fragility curve estimated by the above-mentioned methods can be readily incorporated into this safety-checking format. This method can be used to make safety-checking assessments of an existing RC building --with a specified confidence--employing only one analysis (i.e., the result of code-based procedure for CF=1) based on the bias

and the dispersion factors tabulated for different classes of representative existing structures.

For example, these tables and the updated probability distributions, for various KL's, based on special cases of test and inspection results, are constructed for both static and dynamic non-linear analyses for the case study structure.

Special attention has been focused on seismic record selection and the uncertainty related to the representation of ground motion. In this context, the choice of the parameter (scalar or vector) representative of the ground motion intensity and used in the estimation of the structural performance is fundamental. In order to obtain an assessment of the structural performance which is not affected by the particular choice of the set of records used in the analysis, the representative ground motion parameter adopted as a intensity measure *IM,* should be both sufficient and efficient. A graphical and statistical tool was implemented in the thesis in order to evaluate the fulfillment of the condition of sufficiency for different intensity measures. When this condition is not verified a simplified method using the weighted regression is employed in order to adjust the structural performance assessment in relation to the observed dependencies. The weights are assigned in relation to the results of the seismic hazard disaggregation for the site of interest.

All the methods proposed within this work are based on the definition of probability distributions for uncertain parameters. The uncertain parameters considered include the materials properties, the construction details parameters and, in the case of dynamic analyses, the uncertainty in the ground motion representation. For each knowledge level, the probability distributions for the uncertain parameters are updated using the Bayesian updating framework. The uncertain parameters are divided in groups (emulating various construction zones). It is assumed that the uncertain parameter belonging to distinct groups are fully un-correlated and only the uncertain parameters inside a given group can be correlated. It should be noted that decisions on possible groupings of the uncertain parameters can affect significantly the global performance assessment of the structure.

It should be emphasized that developing prior distributions is probably the most controversial aspect of any Bayesian analysis. Considerable care should be taken when characterizing the prior probability distributions. The process by which priors are selected must be justified carefully. This is because inappropriate choices for priors can lead to incorrect inferences.

To this end, with regard to construction details, a survey for professional engineers has been prepared in order to characterize the prior distributions related to expert opinion. This survey is presented in the thesis together with the preliminary testing results obtained by interviewing a small number of structural engineering professionals.

The aim of this work has been to make a step in the direction of implementing probabilistic performance-based methodologies for the assessment of existing RC buildings accessible to engineering professionals and that can, therefore, be adopted by future seismic codes.

For this aim, a range of methods has been proposed in order to allow the engineering professional to choose the most suitable method as a function of the importance of the structure and the level of precision desired.

As future goals, it can be useful to develop a Bayesian adaptive methodology for optimal programming of in-situ tests and inspections for probabilistic seismic assessment of existing buildings for a set of uncertain modelling parameters.

In fact, the Bayesian framework could be used to incorporate the test results in an adaptive manner in order to obtain a sequence of updated probability distributions for the modelling uncertainties affecting the structural performance based on increasing test results. The structural reliability can be also updated as a function of the updated probability distributions. The decision to stop the test would be reached when the structural reliability becomes effectively insensitive to the increasing number of tests.

Appendices

A.   Lumped Plasticity Model

Two main approaches can be used in order to take into account the inelastic behaviour of materials:

- Lumped plasticity model

- Distributed plasticity model

In the present study, it was decided to use the lumped plasticity model that allows concentrating the member non-linear behaviour in correspondence of their ends; such simplification is particularly indicated in the case of frame structures where the potential plastic hinges are located at the member ends.

In fact, in a frame structure, the moment distribution due to the horizontal lateral loads, not taking into account the gravity loads effects, is linear as reported in Figure A.1 and thus, each member can be considered as a fixed-end cantilever member, with a span equal to L_V, subjected to a force on the free end.

The length L_V is termed as the shear span and it is defined by the distance from the member ends to the inflexion point of the member deformed shape, corresponding to the point in which the moment diagram is equal to zero. The location of the inflexion point can be determined from the linear response of an element to lateral loads. However, once the first plastic regions develop, a redistribution of the flexural moments and a consequent displacement of the

inflexion point happens. Thus, the estimation of the shear span length is not a simple task. In order to simplify the problem, the shear span can be assumed constant due to horizontal loading and equal to $L_V=0,5L$. Such assumption has been adopted in the modeling of the case study structure. Furthermore, the stiffness in the plastic region it is assumed to be constant and equal to that of the cross-section at the beam column interface.
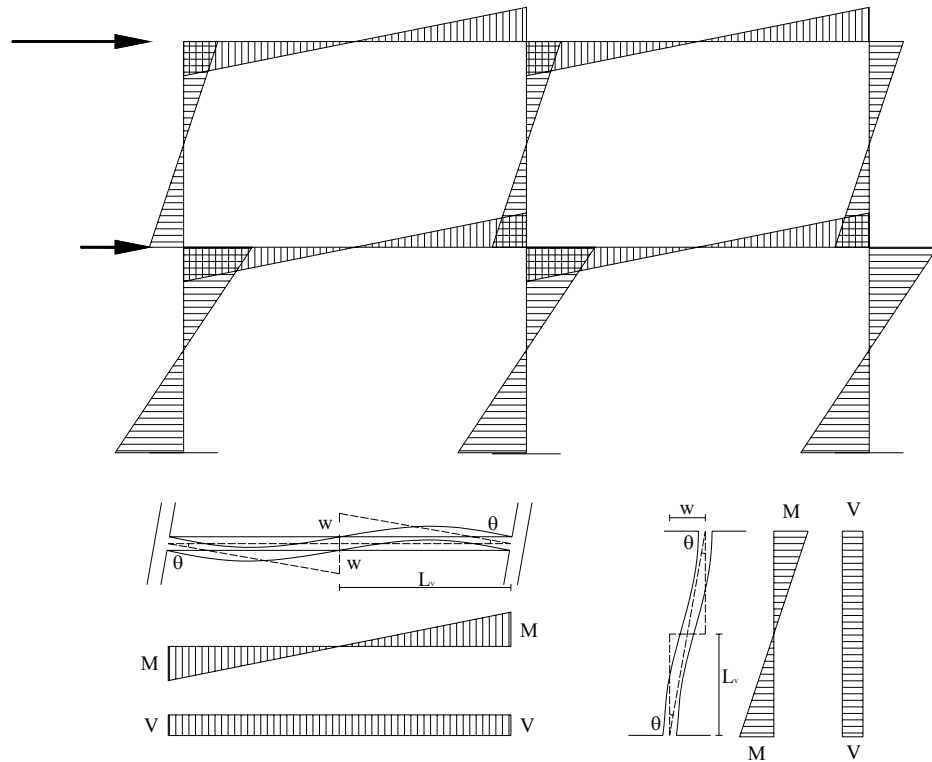
Figure A.1 Moments and deformed shape of frame beams and columns under horizontal loads [1]

The model used is known as *"one component model";* it consists of the coupling of an elastic element with a constant stiffness equal to EI (representative of the elastic behaviour in the member until it reaches the

plasticity) with a rigid-plastic one (representative of the plastic phase) as indicated in Figure A.2.
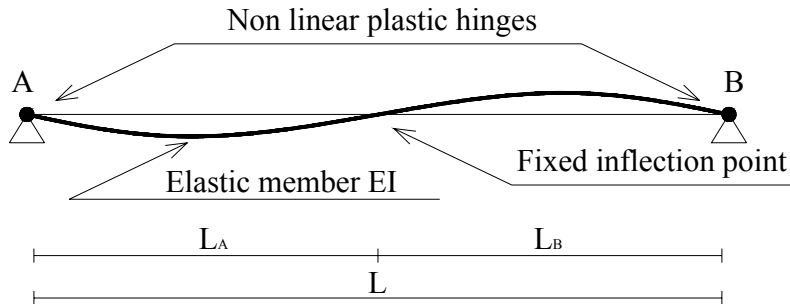
Figure A.2 Member modeling [1]

The main advantage of the model is its simplicity and computational efficiency. On the other hand, the assumption of a constant shear span, L_V, can be considered not very realistic considering that the yielding moments in the members' opposite ends are generally different (due to different reinforcement ratios). Moreover, the model does not allow for computing the formation of plastic hinges along the member due to the horizontal and gravity load interaction.

B. Plastic Hinge Characterization

The moment rotation relationship was obtained based on the moment curvature analysis performed for each element cross-section.

Plastic hinge length, L_{pl}, yielding and ultimate rotation, θ_y and θ_u, were computed according to the Eurocode 8, Part III [2] expressions:

$$L_{pl} = \beta_{flex}L_v + \beta_{shear}h + \beta_{slip}d_{bl}f_y$$

$$\theta_y = \alpha_{flex}\phi_y L_v + \alpha_{shear} + \alpha_{slip}\frac{d_{bl}f_y}{\sqrt{f_c}}$$

$$\theta_u = \gamma\left(\theta_y + \left(\phi_u - \phi_y\right)L_{pl}\left(1 - \frac{0.5L_{pl}}{L_V}\right)\right)$$

Eq. B-1

where L_V is the shear span, h is the cross-section depth, d_{bl} is the diameter of longitudinal bars, f_y and f_c are the average steel and concrete strength, respectively. Factors α_{flex}, α_{shear}, α_{slip} along with β_{flex}, β_{shear}, β_{slip} and γ, have been provided with reference to the seismic guidelines developed by the Italian Department of Civil Protection, Ordinanza 3431 [3]:

$$\begin{cases} \alpha_{flex} = 0.1 \\ \alpha_{shear} = 0.17 \\ \alpha_{slip} = 0.24/\sqrt{f_c} \end{cases} ; \quad \begin{cases} \delta_{flex} = 1/3 \\ \delta_{shear} = 0.0013\left(1 + 1.5\frac{h}{L_V}\right) \\ \delta_{slip} = 0.13\phi_y \end{cases} ; \quad \begin{cases} \gamma = \frac{1}{\gamma_{el}} \end{cases}$$

Eq. B-2

where γ_{el} is a coefficient equal to 1.5 or 1 for primary or secondary members, respectively.

C.   Capacity Spectrum Method

The Capacity Spectrum Method, Fajfar P. [4], is a simplified nonlinear static method for the seismic analysis of structures that combines the pushover analysis of a multi-degree of freedom (MDOF) system with the response spectrum analysis of a single-degree of freedom (SDOF) system.

Starting from the capacity curve of the MDOF system, obtained by pushover analysis, it is possible to obtain an idealized bilinear curve relative to the equivalent SDOF system imposing the equality of areas under the curve ($A_1=A_2$ see Figure C.1).
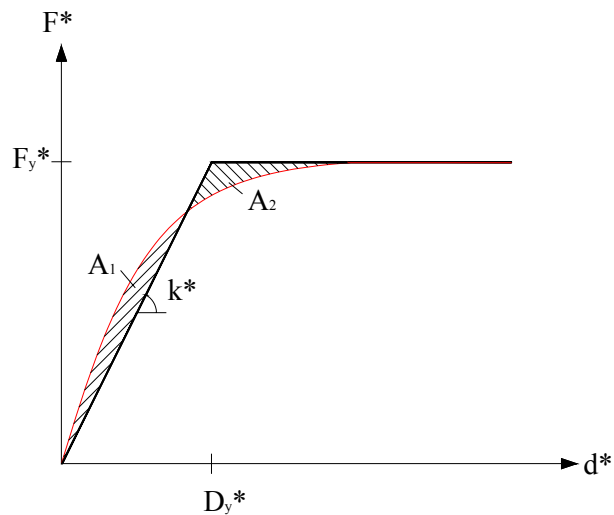
Figure C.1 Determination of the idealized elastic-perfectly plastic force displacement relationship

The SDOF characteristics are mapped to those of the MDOF through the participation coefficient Γ defined as:

$$\Gamma = \frac{\sum m_i \Phi_i}{\sum m_i \Phi_i^2}$$

Eq. C-1

where m_i is the mass relative to each storey i in the building and Φ is the vector representative of the first vibration mode of the considered structure in the analyzed direction, normalized to the unity at the displacement control point.

The SDOF force F^* and displacement d^* are related, in the elastic range, to the corresponding parameters evaluated from the MDOF structure using pushover analysis, through the following relations:

$$F^* = F/\Gamma$$
$$d^* = d/\Gamma$$

Eq. C-2

The obtained bilinear curve, relative to the SDOF system with mass and period equal to $m^* = \sum m_i \Phi_i$ and $T^* = 2\pi\sqrt{m^* D_y^*/F_y^*}$, is characterized by a elastic stiffness equal to F_y^*/ D_y^*.

The target displacement of the inelastic system can be computed as a function of the period T^* and of the assumed response spectrum. In particular, if $T^* \geq T_C$ (medium and low periods), the target displacement of the inelastic system is equal to that of an elastic system and is given by:

$$d_{max}^* = d_{e,max}^* = S_{de}\left(T^*\right)$$

Eq. C-3

In Figure C.2 (a) the equivalent graphical procedure for obtaining such displacement is reported in the ADRS (*Acceleration-Displacement Response*

Spectrum) format, period T^* is represented by the radial line from the origin of the coordinate system to the point at the elastic response spectrum defined by the point d_{max}^* and S_{de} (T^*).

If $T^* < T_C$, the displacement of the inelastic system is lager than that of an elastic system (with the same period) and it is computed as follows:

$$d_{max}^* = \frac{d_{e,max}^*}{q^*}\left[1+\left(q^*-1\right)\frac{T_C}{T^*}\right] \geq d_{e,max}^* \qquad \text{Eq. C-4}$$

where $q^* = S_{ae}(T^*)m^*/F_y^*$ is the ratio between the acceleration in the structure with elastic behaviour, denoted by $S_{ae}(T^*)$, and the acceleration in the structure with yielding strength F_y^*/m^*.

The equivalent graphical procedure is reported in Figure C.2 (b).

(a)   (b)
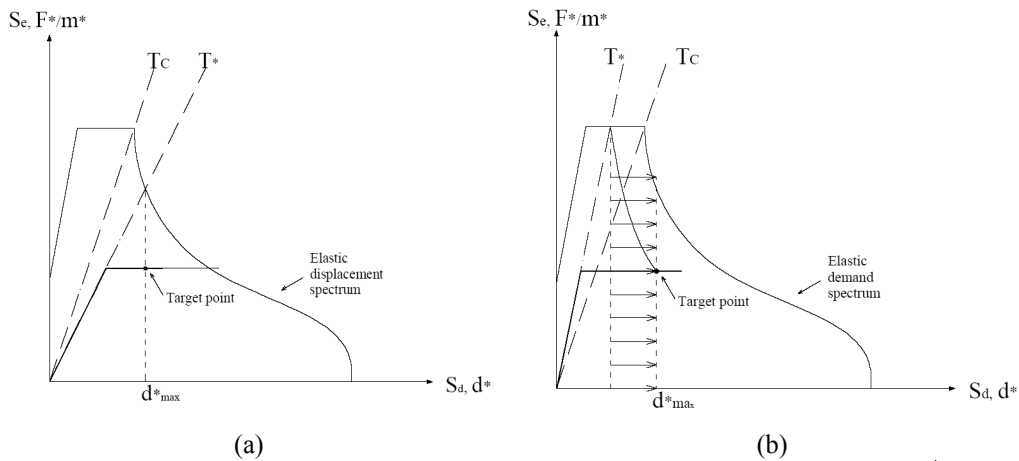
Figure C.2 Graphical procedure for computing the target displacement in the case of $T^* \geq T_C$ *(a)*, and $T^* < T_C$, (b).

Once the target displacement for the equivalent SDOF system has been computed, the target displacement of the MDOF system is given by:

$$d_{max} = \Gamma \cdot d^*_{max}$$
<div align="right">Eq. C-5</div>

D.   Weighted Least Squares

Suppose that in the linear regression model, $y_i = a+bx_i+e_i$, the errors are independent with expected value equal to zero have different variances, that is, $\text{var}(e_i) = \sigma^2 / w_i^2$, were w_i are the corresponding weights [5]. If each observation y_i is multiplied by its corresponding weight:

$$w_i y_i = w_i a + b(w_i x_i) + w_i e_i \qquad \text{Eq. D-1}$$

After defining $z_i = w_i\, y_i$, $u_i = w_i$, $v_i = w_i\, x_i$, and $\delta_i = w_i\, e_i$, the above expression can be transformed as:

$$z_i = au_i + bv_i + \delta_i \qquad \text{Eq. D-2}$$

It can be verified that the variance of the ith error term is equal to:

$$\text{var}(\delta_i) = \text{var}(w_i e_i) = w_i^2\, \text{var}(e_i) = w_i^2 \sigma^2 / w_i^2 = \sigma^2 \qquad \text{Eq. D-3}$$

As a result, the error terms $\delta_i = w_i\, e_i$ in the linear weighted model in equation D-2 can be considered independent and identically distributed (the variance is constant). The linear least squares method can be used to calculate the coefficients a and b by minimizing the sum of the square of the errors $\delta_i = w_i\, e_i$ or in other words by minimizing the sum of the square of the errors e_i in the original regression weighted by the factor w_i^2:

$$\sum_i \delta_i^2 = (z_i - au_i - bv_i)^2 \qquad \text{Eq. D-4}$$

Taking partial derivatives of the sum of the square of errors with respect to the parameters a and b, results in the following pair of equations to solve:

$$\frac{\partial \sum_i \delta_i^2}{\partial a} = -\sum_i 2u_i(z_i - au_i - bv_i) = 0$$

$$\frac{\partial \sum_i \delta_i^2}{\partial b} = -\sum_i 2v_i(z_i - au_i - bv_i) = 0$$

Eq. D-5

Therefore, the coefficients *a* and *b* can be calculated as:

$$b = \frac{(\sum u_i z_i)^2 - (\sum u_i)^2 (\sum v_i z_i)^2}{(\sum u_i v_i)^2 - (\sum u_i)^2 (\sum v_i)^2}$$

$$a = \frac{\sum u_i z_i}{\sum u_i^2} - b\frac{\sum u_i v_i}{\sum u_i^2}$$

Eq. D-6

After substituting $z_i = w_i\, y_i$, $u_i = w_i$, $v_i = w_i\, x_i$, the expressions for coefficients *a* and *b* for the weighted regression model can be written as:

$$b = \frac{(\sum w_i^2 y_i)^2 - (\sum w_i)^2 (\sum w_i^2 x_i y_i)^2}{(\sum w_i^2 y_i)^2 - (\sum w_i)^2 (\sum w_i y_i)^2}$$

$$a = \frac{\sum w_i^2 y_i}{\sum w_i^2} - b\frac{\sum w_i^2 x_i}{\sum w_i^2}$$

Eq. D-7

And the sum of the square of the errors of the weighted regression will be equal to:

$$s = \sum \delta_i^2 = \sum (w_i e_i)^2 = \sum w_i^2 (y_i - a - bx_i)^2$$

Eq. D-8

E.   Shear Failure

The so called *strut and tie* models are the most effective tools for the design and verification of reinforced shear beams because they allow for the visualization of physical resistance mechanisms simultaneously considering the effects of shear and bending. In particular, the *truss with variable slope model* is believed to provide the most realistic estimate of the shear capacity.

The first version of this method, which derives from the theory of plasticity, assumes that the inclination of shear cracks coincides with the inclination of the principal directions of compression. Therefore, there is no shear stress along the cracks and, as result, there is no contribution of concrete to the shear bearing capacity.

The inclination of the compressed struts, indicated with the angle θ, is conditioned by the behavior of the structural element, on the forces inducing fracture in the element and on the construction details.

With reference to the elementary mesh of the truss structure shown in the following figure:
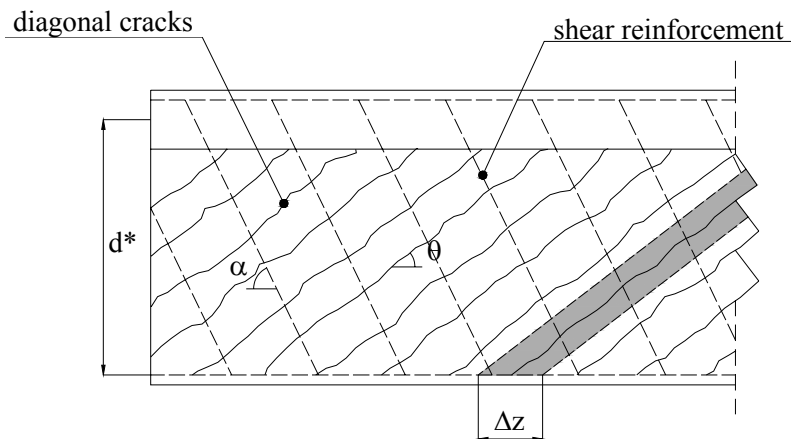
Figure E.1 Variable slope mechanism: elementary mesh [6]

The resistance of the concrete struts and the steel transversal reinforcement ties are analyzed.

The crisis of the compressed strut happens when the following equation is satisfied:

$$S_{cd} = b \cdot t \cdot \alpha_c \cdot \nu \cdot \sigma_{cd} = b \cdot (\Delta z \cdot \sin \theta) \cdot \alpha_c \cdot \nu \cdot \sigma_{cd} \qquad \text{Eq. E-1}$$

where:

$$t = \Delta z \cdot \sin \theta \qquad \text{Eq. E-2}$$

The coefficient ν takes into account the real distribution of stresses along the strut (which is actually inflected). The Italian code requires $\nu = 0.50$. The coefficient α_c takes into account the presence of axial compression forces. The Italian code characterizes α_c as the following:

- $\alpha_c = 1$ for uncompressed element
- $\alpha_c = 1 + \sigma_{cp}/\sigma_{cd}$ for $0 \le \sigma_{cp} < 0.25$
- $\alpha_c = 1.25$ for $0.25\sigma_{cd} \le \sigma_{cp} \le 0.50\sigma_{cd}$
- $\alpha_c = 2.50(1 - \sigma_{cp}/\sigma_{cd})$ for $0.50\sigma_{cd} \le \sigma_{cp} \le \sigma_{cd}$

$$\text{Eq. E-3}$$

where σ_{cp} is the average stress of compression.

If we zoom into the elementary mesh outlined in the following figure:
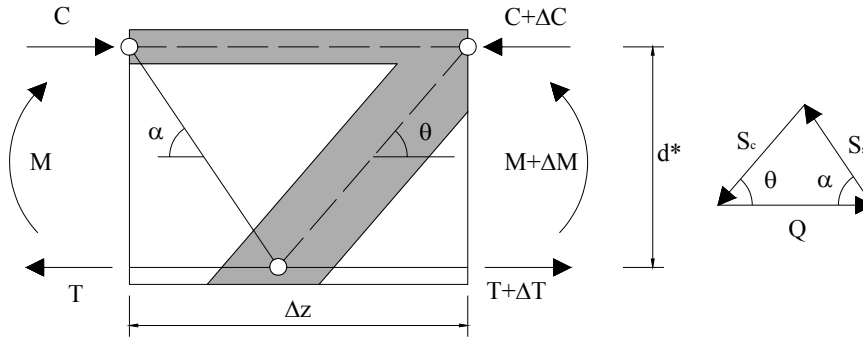
Figure E.2. The elementary mesh [6]

and we indicate its length by Δz and the internal moment arm by $d*$, the resultant force Q has the following value:

$$Q = \Delta C = \Delta T = \frac{\Delta M}{d*} = \frac{V \cdot \Delta z}{d*}$$ Eq. E-4

It is possible to decompose Q in to two stress components: one in the direction of the transverse reinforcement and other one in the direction of the compressed strut.

$$S_c = Q \cdot \frac{\sin \alpha}{\sin(\alpha + \theta)}$$

$$S_s = Q \cdot \frac{\sin \theta}{\sin(\alpha + \theta)}$$ Eq. E-5

Using equations E-4 and E-5 it is possible to derive a relation between the force absorbed by the compressed strut Sc and the shear force:

$$S_c = \frac{V \cdot \Delta z}{d*} \cdot \frac{\sin \alpha}{\sin(\alpha + \theta)}$$ Eq. E-6

By setting equation E-1 equal to equation E-6, one can obtain the critical shear value in the compressed strut:

$$S_{cd} = b \cdot \Delta z \cdot \sin \theta \cdot \alpha_c \cdot \nu \cdot \sigma_{cd} = S_c = \frac{V_{Rcd} \cdot \Delta z}{d^*} \cdot \frac{\sin \alpha}{\sin(\alpha + \theta)} \Rightarrow$$

$$\Rightarrow V_{Rcd} = b \cdot d^* \cdot \nu \cdot \alpha_c \cdot \sigma_{cd} \cdot \sin^2 \theta \cdot (\cot \alpha + \cot \theta) \Rightarrow \qquad \text{Eq. E-7}$$

$$\Rightarrow V_{Rcd} = b \cdot d^* \cdot \nu \cdot \alpha_c \cdot \sigma_{cd} \cdot \frac{\cot \alpha + \cot \theta}{1 + \cot^2 \theta}$$

Considering that only vertical stirrups ($\alpha=90°$) are present in the element, the equation E-7 becomes:

$$V_{Rcd} = b \cdot d^* \cdot \nu \cdot \alpha_c \cdot \sigma_{cd} \cdot \frac{1}{\cot \theta + \tan \theta} \qquad \text{Eq. E-8}$$

It should be noted that the maximum shear resistance corresponds to $\theta = 45°$. If the external shear force is less then the maximum shear resistance, calculated for $\theta = 45°$, the equilibrium in Figure 4 can be achieved for θ values less than 45°.

In the same manner, critical axial force in the transverse reinforcement is reached on the onset of yielding:

$$S_{sd} = \Omega_{sw} \cdot f_{yd} \qquad \text{Eq. E-9}$$

where Ω_{sw} is the total area of the reinforcement present in the length Δz. If the area of the single transverse reinforcement rebar is indicated with A_{sw}, we have:

$$\Omega_{sw} = A_{sw} \frac{\Delta z}{s} \qquad \text{Eq. E-10}$$

where s is the transverse reinforcement spacing.

Using equations E-4 and E-5, one can derive a relation between the axial force in the transverse reinforcement S_s and the shear force V:

$$S_s = \frac{V \cdot \Delta z}{d*} \cdot \frac{\sin\theta}{\sin(\alpha + \theta)}$$ Eq. E-11

By setting equation D-8 equal to equation D-11, we can obtain the shear critical force that corresponds to the yielding of the transverse reinforcement:

$$S_{sd} = \frac{A_{sw} \cdot \Delta z}{s} \cdot f_{yd} = S_s = \frac{V_{Rsd} \cdot \Delta z}{d*} \cdot \frac{\sin\theta}{\sin(\alpha + \theta)} \Rightarrow$$

$$\Rightarrow V_{Rsd} = A_{sw} \cdot f_{yd} \cdot \frac{d*}{s} \cdot \sin\alpha \cdot (\cot\alpha + \cot\theta)$$ Eq. E-12

Considering that only vertical stirrups ($\alpha = 90°$) are present, the equation becomes:

$$V_{Rsd} = A_{sw} \cdot f_{yd} \cdot \frac{d*}{s} \cdot \cot\theta$$ Eq. E-13

It should be noted, from the previous equation, that the shear resistance decreases with the increasing slope angle θ.

The Italian code limits that the inclination θ of the concrete struts with the beam axis in the following interval:

$$1 \leq \cot\theta \leq 2.5 \Rightarrow 45° \geq \theta \geq 21.81°$$ Eq. E-14

References

[1] Verderame, G., "Analisi sismica di edifici in C.A. progettati per carichi gravitazionali," *PhD. Thesis,*, XII ciclo, 1999.

[2] CEN, European Committee for Standardisation TC250/SC8/ [2003] *"Eurocode 8: Design Provisions for Earthquake Resistance of Structures, Part 1.1: General rules, seismic actions and rules for buildings*," PrEN1998-1.

[3] Ordinanza del Presidente del Consiglio dei Ministri (OPCM) n. 3431, "Ulteriori modifiche ed integrazioni all'ordinanza del Presidente del Consiglio dei Ministri n. 3274 del 20 marzo 2003". Gazzetta Ufficiale della Repubblica Italiana n. 107 del 10-5-2005 (Suppl. Ordinario n.85), 2005 (*in Italian*).

[4] Fajfar, P. "Capacity spectrum method based on inelastic demand spectra", *Earthquake Engineering and Structural Dynamics*; 28:979–93, 1999.

[5] Rice J. A., (1995) *Mathematical Statistics and Data Analysis*, Belmont, CA: Duxbury/Wadsworth.

[6] Cosenza E., Manfredi G., Pecce M., Strutture in cemento armato – basi della progettazione. Hoepli, 2008.